

LESSONS LEARNED FROM DYNAMIC ANALYSES OF MEXICO CITY AND APPLIED
TO RICHMOND B.C.

by

ANDREW M. NICHOLS

B.A.Sc., University Of British Columbia, 1983

A THESIS SUBMITTED IN PARTIAL FULFILMENT OF
THE REQUIREMENTS FOR THE DEGREE OF
MASTER OF APPLIED SCIENCE

in

THE FACULTY OF GRADUATE STUDIES
Department Of Civil Engineering

We accept this thesis as conforming
to the required standard

THE UNIVERSITY OF BRITISH COLUMBIA

September 1987

© Andrew M. Nichols, 1987

In presenting this thesis in partial fulfilment of the requirements for an advanced degree at the University of British Columbia, I agree that the Library shall make it freely available for reference and study. I further agree that permission for extensive copying of this thesis for scholarly purposes may be granted by the head of my department or by his or her representatives. It is understood that copying or publication of this thesis for financial gain shall not be allowed without my written permission.

Department of Civil Engineering

The University of British Columbia
1956 Main Mall
Vancouver, Canada
V6T 1Y3

Date Oct 9 1987

Abstract

The implications of the acceleration data recorded during the September 19, 1985 Mexican earthquake for seismic design in Canada are investigated by determining if the deep deposits of the Fraser Delta could cause large amplification of earthquake motions. The conditions for amplification of low level incoming ground motions at deep sites are identified; in particular, the critical role of variation in shear modulus with shear strain. The current procedure for determining site specific ground motions is evaluated and major sources of uncertainty in the results identified. Criteria for selecting representative input motions for site response studies are recommended based on analyses of Mexico City sites. A comparative study of sites in the Fraser Delta area of British Columbia showed that offshore subduction earthquakes should be considered when developing design spectra for deep sites in the Delta.

Table of Contents

Abstract	ii
List of Tables	v
List of Figures	ix
Acknowledgement	xi
1.0 INTRODUCTION	1
2.0 GROUND MOTIONS AND DAMAGE DURING THE 1985 MEXICAN EARTHQUAKE	4
2.1 Ground Motions Recorded During The 1985 Mexican Earthquake	4
2.2 Ground Motions And Damage In Mexico City	19
3.0 GEOLOGY AND PROPERTIES OF MEXICO CITY SOILS	24
3.1 Location	24
3.2 Geologic History Of The Valley Of Mexico	24
3.4 Index Properties Of Mexico City Soils	31
3.5 Dynamic Properties Of Mexico City Lakebed Deposits	32
4.0 ANALYSES OF MEXICO CITY SITES USING REPRESENTATIVE INPUT MOTIONS	36
4.1 Selection Of Representative Input Motions	36
4.2 Results Of Analyses At The SCT Site	38
4.3 Results Of Analyses At The CAF Site	39
4.4 Results Of Analyses At The CAO Site	39
4.5 Summary Of Results Using The Modified Pasadena Record As Input	42
5.0 ANALYSES OF MEXICO CITY SITES USING ROCK OUTCROP MOTIONS AS INPUT	45
5.1 Results Of Analyses At The SCT Site	45
5.2 Results Of Analyses At The CAO Site	52
5.3 Results Of Analyses At The CAF Site	54
5.3 Summary Of Analyses Of Mexico City Sites Using Rock Outcrop Motions As Input	57
6.0 INPUT MOTIONS, SOIL PROFILES AND SOIL PROPERTIES FOR DYNAMIC ANALYSES OF FRASER DELTA SITES	59
6.1 Selection Of Representative Input Motions	59
6.2 Soil Properties And Profile - Annacis Site	65
6.3 Soil Properties And Profile - Brighthouse Site	68
6.4 Soil Properties And Profile - McDonald Farm Site	70
7.0 RESULTS OF DYNAMIC ANALYSES OF FRASER DELTA SITES	71
7.1 Results Of Analyses At The Annacis Site	71
7.2 Summary Of Analyses At The Annacis Site	81
7.3 Results Of Analyses At The Brighthouse Site	82
7.4 Results Of Analyses At The McDonald Farm Site	85
7.5 Summary Of Analyses Of Fraser Delta Sites	88

8.0 REVIEW OF RESULTS AND SUGGESTIONS FOR FURTHER STUDY ..	91
8.1 Review Of Mexico City Analyses	91
8.2 Review Of Fraser Delta Analyses	92
8.3 Suggestions For Further Research	93
REFERENCES	95
APPENDIX--THE GEOLOGY OF THE FRASER LOWLAND	102
Geologic History Of The Fraser Lowland	102
Geological History Of The Fraser Delta	108
Geology Of The Fraser River Delta	111

List of Tables

Table 3.1: Average Values of Properties of the Clays
of the Tacubaya Formation32

Table I: Stratigraphy of the Fraser Lowland103

List of Figures

Figure 2.1: Earthquake Epicenters And Tectonic Features Of The Mexican Coast	5
Figure 2.2: N00E Component Of Acceleration Recorded At The CALE Site	6
Figure 2.3: N90W Component Of Acceleration Recorded At The CALE Site	6
Figure 2.4: Accelerograph Sites In Mexico City	8
Figure 2.5: N00E Component Of Acceleration Recorded At The CUO1 Site	9
Figure 2.6: N90W Component Of Acceleration Recorded At The CUO1 Site	9
Figure 2.7: N00E Component Of Acceleration Recorded At The CUIP Site	10
Figure 2.8: N90W Component Of Acceleration Recorded At The CUIP Site	10
Figure 2.9: N00E Component Of Acceleration Recorded At The SCT Site (First 20 Seconds Cutoff)	11
Figure 2.10: N90W Component Of Acceleration Recorded At The SCT Site (First 20 Seconds Cutoff)	11
Figure 2.11: N00E Component Of Acceleration Recorded At The CAO Site (First 30 Seconds Cutoff)	12
Figure 2.12: N90W Component Of Acceleration Recorded At The CAO Site (First 30 Seconds Cutoff)	12
Figure 2.13: N00E Component Of Acceleration Recorded At The CAF Site	13
Figure 2.14: N90W Component Of Acceleration Recorded At The CAF Site	13
Figure 2.15: Response Spectra (5% Damping) Of Motions Recorded At The SCT Site	16
Figure 2.16: Response Spectra (5% Damping) Of Motions Recorded At The CAO Site	16
Figure 2.17: Response Spectra (5% Damping) Of Motions Recorded At The CAF Site	17

Figure 2.18: Response Spectra (5% Damping) Of Motions Recorded At The CUO1 And CUIP Sites	17
Figure 2.19: Response Spectra (5% Damping) Of Motions Recorded At The CALE Site	18
Figure 2.20: Zones Of Damage In Mexico City Earthquakes ..	20
Figure 2.21: Damage Rates As A Function Of Building Height	22
Figure 3.1: The Basin Of The Valley Of Mexico	25
Figure 3.2: Geological Sequence And Soil Depsoits Below The Central Area Of Mexico City	27
Figure 3.3: The Subsoil Zones Of Mexico City	29
Figure 3.4: Cross Sections Through Mexico City	30
Figure 3.5: Site Models For The SCT, CAF And CAO Sites ...	34
Figure 3.6: Range In Shear Dependent Moduli And Damping For Mexico City Clay Compared To The Shear Dependent Modulus For A Typical Clay	35
Figure 4.1: Response Spectra (5% Damping) Of Pasadena Record Showing Effect Of Frequency Scaling	37
Figure 4.2: Response Spectra (5% Damping) Of Computed Motions And Average Response Spectrum Of The Recorded Motions At The SCT Site	37
Figure 4.3: Response Spectra (5% Damping) Of Computed Motions Using The Modified Pasadena Record Scaled To .035g And Average Response Spectrum Of The Recorded Motions At The CAF Site	40
Figure 4.4: Response Spectra (5% Damping) Of Computed Motions Using The Modified Pasadena Record Scaled To .045g And Average Response Spectrum Of The Recorded Motions At The CAF Site	40
Figure 4.5: Response Spectra (5% Damping) Of Computed Motions And Average Response Spectrum Of The Recorded Motions At The CAO Site	41
Figure 4.6: Response Spectra (5% Damping) Of Computed Motions At The SCT Site Showing The Effect Of Soil Properties	43
Figure 4.7: Response Spectra (5% Damping) Of Computed Motions At The SCT Site Showing The Effect Of The Period Content Of The Input Motion	43

Figure 5.1: Response Spectra (5% Damping) Of Recorded And Computed Motions In The N90W Direction At The SCT Site	46
Figure 5.2: Response Spectra (5% Damping) Of Recorded And Computed Motions In The N00E Direction At The SCT Site	46
Figure 5.3: Acceleration Path At The SCT Site During The 1985 Earthquake	48
Figure 5.4: Acceleration Path At The CUIP Site During The 1985 Earthquake	48
Figure 5.5: Response Spectra (5% Damping) Of Recorded And Computed Motions In The N90W Direction At The SCT Site Using Scaled Input Motions	49
Figure 5.6: Response Spectra (5% Damping) Of Recorded And Computed Motions In The N90W Direction At The SCT Site Using A Deep Site Model	51
Figure 5.7: Response Spectra (5% Damping) Of Recorded And Computed Motions In The N00E Direction At The SCT Site Using A Deep Site Model	51
Figure 5.8: Response Spectra (5% Damping) Of Recorded And Computed Motions In The N90W Direction At The CAO Site	53
Figure 5.9: Response Spectra (5% Damping) Of Recorded And Computed Motions In The N00E Direction At The CAO Site	53
Figure 5.10: Response Spectra (5% Damping) Of Recorded And Computed Motions In The N90W Direction At The CAO Site Using Scaled Input Motions	55
Figure 5.11: Response Spectra (5% Damping) Of Recorded And Computed Motions In The N90W Direction At The CAF Site	56
Figure 5.12: Response Spectra (5% Damping) Of Recorded And Computed Motions In The N00E Direction At The CAF Site	56
Figure 6.1: The Fraser Delta And Fraser Lowland	60
Figure 6.2: Location Map Of The Delta Sites	60
Figure 6.3: Plate Boundaries Of The West Coast Of North America: 1) Dellwood-Wilson, 2) Revere-Dellwood, 3) Sovanco, 4) Nootka, 5) Blanco, 6) Gorda, 7) Mendocino, 8) Sandspit, 9) Beaufort	61

Figure 6.4: Response Spectra (5% Damping) Of Motions Recorded At Taft During The 1952 Kern County Earthquake Scaled To .2 G And .25 G	64
Figure 6.5: Soil Profile And Properties Developed By Golder Associates At The Annacis Site	66
Figure 6.6: Shear Dependent Modulus And Damping For Sand	66
Figure 6.7: Shear Dependent Modulus And Damping For Silty Clay	67
Figure 6.8: Shear Dependent Modulus And Damping For Till	67
Figure 6.9: Soil Profile And Properties Developed By Wallis At The Brighthouse Site	69
Figure 6.10: Soil Profile And Properties Developed At The McDonald Farm Site	69
Figure 7.1: Response Spectra (5% Damping) Of Computed Motions At The Annacis Site, Taft .25g As Input	72
Figure 7.2: Response Spectra (5% Damping) Of Computed Motions At The Annacis Site	72
Figure 7.3: Response Spectra (5% Damping) Of Input And Computed Motions At The Annacis Site	74
Figure 7.4: Response Spectra (5% Damping) Of Input And Computed Motions At The Annacis Site	74
Figure 7.5: Response Spectra (5% Damping) Of Input And Computed Motions At The Annacis Site	75
Figure 7.6: Response Spectra (5% Damping) Of Input And Computed Motions At The Annacis Site	75
Figure 7.7: Spectral Acceleration (5% Damping) As A Function Of The Predominant Period Of The Input Motion ...	77
Figure 7.8: Response Spectra (5% Damping) Of Computed Motions At The Annacis Site	77
Figure 7.9: Response Spectra (5% Damping) Of Computed Motions At The Annacis Site	79
Figure 7.10: Spectral Acceleration (5% Damping) As A Function Of The Predominant Period Of The Input Motion ...	79
Figure 7.11: Response Spectra (5% Damping) Of Computed Motions At The Annacis Site	80
Figure 7.12: Response Spectra (5% Damping) Of Computed	

Motions At The Annacis Site	80
Figure 7.13: Response Spectra (5% Damping) Of Computed Motions At The Brighthouse Site, Taft .25g As Input	83
Figure 7.14: Response Spectra (5% Damping) Of Computed Motions At The Brighthouse Site Showing Dependence Of Site Response On Shear Dependence Of Modulus And Damping	83
Figure 7.15: Response Spectra (5% Damping) Of Computed Motions At The Brighthouse Site	84
Figure 7.16: Spectral Acceleration (5% Damping) At The Brighthouse Site As A Function Of The Predominant Period Of The Input Motion	84
Figure 7.17: Response Spectra (5% Damping) Of Computed Motions At The Brighthouse Site	86
Figure 7.18: Response Spectra (5% Damping) Of Computed Motions At The McDonald Site	87
Figure 7.19: Spectral Acceleration (5% Damping) At The McDonald Farm Site As A Function Of The Predominant Period Of The Input Motion	87
Figure 7.20: Response Spectra (5% Damping) Of Computed Motions At The McDonald Site	89
Figure I: Quaternary Depsoits Of The Fraser Lowland	107
Figure II: Cross Section And Borehole At Mitchell Island	110
Figure III: Soil Type And Depth Of Surficial Deltaic Deposits In Richmond	112

Acknowledgement

The writer wishes to thank his research supervisor Dr. W.D.L. Finn for his guidance. He further wishes to express his appreciation to Mr. M. Yogendrakumar for his help.

Data on soil properties in Mexico City was obtained from Dr. R. Lo of Klohn Leonoff Consultants. Accelerograms from the Mexican earthquake were made available by the Institute of Geophysics and Planetary Physics of the University of California, San Diego and the Instituta de Ingenieria at the Universidad Nacional Autonoma de Mexico, Mexico City. Data on soil properties in the Fraser Delta were made available by the British Columbia Ministry of Transportation and Highways.

The writer would also like to thank the National Research Council of Canada who provided financial support.

1.0 INTRODUCTION

The presence of site dependent effects during earthquake shaking has been reported by many authors; Gutenberg(1957), Duke(1958), Ohsaki(1969) and Seed and Idriss(1969). Engineers must be able to quantitatively account for site effects in design but due to the large number of variables affecting the response such as source and travel path, site topography, soil profile and soil properties, the prediction of site effects is very difficult. Two possible means of obtaining site dependent spectra for use in design are the use of generalised site dependent spectra, (Seed et al. 1976), and one dimensional analysis using programs such as SHAKE, (Schnabel et al., 1972), or Desra-2, (Lee and Finn, 1978). A two dimensional analysis using the programs discussed by Bard and Bouchon(1980) or Finn et al.(1986) is necessary if the effects of site topography or soil structure interaction are to be included.

Site dependent effects were observed in Mexico City during the September 19, 1985 Mexican earthquake of magnitude $M_s=8.1$. The epicenter of the earthquake was located 300 km from Mexico City in the subduction zone off the Pacific Coast of Mexico between Jalisco and Oaxaca. Despite the large epicentral distance, damage was severe in the sections of Mexico City built on the former lakebed of Lake Texcoco. Peak horizontal accelerations at hard sites at the edge of the lakebed were .035g, while, at sites on the lakebed, peak horizontal accelerations were as high as .17g, an amplification of approximately 5 as the motions passed through the lakebed

deposits. The duration of strong shaking on the lakebed was very long, up to 3 minutes at some sites. The long duration of the strong shaking produced severe damage and heavy loss of life in Mexico City.

The dramatic effects of amplification of earthquake motions by the lakebed deposits in Mexico City have led to concern that large amplification of earthquake motions could occur at other sites such as the Bay Mud deposits in San Francisco (Seed, 1986) and the deep soil deposits of the Fraser Delta in British Columbia (CANCEE, 1986). The purpose of this study is to determine if the Fraser Delta deposits could cause large amplification of earthquake motions.

The 1985 Mexican earthquake also altered opinions on the seismicity of the west coast of British Columbia. The earthquake led to studies which suggest that a subduction earthquake with magnitude $M=8+$ with a return period of 400 to 600 years could occur with 200 km of Vancouver (Weichert and Rogers, 1987; Heaton and Hartzell, 1987). This earthquake could cause motions in the bedrock beneath the deposits of the Fraser Delta similar to those in the materials underlying the lakebed deposits of Mexico City.

There are no strong motion earthquake records available for the Fraser Delta. Therefore, the determination of whether amplification of the subduction type earthquake motions similar to that which occurred in Mexico City could occur in the Fraser Delta will have to be made using one dimensional (1-D) analysis techniques. Because of the uncertainties in dynamic analyses,

verification of the current procedures is desirable. In this study verification is carried out using recorded motions from Mexico City.

During the 1985 Mexican earthquake many strong motion accelerograms were recorded in the near and far field, and on hard and soft sites. These records present an excellent opportunity to verify dynamic analysis procedures and isolate the important factors determining whether large amplification of base motions will occur or not. If the characteristics of the lakebed motions in Mexico City can be reproduced the same procedures will be applied to Fraser Delta sites to determine if similar amplification may take place.

2.0 GROUND MOTIONS AND DAMAGE DURING THE 1985 MEXICAN EARTHQUAKE

The 1985 Mexican earthquake occurred near the seismically active west coast as shown in Figure 2.1. These earthquakes are caused by the subduction of the Cocos Plate beneath the North America Plate at the rate of 60 mm/year (Mitchell et al., 1986). Earthquakes in this zone are shallow and have return periods of 32 to 56 years (Singh et al., 1981). Figure 2.1 also shows two seismic gaps that existed prior to the September, 1985 earthquake. The Mihoacan and Tehuantepec areas had not experienced earthquakes since 1800 or earlier (Singh et al., 1981) and thus until the September, 1985 earthquake, it was considered a possibility that strains were being released aseismically in the Mihoacan area. Because the Mihoacan gap had not experienced any movement for at least 150 years the magnitude of the 1985 event was much larger than most events occurring on the coast of Mexico. It had a magnitude of 8.1 and since 1900 there have only been three earthquakes on the west coast of Mexico with a magnitude greater than 8.0 and only one with a magnitude greater than 8.1 (Singh et al., 1981).

2.1 Ground Motions Recorded During the 1985 Mexican Earthquake

Accelerograms of the N00E and N90W components of motion recorded at Caleto de Campos or CALE site, 40 km from the epicenter are shown in Figures 2.2 and 2.3. Both components have peak accelerations of $A_{max} = .14g$. From the records it was determined that the earthquake consisted of two separate events

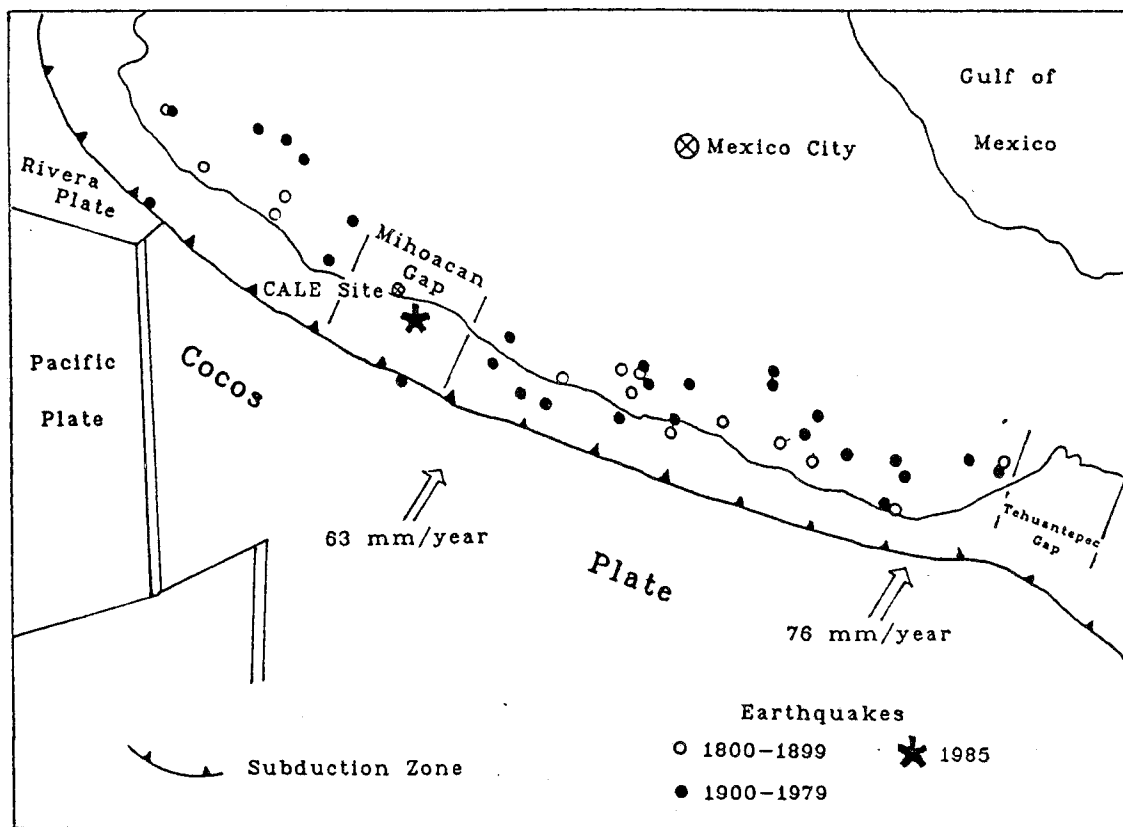


Figure 2.1: Earthquake Epicenters and Tectonic Features of the Mexican Coast

(Adapted from Mitchell et al., 1986)

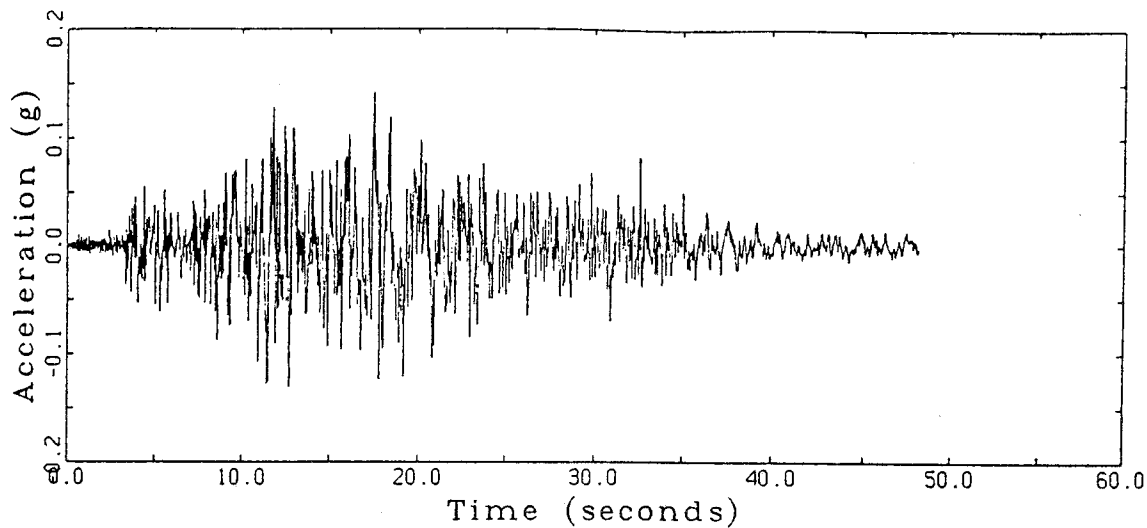


Figure 2.2: N00E Component of Acceleration Recorded at the CALE Site

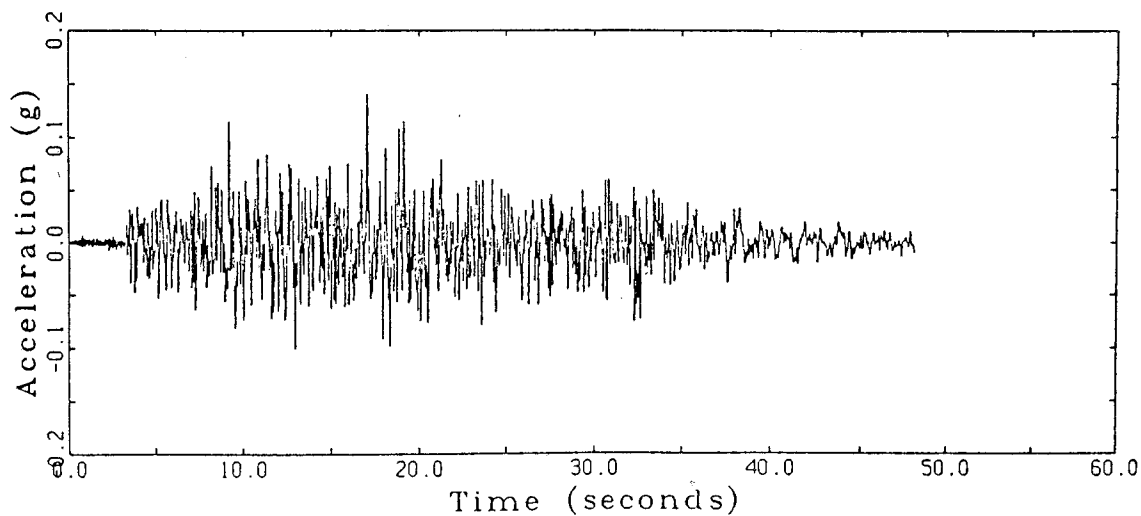


Figure 2.3: N90W Component of Acceleration Recorded at the CALE Site

(Mitchell et. al., 1986). An initial rupture on the slip plane propagated at about 4 km/sec and released energy for 30 to 40 seconds. A second slip, 40 seconds after the initial event, provided additional energy and extended the duration of the shaking.

During the 1985 earthquake, accelerograms were also recorded in Mexico City at the sites shown in Figure 2.4. The hard UNAM site consists of two sites; designated CUO1 and CUIP. The N00E and N90W components of the motion at the CUO1 site were recorded in the first floor of a 3 story building and are shown in Figures 2.5 and 2.6. The N00E and N90W components of the motion at the CUIP site were recorded in the free field and are shown in Figures 2.7 and 2.8.

Motions were also recorded at three lakebed sites during the 1985 earthquake. The N00E and N90W components of the motion recorded at the free field SCT site (Figure 2.4) are shown in Figures 2.9 and 2.10. The Central de Abastos site consists of two sites designated CAO and CAF. The N00E and N90W components of the motions recorded in the building at the CAO site are shown in Figures 2.11 and 2.12. The N00E and N90W components of the motion recorded in the free field at the CAF site are shown in Figures 2.13 and 2.14. Two observations can be made about the character of the motions shown in Figures 2.2 and 2.3 and Figures 2.5 to 2.14. The first is that the epicentral motions (Figures 2.2 and 2.3) have a higher frequency content than the hard site motions recorded in Mexico City (Figures 2.5 to 2.8). This is due to the attenuation of the higher frequency motions

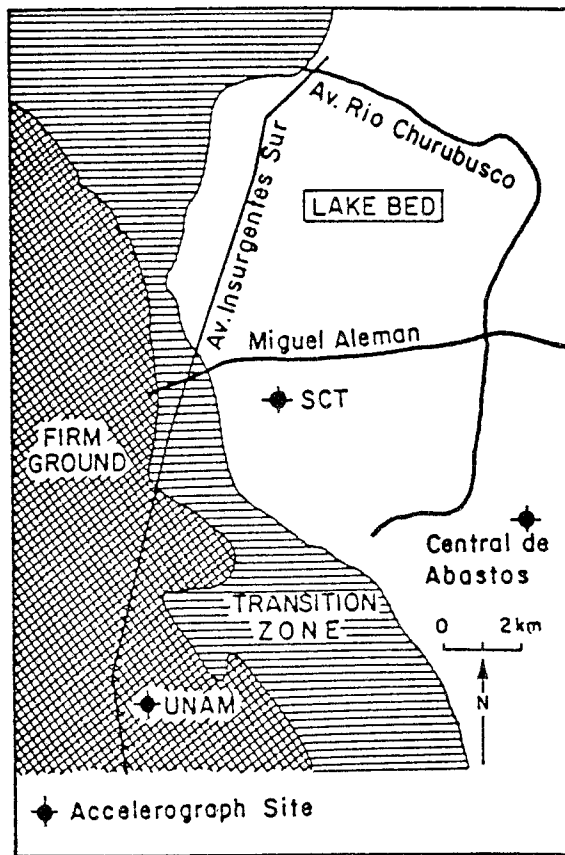


Figure 2.4: Accelerograph Sites in Mexico City
(Adapted from Mitchell et al., 1986)

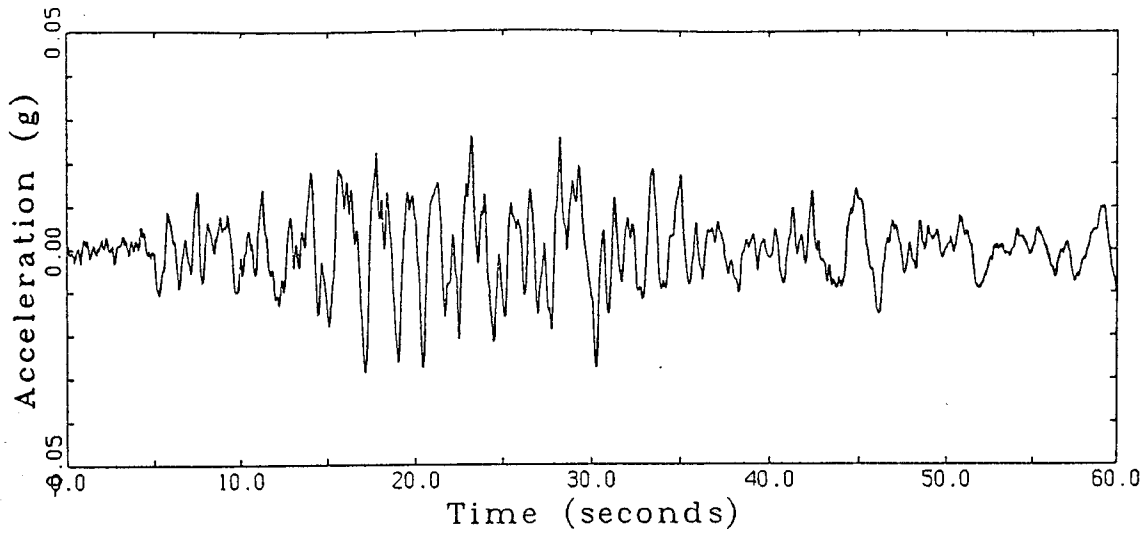


Figure 2.5: N00E Component of Acceleration Recorded at the CUO1 Site

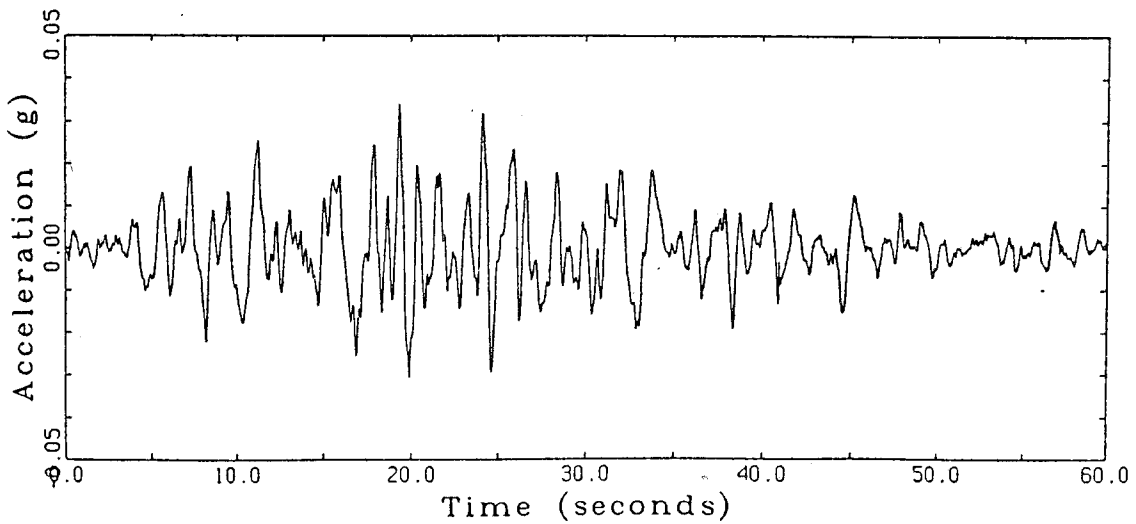


Figure 2.6: N90W Component of Acceleration Recorded at the CUO1 Site

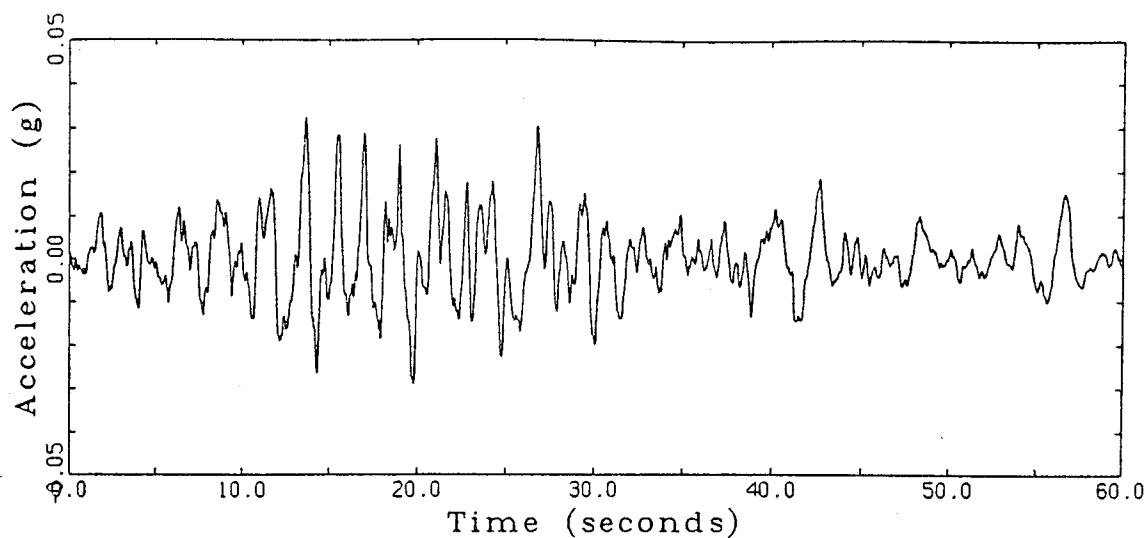


Figure 2.7: N00E Component of Acceleration Recorded at the CUIP Site

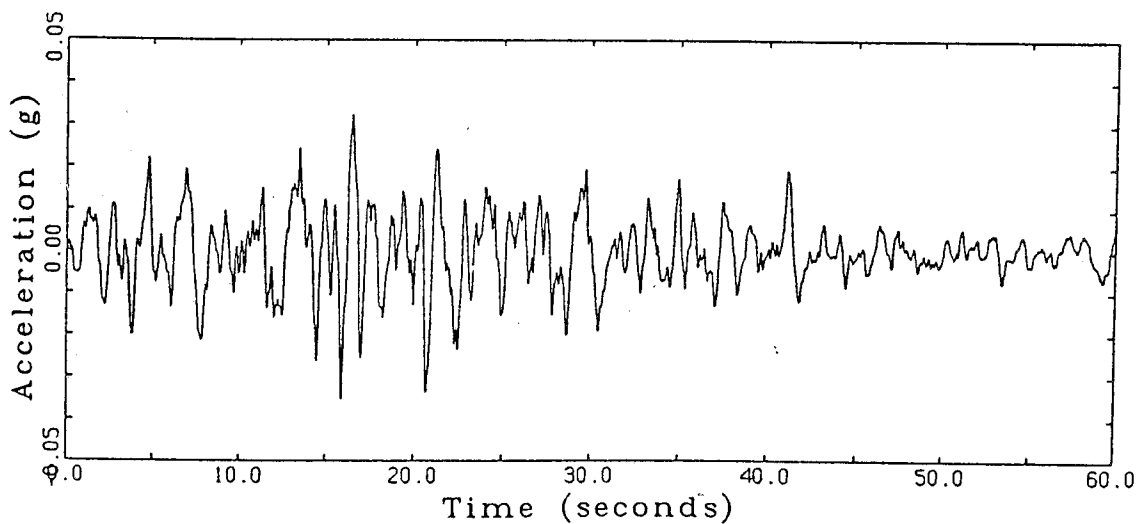


Figure 2.8: N90W Component of Acceleration Recorded at the CUIP Site

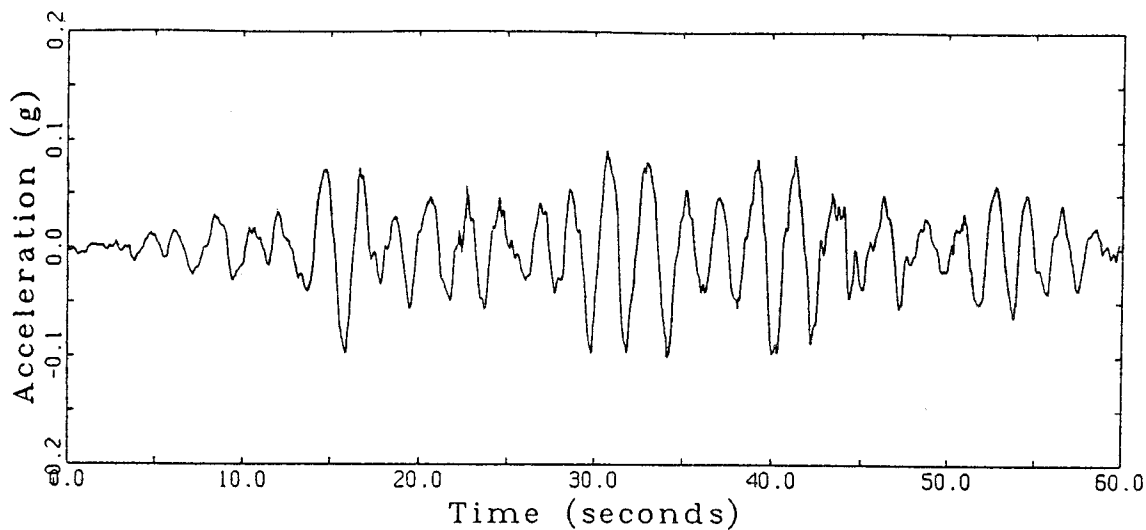


Figure 2.9: N00E Component of Acceleration Recorded at the SCT Site (First 20 seconds cutoff)

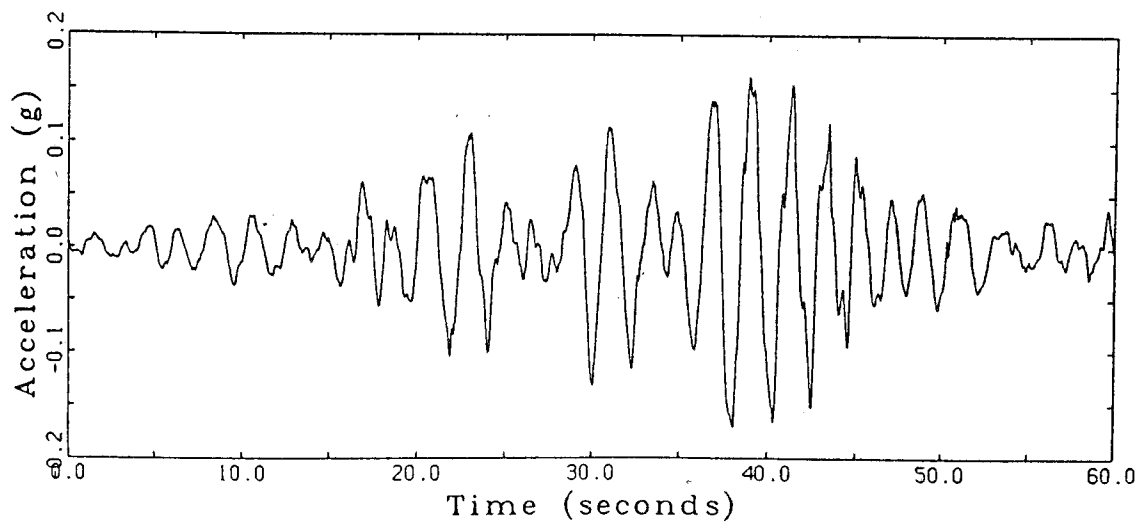


Figure 2.10: N90W Component of Acceleration Recorded at the SCT Site (First 20 seconds cutoff)

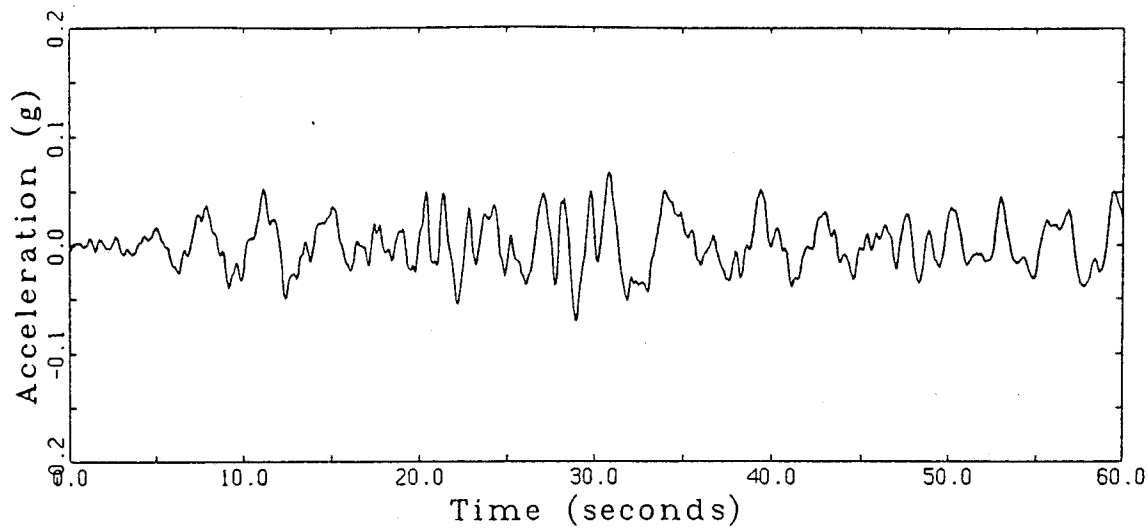


Figure 2.11: N00E Component of Acceleration Recorded at the CAO Site (First 30 seconds cutoff)

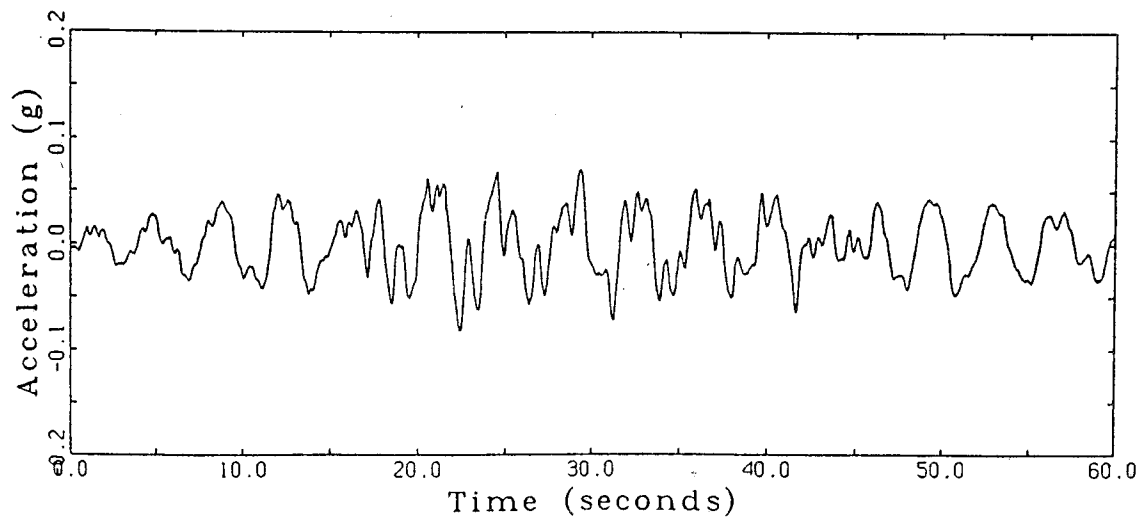


Figure 2.12: N90W Component of Acceleration Recorded at the CAO Site (First 30 seconds cutoff)

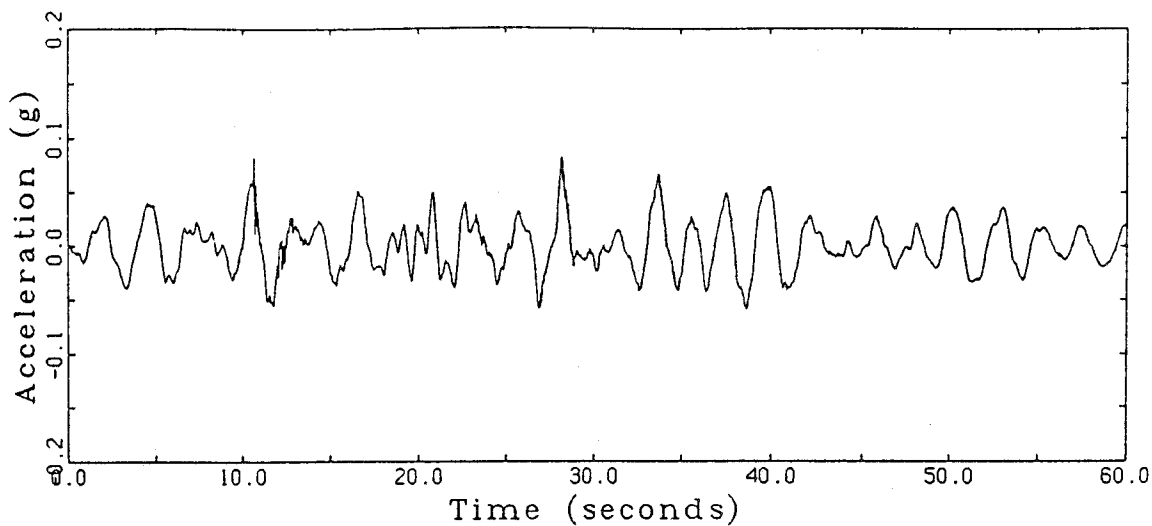


Figure 2.13: N00E Component of Acceleration Recorded at the CAF Site

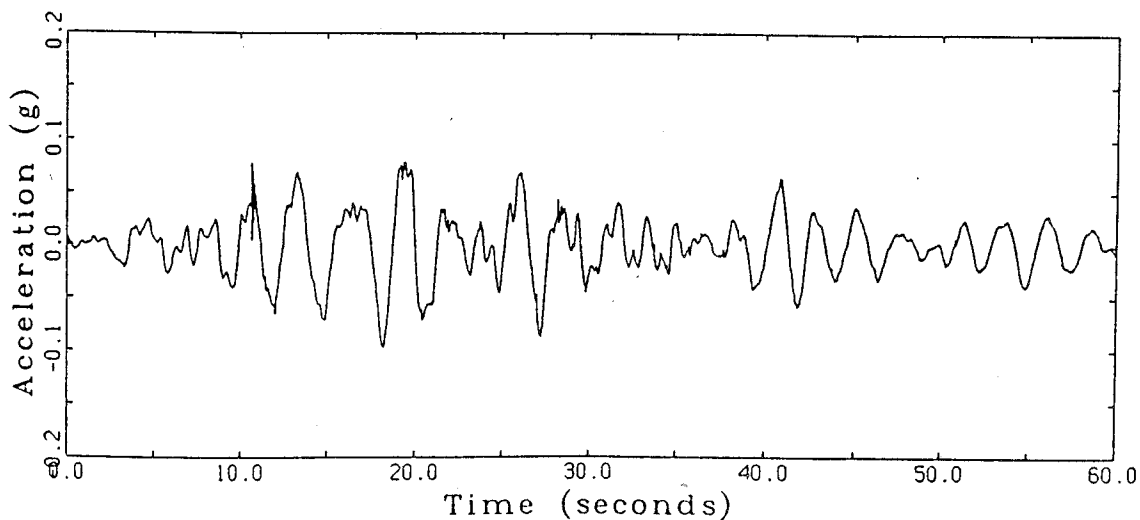


Figure 2.14: N90W Component of Acceleration Recorded at the CAF Site

relative to the lower frequency motions as the disturbance travelled from the epicenter to Mexico City.

The second observation is that the maximum acceleration levels recorded on the lakebed (Figures 2.9 to 2.14) are much higher than those recorded at hard sites in Mexico City (Figures 2.5 to 2.8). The peak horizontal accelerations recorded on the lakebed ranged from .07 to .17g while the peak horizontal accelerations recorded at hard sites ranged from .028 to .035g. The acceleration levels at the hard sites are consistent with those predicted by the attenuation relation developed by Esteva and Villaverde(1973) given by Equation 2.1. For the September

$$A_{max} = (5600 \exp(.8M)) / (R+40)^2 \quad 2.1$$

where A_{max} = maximum acceleration-cm/sec²

M = magnitude

R = hypocentral distance-km

1985, M=8.1 earthquake, equation 2.1 predicts accelerations on firm ground in Mexico City with R=300 km of .032g.

Similar conclusions may be drawn by examining the response spectra or Fourier spectra of the recorded motions. In addition, response spectra or Fourier spectra of recorded motions also provide information on the frequency content of the motions which is useful in determining the effect a motion will have on a soil deposit or a structure. For example, if a record is largely made up of motions of a particular period, the motions of that period will be amplified by sites or structures with similar periods. This amplification will appear as a peak in the response or Fourier spectra of the record.

Response spectra of the motions recorded at the three lakebed sites are shown in Figures 2.15 to 2.17. From the figures it can be seen that there is a very strong response at a period of 2 seconds in Figure 2.15, at periods of 3.5 and 4.0 seconds in Figure 2.16, and periods of 2 and 3 seconds in Figure 2.17. This type of response is indicative of resonance in the soil deposits whereby motions at the base of the deposit with periods near the natural periods of the sites are amplified as they pass through them. The input motions were amplified by the lakebed deposits because they contained energy over a broad range of periods that spanned the natural site periods. The broad band energy of the rock motions is shown by the response spectra of the CUIP and CUO1 motions in Figure 2.18. These spectra show that the rock motions contained energy in the range of periods from .75 to 2.75 seconds. The rock motions are rich in long period energy not only because of the effect of distance but also due to the presence of significant long period energy at the source caused by the source mechanism. This is shown by the peak at a period of 2 seconds in the response spectra of the epicentral motions recorded at CALE in Figure 2.19.

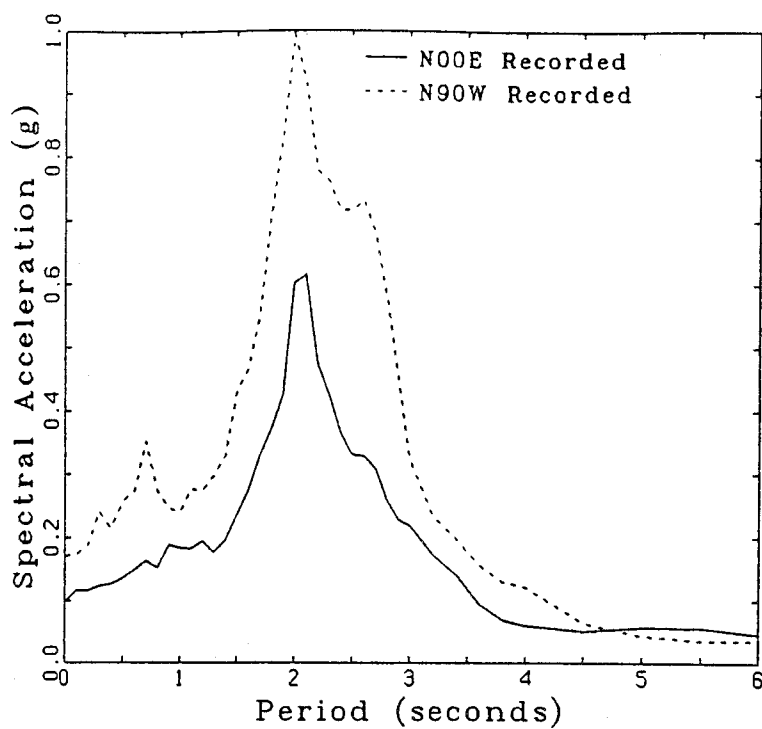


Figure 2.15: Response Spectra (5% Damping) of Motions Recorded at the SCT Site

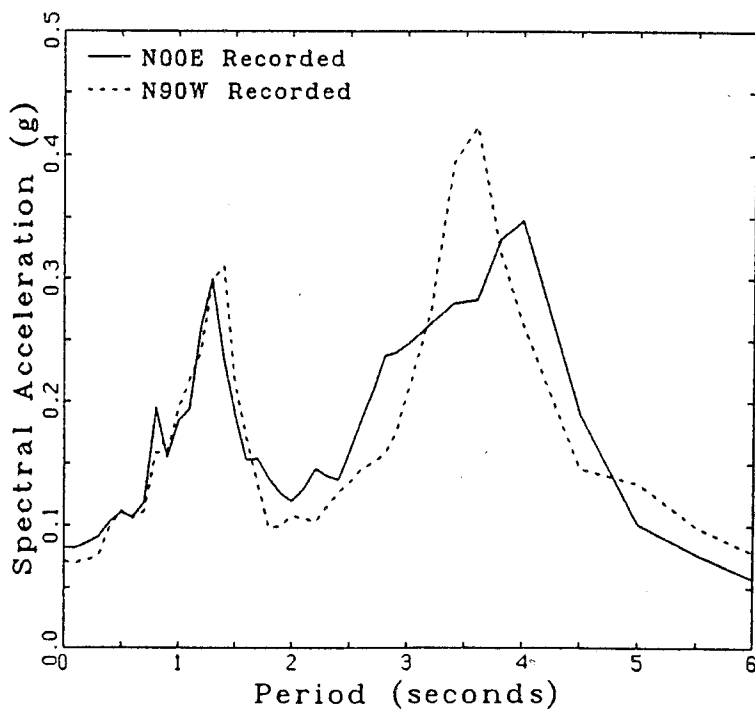


Figure 2.16: Response Spectra (5% Damping) of Motions Recorded at the CAO Site

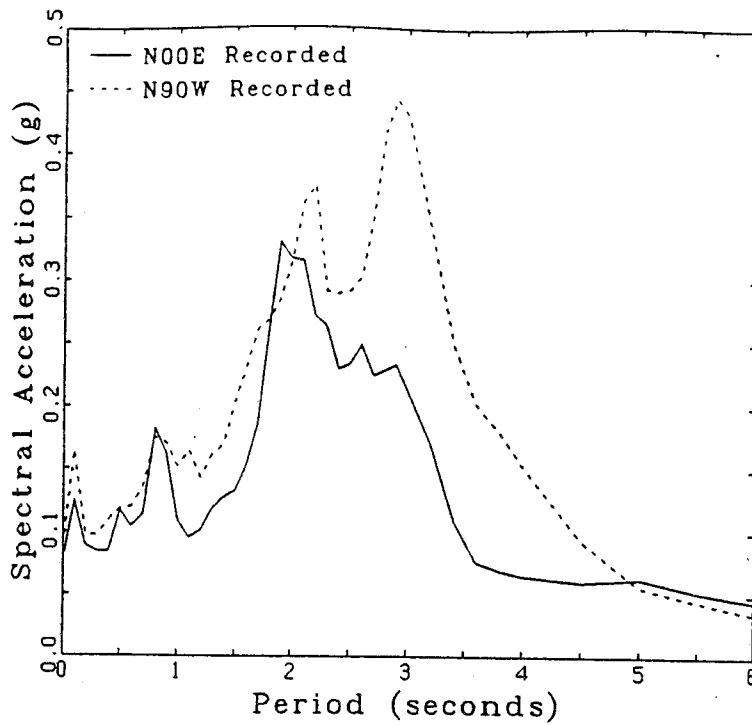


Figure 2.17: Response Spectra (5% Damping) of Motions Recorded at the CAF Site

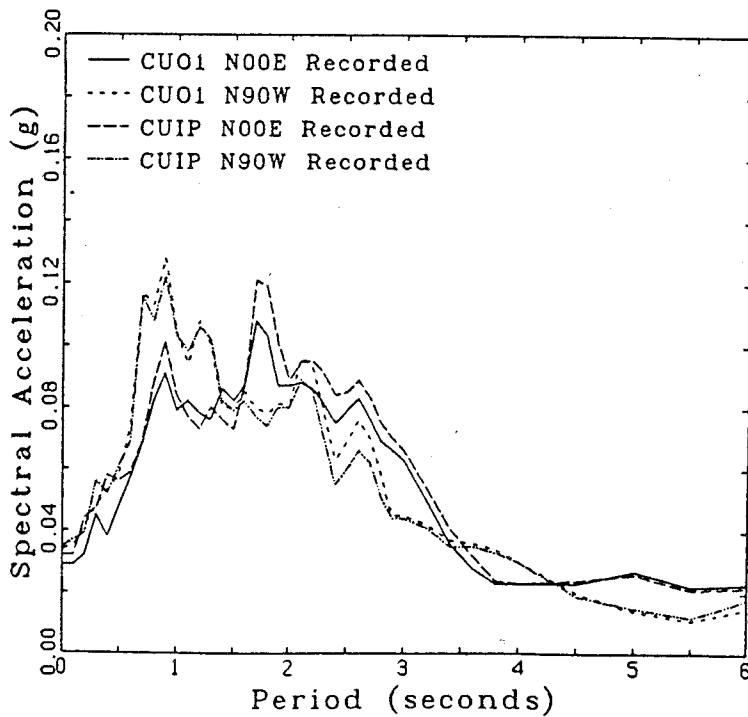


Figure 2.18: Response Spectra (5% Damping) of Motions Recorded at the CUO1 and CUIP Sites

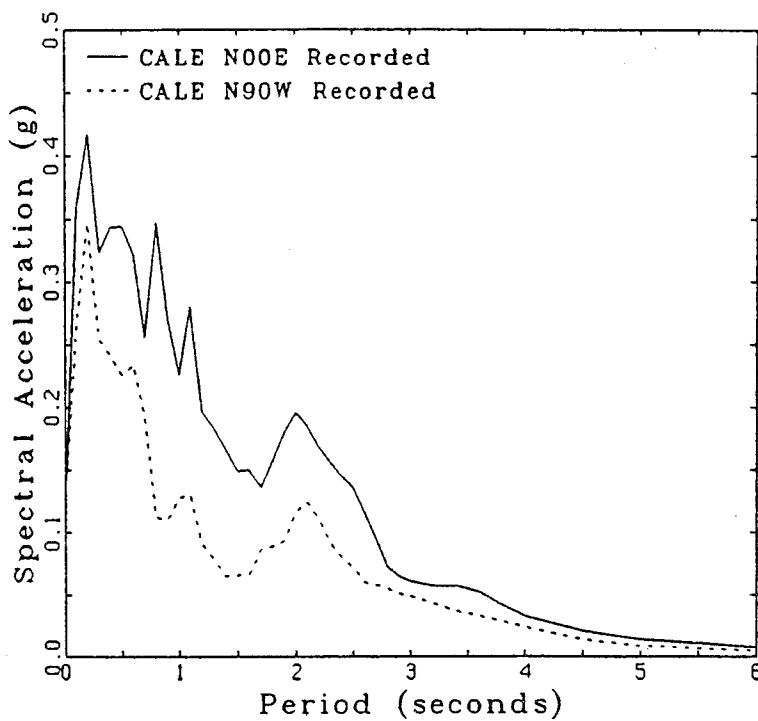


Figure 2.19: Response Spectra (5% Damping) of Motions Recorded at the CALE Site

2.2 Ground Motions and Damage in Mexico City

Because of the amplifying effect of the lakebed deposits, the accelerations on the lakebed were very high. The high accelerations combined with the extended duration of the shaking caused damage levels to structures to be much higher on the lakebed than on the surrounding firm ground during the 1985 event. The large amplification of motions that occurred during the September 1985 earthquake has occurred in past earthquakes affecting Mexico City. However, the 1985 earthquake was of much greater magnitude which resulted in larger input motions. The net effects were large peak accelerations and longer duration of strong shaking than previously. During the 1985 event and past events over 90% of the damage occurred on the lakebed (Rosenblueth, 1960, Duke and Leeds, 1959 and Mitchell et al., 1986). Figure 2.20 shows that the heavily damaged areas from three earthquakes affecting Mexico City were principally on the west side of the lakebed.

The amplified motions of long duration caused damage to a wide range of structures built on the lakebed, from 1 story homes to multistory buildings (Rosenblueth, 1960 and Mitchell et al., 1986). Damage levels on the lakebed are also higher due to resonance between the motions in the lakebed soils and the structures built on the lakebed. Resonance between lakebed motions and structures built on the lakebed has also been observed before. Duke and Leeds(1959) and Rosenblueth(1960) report that damage was most marked in 5 to 18 story buildings and that damage was greatest in 11 to 16 story buildings. In

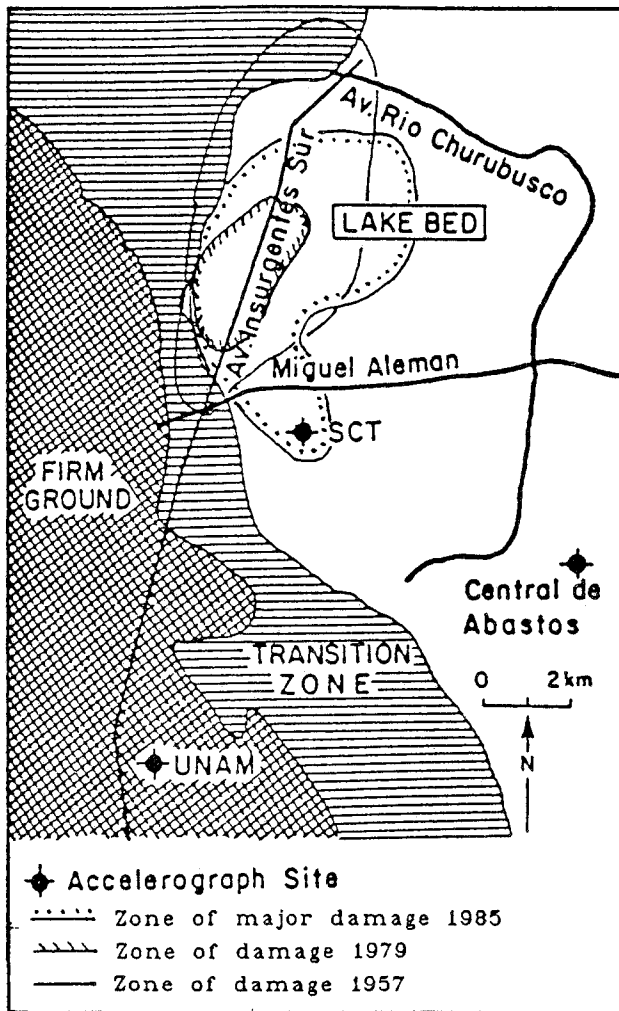


Figure 2.20: Zones of Damage in Mexico City Earthquakes

(Adapted from Mitchell et al., 1986)

hist of
eq. data

the September 1985 earthquake the highest percentage of damaged buildings lay in the 9 to 12 story range and buildings greater than 12 stories had almost as high a damage rate as shown in Figure 2.21. Although the periods of the most heavily damaged buildings were initially less than the natural periods of the lakebed sites, damage due to strong shaking increased their periods, (Mitchell et al., 1986), and brought them into the range of resonant response.

In summary structural damage in the lake zone of Mexico City was higher than the the damage usually associated with earthquakes occurring at large epicentral distances because of the following set of circumstances. The high levels of long period motion present in the epicentral motions, when combined with the large epicentral distance, caused the motions in Mexico City to be predominantly long period. The period of the Mexico City bedrock motions coincided with the natural period of the soft soil deposits located in the lakebed zone of Mexico City and the resulting resonance caused large amplification of the input motions. The amplified motions when combined with their extended duration caused high damage levels in a wide range of structural types. Resonance between the motions in the lakebed soils and the buildings themselves also contributed to the high damage levels, especially in the case of buildings more than 5 stories high.

Since it has been demonstrated that a great deal of damage can be caused by large, distant earthquakes, it is important to be able to predict the response of sites at other locations

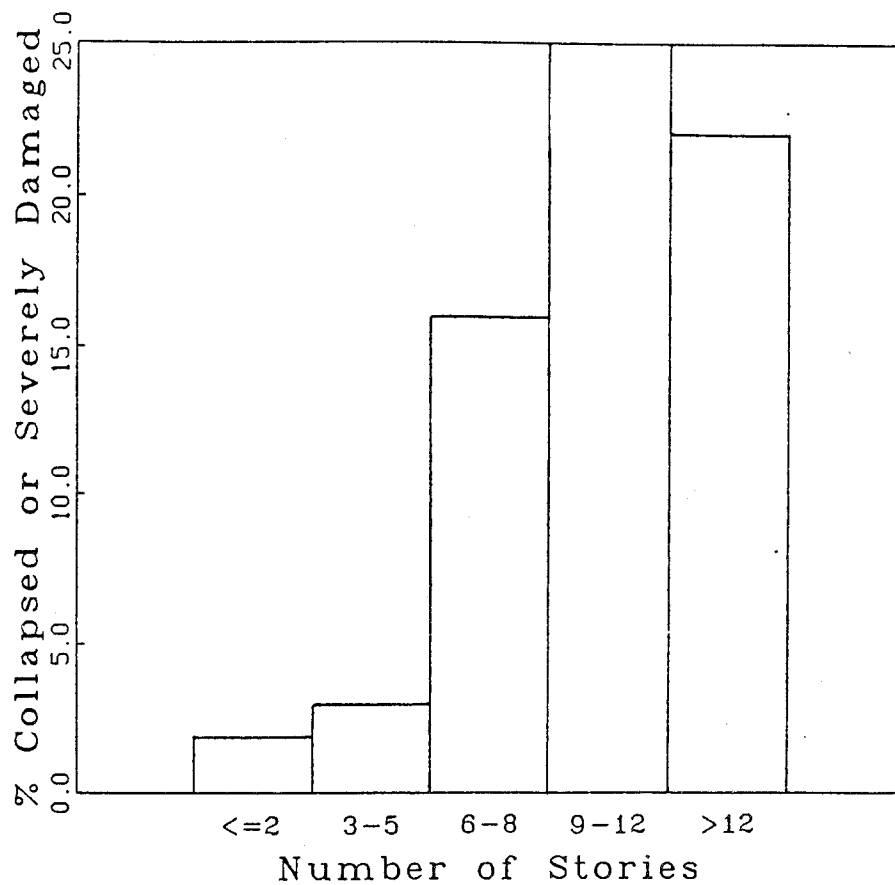


Figure 2.21: Damage Rates as a Function of Building Height

(Adapted from Mitchell et al., 1986)

around the world to these kinds of earthquakes, especially the response of sites for which previous strong motion data are not available. Therefore, current procedures for site specific analyses will be evaluated by applying them to the Mexico City sites and comparing computed and measured site responses. The first step in this process is to study the geology of Mexico City and establish the dynamic properties of the underlying soils.

3.0 GEOLOGY AND PROPERTIES OF MEXICO CITY SOILS

3.1 Location

Mexico City is located at an elevation of 2240 m in the southwestern end of the Valley of Mexico. The Valley forms the south end of the highest part of the Mexican Plateau which is bounded on the east by the Sierra Nevada Mountains, on the west and north by the Sierra Madre Occidental, on the south by the Ajusco Range and on the north by the Pachuca Range as shown in Figure 3.1.

The city was originally constructed on an island in Lake Texcoco but large population growth has caused the city to grow on to the lakebed and the surrounding hills of the Sierra de la Cruces. Construction on the lakebed was made possible by a drainage program initiated in 1789 (Mitchell et al., 1986).

3.2 Geologic History of the Valley of Mexico

The basin of the Valley of Mexico formed in Pliocene times with the growth of the surrounding mountains by volcanic activity (Zeevaert, 1953). By the late Pliocene, volcanic activity had ceased. In the semi-arid climate during the subsequent Pleistocene period, eroded materials were not carried away and alluvial fans formed in the basin. The Tarango formation which underlies Mexico City, as shown in Figure 3.2, formed during this period. During the early Pleistocene the

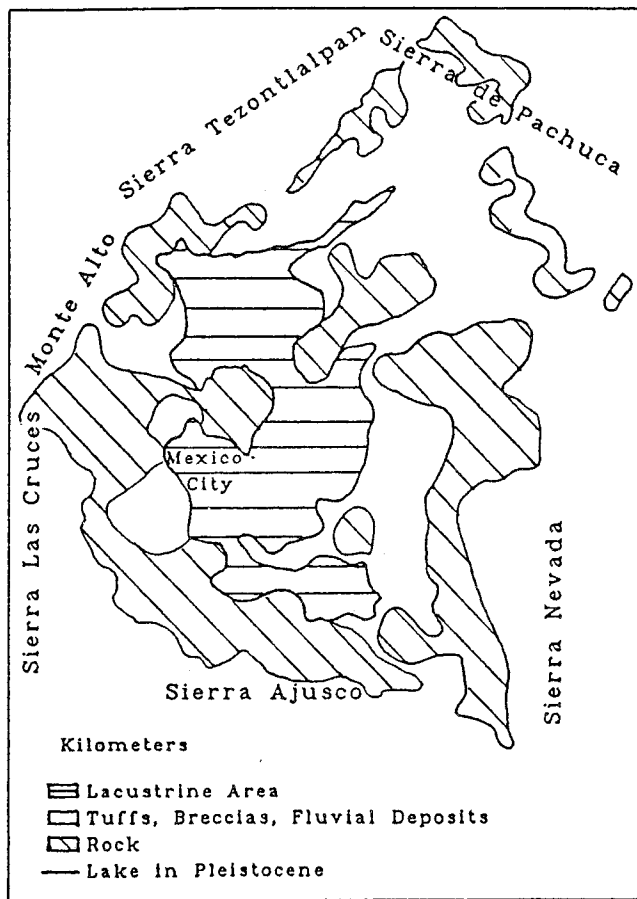


Figure 3.1: The Basin of the Valley of Mexico

(Adapted from Zeevaert, 1953)

climate became colder and damper, causing the formation of glaciers on the mountains. The glaciers, combined with runoff, caused the the formation of two large valleys with their heads in the Pachuca Hills and ending in the basin of Almuto Amacuzoc (Marsal and Mazari, 1959). Another cycle of volcanic activity cut off the southern drainage in the valleys which allowed alluvial and lacustrine deposits of silt and sand to be laid down, as well as lenses of air transported volcanic ash (Marsal, 1959). These materials continued to collect throughout Pleistocene times and are still being deposited today by streams coming out of the mountains surrounding the Valley of Mexico.

The geologic history of the central area of Mexico City is similar to that of the valley except that in Wisconsin times Lake Texcoco formed causing the purely lacustrine sediments of the Tacubaya formation (Figure 3.2) to be laid down. The layers of calcium carbonate or caliche present in the Tacubaya formation (Figure 3.2) formed during periods when the lake dried up. The waters of the lake were rich in silica from nearby volcanic eruptions. This allowed the growth of siliceous diatoms which form 55 to 65% of the clays of the Tacubaya formation (Mesri et al., 1975). The Becerra formation (Figure 3.2) above the the Tacubaya deposits are of Holocene age and another period of lake disappearance is indicated by the presence of caliche.

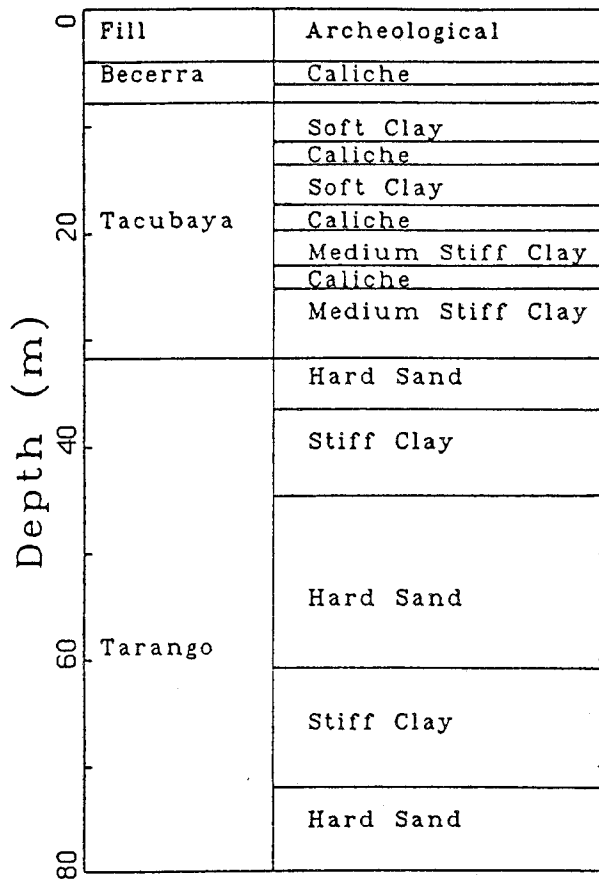


Figure 3.2: Geological Sequence and Soil Depsoits Below the Central Area of Mexico City

(Adapted from Zeevaert, 1953)

3.3 Geology of Mexico City

Because Mexico City is in a valley, the soil profile varies with the location of the site. To account for this variation in stratigraphy, the city has been divided into 3 zones as shown in Figure 3.3. The zones of Figure 3.3 are shown in cross section in Figure 3.4. Figure 3.4 shows that the surface layer over much of Mexico City consists of fill ranging in thickness from 2 to 8 m. The fill is thickest in the central area of the city around the Plaza de la Republica. Below the surface layer is an upper layer of compressible clay 15 to 30 m thick. The compressible upper clay is underlain by 3 m of dense cemented silt and sand as shown in Figure 3.4. This layer forms the base of most of the piled foundations in the lake zone. Beneath the area surrounding the Plaza de la Republica, where the cross sections of Figure 3.4 intersect, the 3 m thick dense silt and sand layer overlies a lower layer of stiff clay 4 to 14 m thick. Beneath the lower clay layer are deep dense deposits of sand and gravel extending to bedrock. Away from the Plaza de la Republica the upper clay layer rests directly on the dense deposits of sand and gravel as shown in Figure 3.4. The total thickness of the lacustrine and alluvial deposits at the deepest point is estimated to be 1000 m (Marsal and Mazari, 1959). The water table in the lake zone ranges from 2 to 3 m below ground surface (Marsal, 1959).

In the transition zone of Mexico City (Figure 3.3) volcanic flow and alluvial materials of low compressibility are found within 40 m of the surface. Also, deposits of alluvial fan

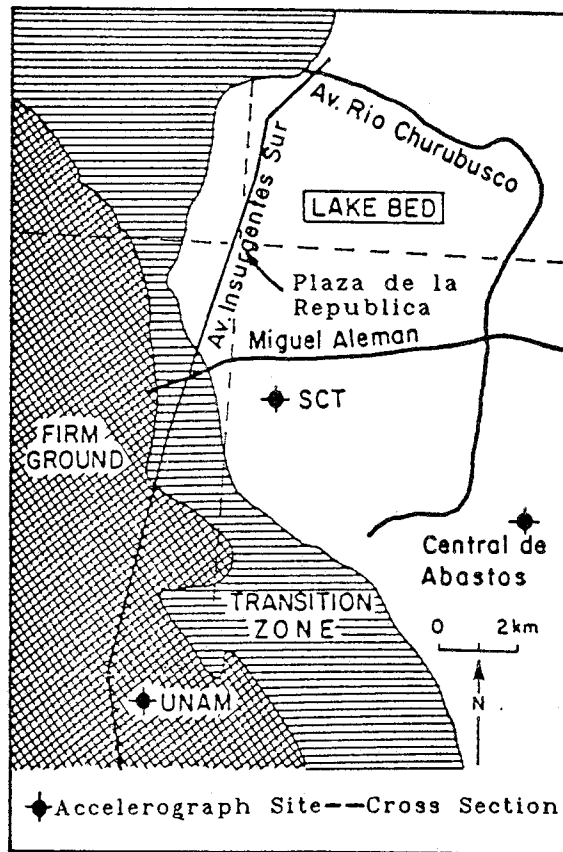


Figure 3.3: The Subsoil Zones of Mexico City
 (Adapted from Mitchell et al., 1986)

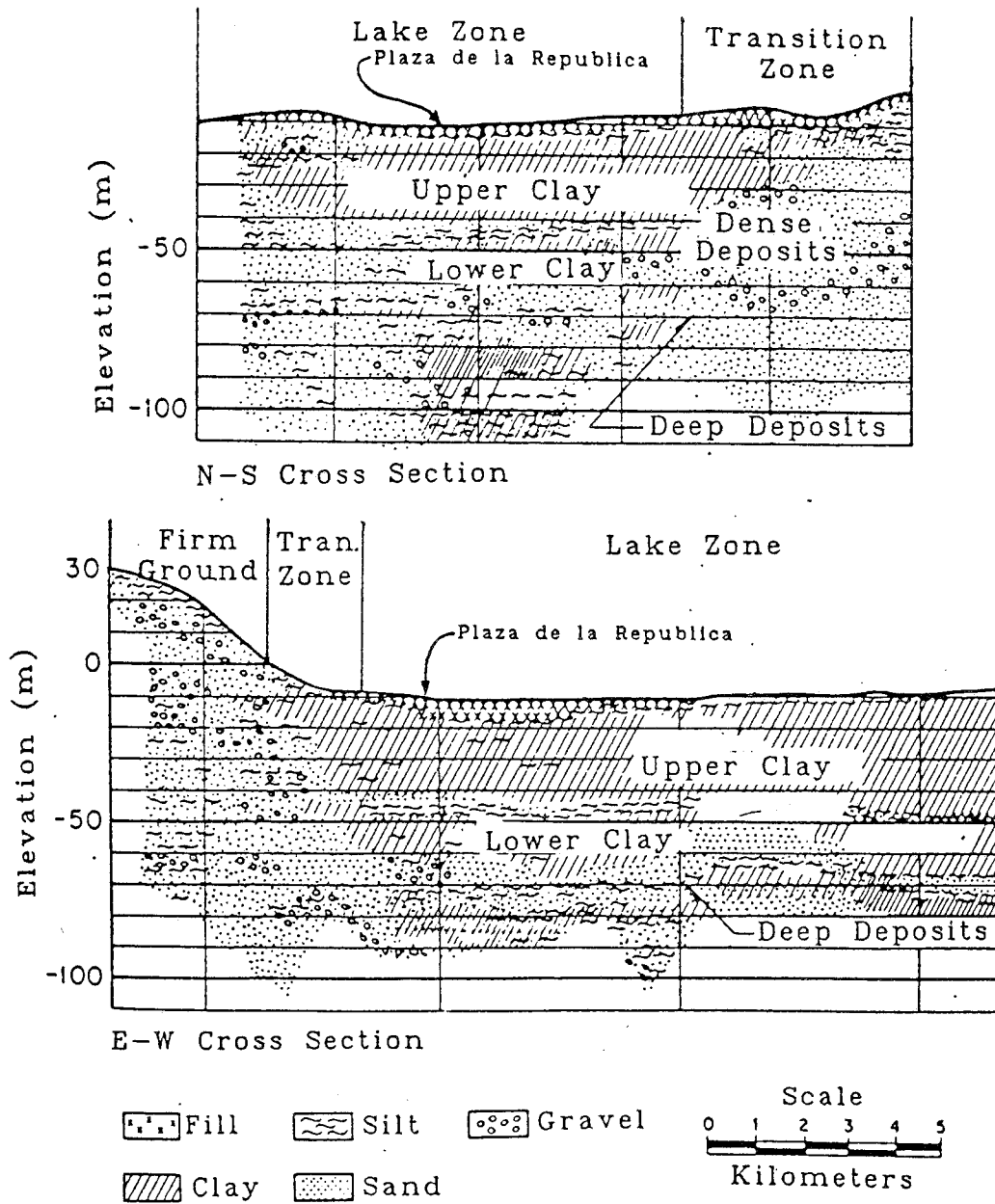


Figure 3.4: Cross Sections Through Mexico City

(Adapted from Marsal and Mazari, 1959)

materials are often interspersed with the silty clays, which are stiffer than the clays contained in the lake zone (Rosenblueth, 1960).

The firm or hilly zone of Mexico City is built on the southern and western slopes of the Sierras and the subsoil consists of volcanic tuffs, conglomerates and cemented or dense sands (Rosenblueth, 1960).

3.4 Index Properties of Mexico City Soils

The most striking material property of the upper clays and silty clays is their high water content, up to 400%. This in turn causes them to be highly compressible with settlements in the central area of the city of up to 9 m. The main cause of the settlement was the pumping of water from the clays beneath Mexico City (Marsal, 1959). During the 1950's restrictions were placed on the pumping of water and the settlement rate was reduced from a high of 50 cm/year around 1950 to 10cm/year in 1975 (Marsal, 1975).

Averaged index properties for the clays of the Tacubaya Formation are shown in Table 3.1. The clays of the Tacubaya Formation are heterogeneous, with water contents ranging from 50 to 300% in the same deposit. The clays are normally consolidated to lightly overconsolidated. Consolidation tests performed on Mexico City clay show an overconsolidation ratio of between 1.5 (Mesri et al., 1975) and 4 (Lo, 1962). The overconsolidation was caused by a lowering of the porewater pressure by pumping, followed by a reduction in

Property	Average Value
Density of Solids	2.404
Initial Void Ratio	7.1
Natural Water Content	289.1
Liquid Limit	295.3
Plastic Limit	86.5
Plasticity Index	208.7
Shear Strength kPa	80.4

Table 3.1: Average Values of Properties of the Clays of the Tacubaya Formation

(Adapted from Marsal and Mazari, 1959)

the pumping rate which allowed the porewater pressure to increase.

The friction angle of the clay at a depth of 8 m is reported by Lo(1962) as 47° . Lo also reports a value determined by Marsal and Rasines(1960) of 43° . Mesri et al.(1975) suggest that it is the interlocking nature of the diatoms that make up the clay that cause it to have a high friction angle despite its high compressibility.

3.5 Dynamic Properties of Mexico City Lakebed Deposits

The subsoil of the central area of Mexico City consists of compressible clays overlying dense sands and stiff clays. Romo and Seed(1986) modelled three sites, the CAF, CAO, and SCT sites as homogeneous clay deposits overlying the dense sand layer. The site models are shown in Figure 3.5. The values of initial modulus were obtained from $G=\rho V_s^2$ where V_s was obtained from the Fourier Spectra of the recorded motions using $V_s=4H_f/(2n-1)$,

where H is the thickness of the deposit, f is the peak frequency of the Fourier Spectrum, and n is the mode number (Romo and Seed, 1986). The mode number of the peak frequency was taken as 1. If the site is behaving elastically the other peaks will be related to the first by $1/(2n-1)$. These computed moduli compared well with the moduli from resonant column and cyclic triaxial tests (Romo and Jaime, 1986).

In their 1986 study Romo and Seed used laboratory data from Leon et al. (1974) and Romo and Jaime (1986) relating shear modulus and damping to shear strain; the range of the laboratory data is shown in Figure 3.6. For comparison the typical modulus reduction and damping curves suggested by Seed and Idriss (1970) for clay are also shown in Figure 3.6. The damping shear strain relation for Mexico City clay is similar to the suggested relation for strains less than .001% but at greater strains Mexico City clay exhibits less damping. Mexico City clay has a very different modulus reduction curve from that of a typical clay; retaining 95% of its original stiffness until .1% strain while the typical clay has only 15% of its original stiffness at the same strain. The differences between the two sets of curves in Figure 3.6 indicate the dangers inherent in relying on generalised soil properties. Whenever possible site dependent properties should be determined.

Dynamic analyses of the responses of the Mexico City sites will be conducted using the site models developed by Romo and Seed (1986) and the soil properties described above and shown in Figure 3.6.

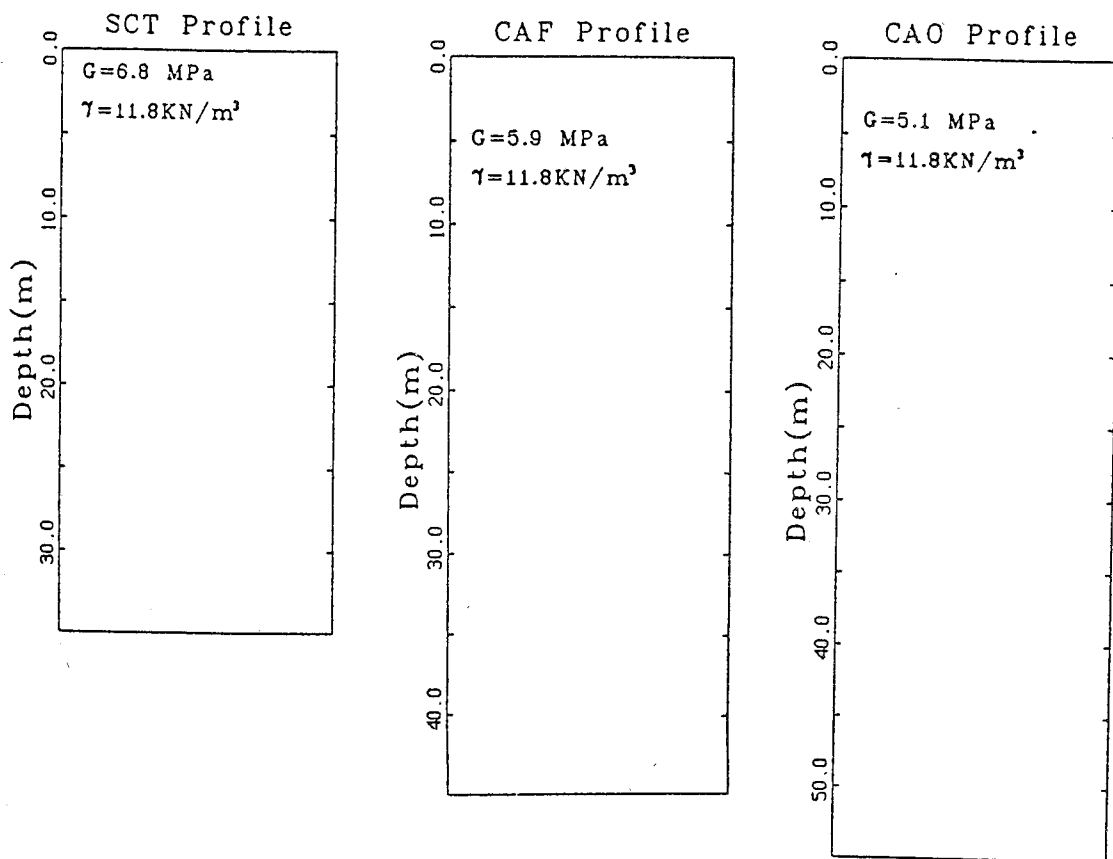


Figure 3.5: Site Models for the SCT, CAF and CAO Sites

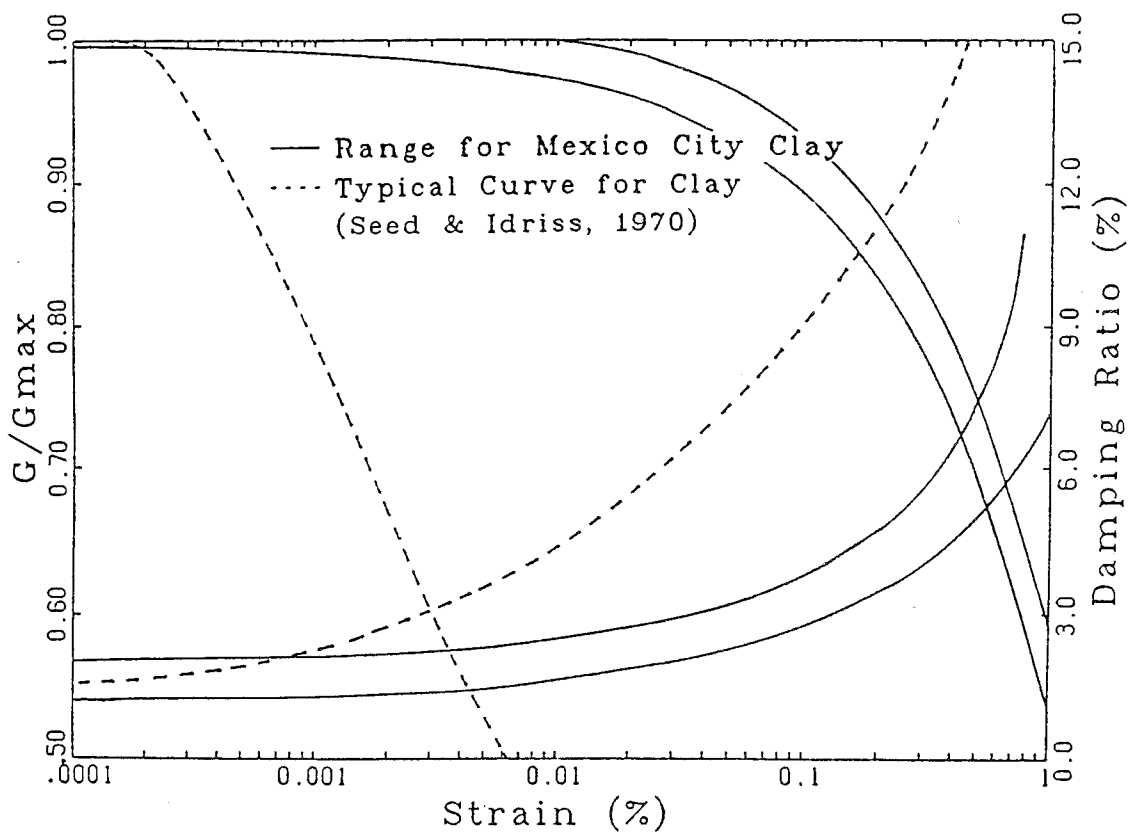


Figure 3.6: Range in Shear Dependent Moduli and Damping for Mexico City Clay Compared to the Shear Dependent Modulus for a Typical Clay

4.0 ANALYSES OF MEXICO CITY SITES USING REPRESENTATIVE INPUT MOTIONS

Input motions for dynamic analyses of the Mexico City sites can be obtained by two methods; the appropriate scaling of recorded motions from previous earthquakes or by using the recorded rock outcrop motions. In this chapter, dynamic analyses will be described using input motions obtained by scaling motions from the 1952 Kern County earthquake following the procedures of Romo and Seed(1986). In the following chapter, analyses will be described using the motions recorded at the CUO1 and CUIP sites as input.

4.1 Selection of Representative Input Motions

In their 1986 analysis Romo and Seed used an appropriately scaled version of the 1952 Kern County earthquake recorded at the Athaeneum on the Pasadena Campus of Cal Tech. The record was scaled to have a maximum acceleration of .035g and a predominant period of about 2 seconds. The response spectra of the scaled and unscaled records are shown in Figure 4.1. As can be seen, a substantial shift in predominant period was required, from .9 seconds to 2 seconds. This shift was indicated by the predominant period of the 1985 earthquake motions. The predominant period indicated by correlations developed by Seed et al. (1969) between predominant period, distance from the causative fault, and magnitude is of the order of 1.5 seconds.

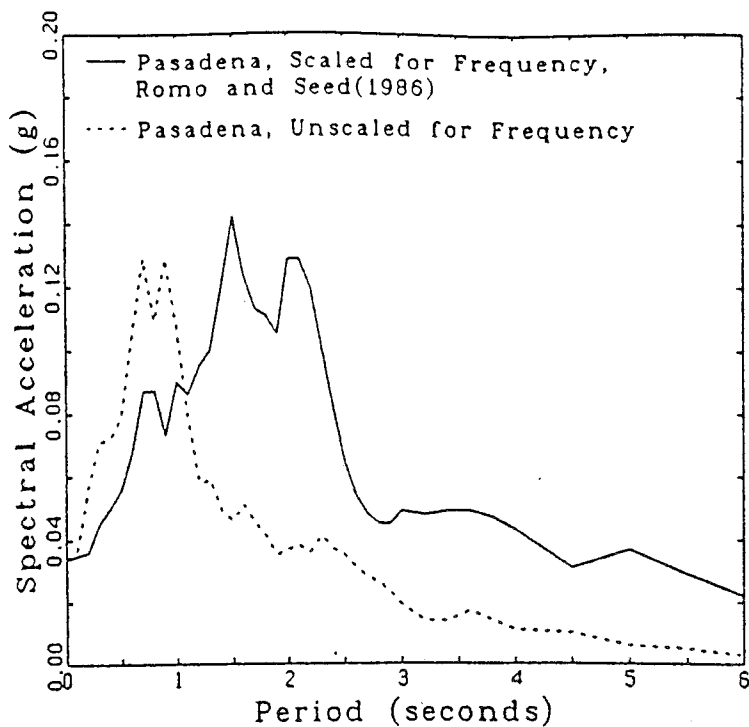


Figure 4.1: Response Spectra (5% Damping) of Pasadena Record Showing Effect of Frequency Scaling

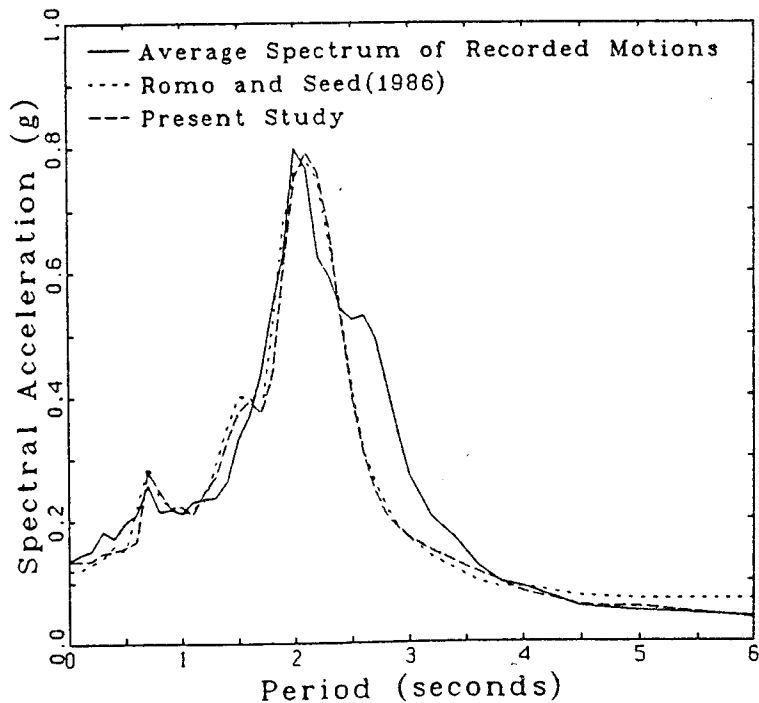


Figure 4.2: Response Spectra (5% Damping) of Computed Motions and Average Response Spectrum of the Recorded Motions at the SCT Site

4.2 Results of Analyses at the SCT Site

The response spectra computed for the SCT site both in this study and by Romo and Seed(1986), using the modified Pasadena record as input, are shown in Figure 4.2. Also shown in the figure is the average of the spectra of the two components of motion recorded at the SCT site. The figure shows that the spectrum of the computed motions matches the average spectrum of the recorded motions very well. The large response at a period of 2 seconds is due to the coincidence of the predominant period of the input motion, visible as the peak at 2 seconds in the input spectrum (Figure 4.1), and the natural period of the site, which causes resonance to occur. The natural periods of the site are computed from the eigen values of the site using the strain-softened soil stiffness that exists during shaking. If the site is behaving in an approximately linear fashion, the peaks in the response spectra corresponding to the natural periods of the site will be related by $1/(2n-1)$. The second mode of the site is also visible as a peak at 0.7 seconds. Since this second mode is related to the first by $1/(2n-1)$ it may be concluded that the site response is close to linear. The linearity of the response of the soil deposit is caused by the limited strain softening that takes place in Mexico City soils during shaking. The computed strains at the mid-depth of the deposit are about .2%, which corresponds to a modulus reduction of only about 20% (Figure 3.6).

4.3 Results of Analyses at the CAF Site

The computed response spectrum for the CAF site, using the modified Pasadena record as input, as well as the average of the response spectra of the two components of motion recorded at the site, is shown in Figure 4.3. The match is reasonable, although a better match can be obtained by scaling the input motion to a maximum acceleration of .045g, rather than .035g, as shown in Figure 4.4. The response of the CAF site is less than that of the SCT site because the predominant period of the input motion, which is around 2 seconds, and the natural period of the site, computed as 2.9 seconds, do not coincide and thus resonance does not occur.

4.4 Results of Analyses at the CAO Site

The response spectra of the motions computed at the CAO site in this study, and by Romo and Seed(1986), using the modified Pasadena record as input are shown in Figure 4.5. The average spectrum of the components of motion recorded at the CAO site is also shown in Figure 4.5. The match between the spectra of the computed and average recorded motions is reasonable but unlike the CAF site, scaling the input motions does not cause a better match since the computed response becomes greater than the recorded response at a period of 2 seconds. The peaks in the spectra of the computed and recorded motions at 3.8 and 1.3 seconds are due to the site vibrating in its first and second modes respectively.

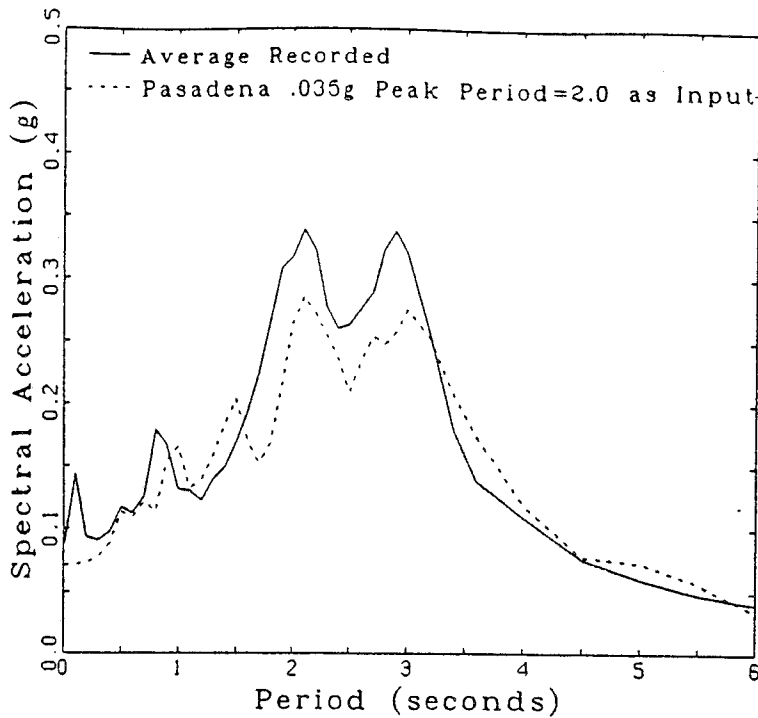


Figure 4.3: Response Spectra (5% Damping) of Computed Motions Using the Modified Pasadena Record Scaled to .035g and Average Response Spectrum of the Recorded Motions at the CAF Site

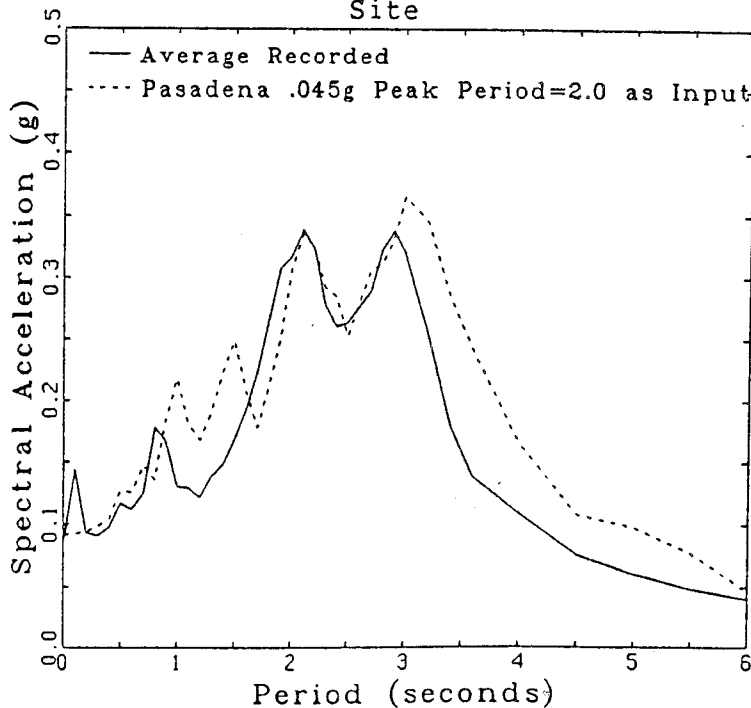


Figure 4.4: Response Spectra (5% Damping) of Computed Motions Using the Modified Pasadena Record Scaled to .045g and Average Response Spectrum of the Recorded Motions at the CAF Site

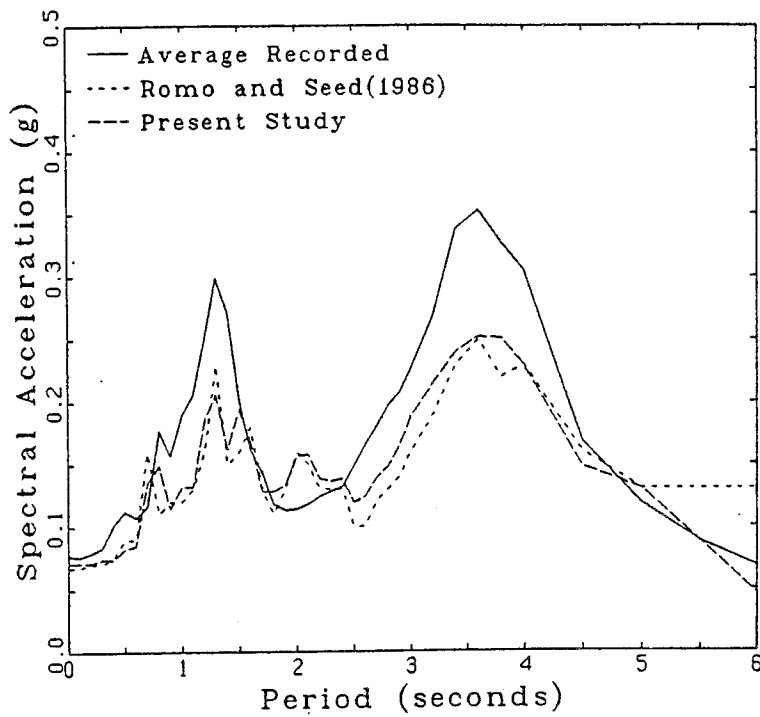


Figure 4.5: Response Spectra (5% Damping) of Computed Motions and Average Response Spectrum of the Recorded Motions at the CAO Site

4.5 Summary of Results Using the Modified Pasadena Record as Input

The above analyses show that if recorded motions and site specific soil properties are available, it is possible to modify an input motion so that the average spectrum of the recorded motions can be matched. The importance of using site specific soil properties is shown in Figure 4.6. The figure shows the response spectra of the motions computed at the SCT site using the modified Pasadena record as input, and the range of modulus and damping curves for Mexico City clay shown in Figure 3.6. The computed peak acceleration stays relatively constant but the peak spectral response varies by 20%. The response spectrum of the motions computed using the modified Pasadena record and the modulus reduction curve for a typical clay (Figure 3.6) is also shown in Figure 4.6. The response is much lower, almost negligible; the much greater strain softening occurring during shaking has so increased the period of site response that the mismatch between site and input periods precludes any resonance effects. Therefore modulus reduction and damping relationships should be site specific and typical relations should not be used. It is clear that changes in stiffness of the Mexico City clays due to strain softening were a key factor in the resonant response of the SCT site.

The importance of the modification of the predominant period of the Pasadena motion on site response is shown in Figure 4.7. The figure shows the response spectra of the motions computed at the SCT site using the Pasadena record

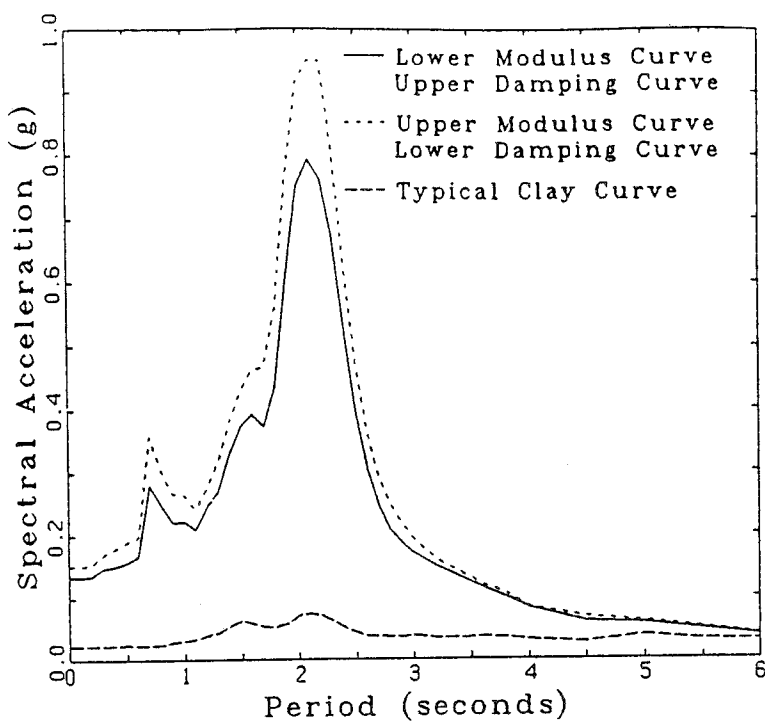


Figure 4.6: Response Spectra (5% Damping) of Computed Motions at the SCT Site Showing the Effect of Soil Properties

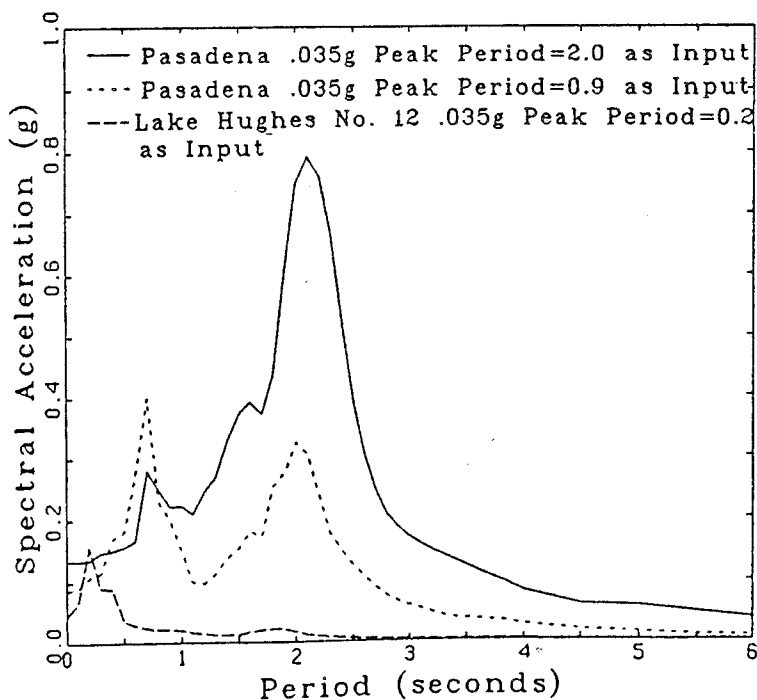


Figure 4.7: Response Spectra (5% Damping) of Computed Motions at the SCT Site Showing the Effect of the Period Content of the Input Motion

scaled for period and maximum acceleration, and scaled for maximum acceleration only. If the predominant period is not scaled, the response is much less because resonance does not occur. Resonance does not occur because the natural period of the site is 2.1 seconds and the predominant period of the unscaled input motion is .9 seconds, as shown by the peak in the spectrum of the unmodified Pasadena record at .9 seconds in Figure 4.1. The importance of the frequency content of the input motion on site response is further emphasized when an input motion with a predominant period of .2 seconds, such as the Lake Hughes No. 12 record of the 1971 San Fernando earthquake, with a scaled maximum acceleration of .035 g is used as input, as shown in Figure 4.7. The computed response for the SCT site is very low because the input motions contain very little energy at the periods of the first or second modes of site response.

Since the frequency content of the input motion is a function of the magnitude, source mechanism, and epicentral distance the results shown in Figure 4.7 illustrate the importance of considering these parameters when selecting input motions for use in dynamic analyses. A series of input motions should be selected that bracket the expected range of these parameters for the site in question in order to provide realistic input for the analysis of the response of a site to earthquake motions.

5.0 ANALYSES OF MEXICO CITY SITES USING ROCK OUTCROP MOTIONS AS INPUT

Having calibrated the present analyses by matching the analyses of Romo and Seed(1986), the motions recorded at hard sites in Mexico City during the 1985 Mexico earthquake will be used as input motions at the three Mexcio City sites analysed in Chapter 4.0. The peak horizontal accelerations at the hard CUO1 and CUIP sites are as follows: CUO1-N90W=.034g, CUO1-N00E=.028g, CUIP-N90W=.035g, and CUIP-N00E=.032g. The records were shown in Figures 2.5 to 2.8 and the response spectra of the motions were shown in Figure 2.18.

5.1 Results of Analyses at the SCT Site

The response spectra of the motions computed for the SCT site, using the N90W component of the CUO1 and CUIP records, are shown in Figure 5.1. Also shown in the figure is the response spectrum of the recorded motions in the N90W direction. The spectrum of the computed motions has the same general shape as the spectrum of the recorded motions but underestimates the response at all periods.

The response spectra of the computed motions at the SCT site, using the N00E component of the CUO1 and CUIP records as input, are shown in Figure 5.2. Also shown in the figure is the response spectrum of the recorded motion in the N00E direction. The match between the spectra of the recorded and computed motions in the N00E direction is much better than it was in the

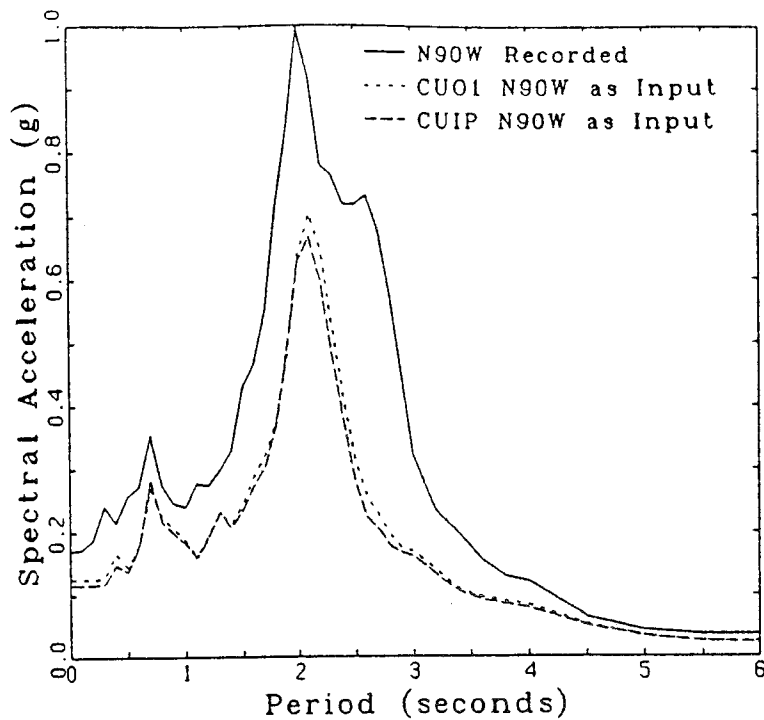


Figure 5.1: Response Spectra (5% Damping) of Recorded and Computed Motions in the N90W Direction at the SCT Site

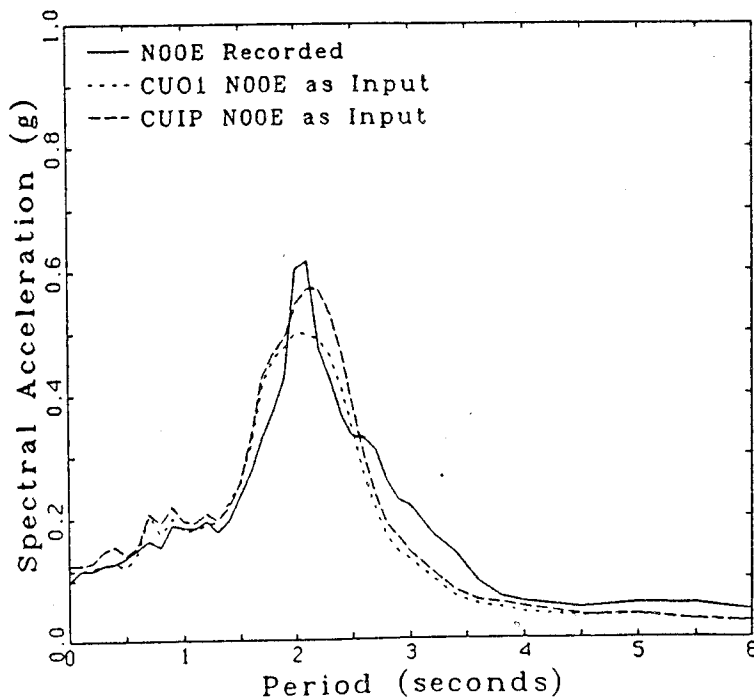


Figure 5.2: Response Spectra (5% Damping) of Recorded and Computed Motions in the N00E Direction at the SCT Site

N90W direction (Figure 5.1).

An examination of Figures 5.1 and 5.2 shows that the recorded motion at the SCT site has a directional bias. The peak response in the N90W direction is 1g, while in the N00E direction the peak response is .65g. On the other hand the computed responses show very little bias. The peak responses computed in the N90W direction are .7 and .67g, while in the N00E direction the computed peak responses are .5 and .56g. The lack of directionality in the computed motions is due to the fact that the input CUO1 and CUIP motions show little or no bias as shown by the similarity of their response spectra (Figure 2.18).

This difference in directionality between the lakebed SCT site and rock outcrop sites is also shown in Figures 5.3 and 5.4. The figures show the acceleration path followed during the earthquake. At the SCT site (Figure 5.3) it can be seen there is a strong bias in the N-E direction while at the CUIP site (Figure 5.4) there is little bias in the motions.

If the N90W components of the CUIP and CUO1 motions are scaled from .035g to .095g a good match between the spectra of the computed and recorded motions is obtained as shown in Figure 5.5. Not only does the scaling cause the peak spectral responses to match, but the shoulder in the recorded spectrum to the right of peak response is also reproduced. The fact that a better match is obtained by scaling the input motions indicates that the motions may be amplified directionally as they travel across the lakebed or as they enter the dense sands from below.

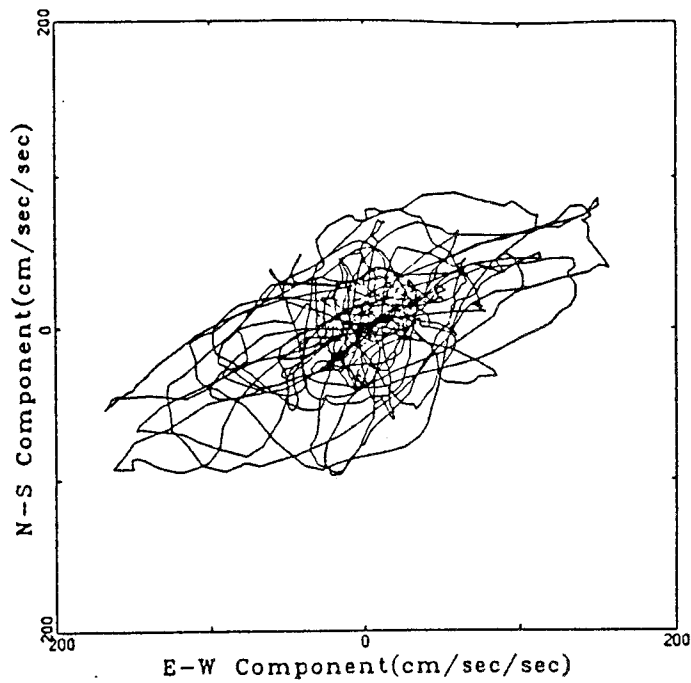


Figure 5.3: Acceleration Path at the SCT Site during the 1985 Earthquake

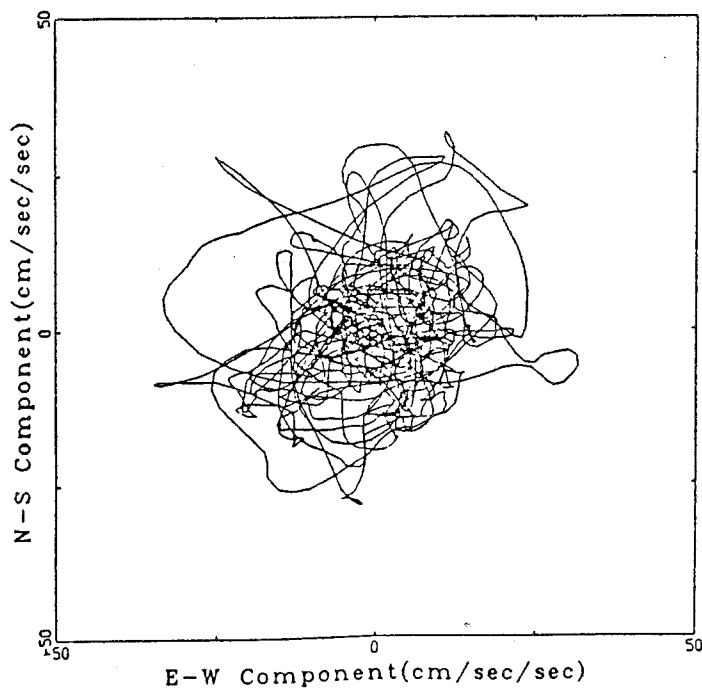


Figure 5.4: Acceleration Path at the CUIP Site during the 1985 Earthquake

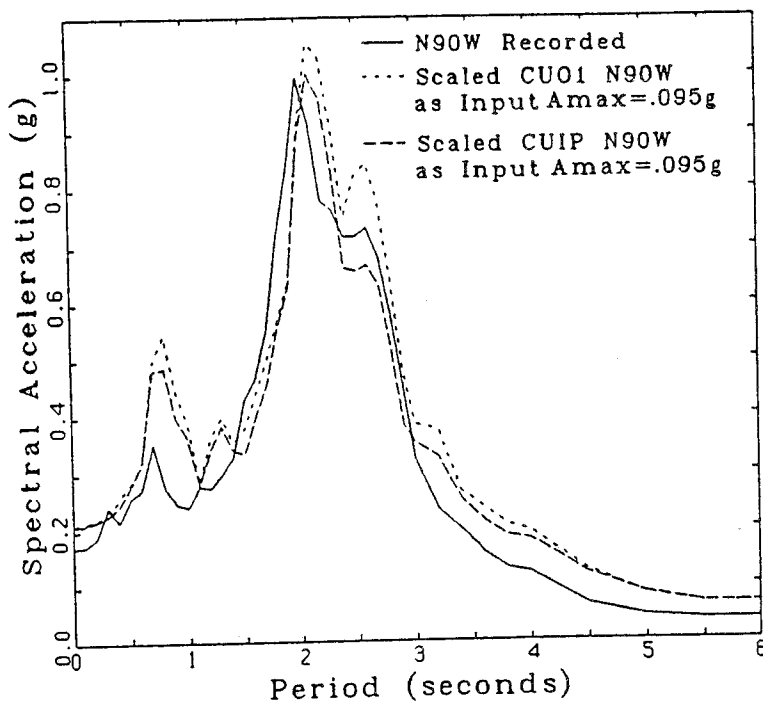


Figure 5.5: Response Spectra (5% Damping) of Recorded and Computed Motions in the N90W Direction at the SCT Site Using Scaled Input Motions

In the above analyses the motions have been input at the base of the soft clay deposits. To explore the effects of these motions being input at bedrock, a deep site model was developed using data from Herrera et al.(1965). Herrera et al.(1965) used a shear wave velocity of 1000 m/sec for the dense sands and suggested a range of depths of 400 to 1000 m. For this study a depth of 500 m was chosen. Because the sand has the properties of soft rock, flat modulus reduction and damping curves were required, and it was deemed appropriate to use the same modulus reduction and damping curves as for the clay.

The results of the analyses using the deep site model and the N90W component of the CUIP motions as input are shown in Figure 5.6. The match between the spectra of the recorded and computed motions in the N90W direction is very good. The shoulder to the right of the peak response is reproduced and the spectra match at all periods. The maximum acceleration at the top of the sand was .094g which is roughly equal to the value of .095 g used in the analyses with scaled input motions. When the deep site model is used for computing the motions in the N00E direction the computed motions greatly overestimate the recorded motions. These results suggest that the differences in the field responses in the N00E and N90W directions is due to factors outside the scope of 1-D analysis. Either the input motions at the base of the clay layer have strong directionality, acquired on passage from the rock walls into the valley deposits, or the recorded surface motions include surface waves on the lakebed in addition to the motions from vertically

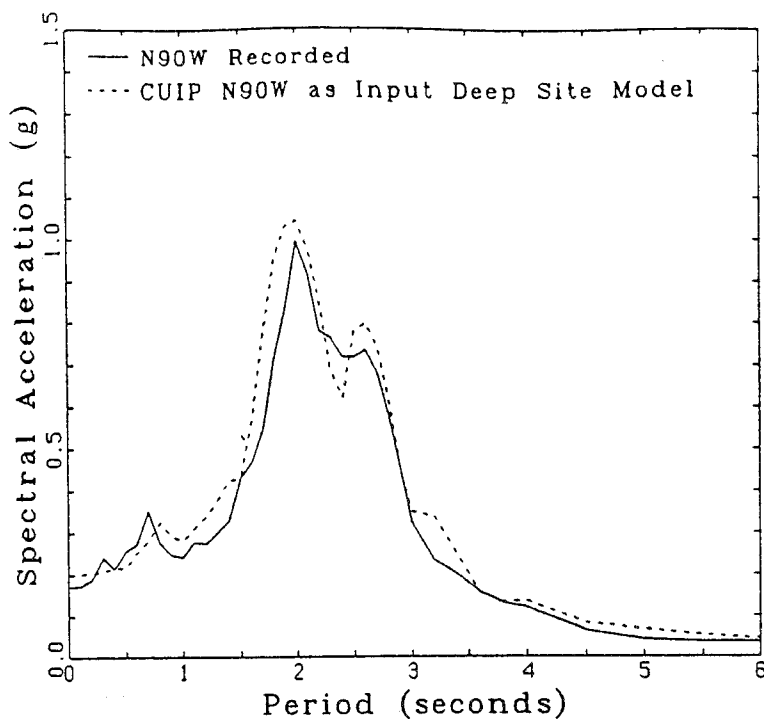


Figure 5.6: Response Spectra (5% Damping) of Recorded and Computed Motions in the N90W Direction at the SCT Site Using a Deep Site Model

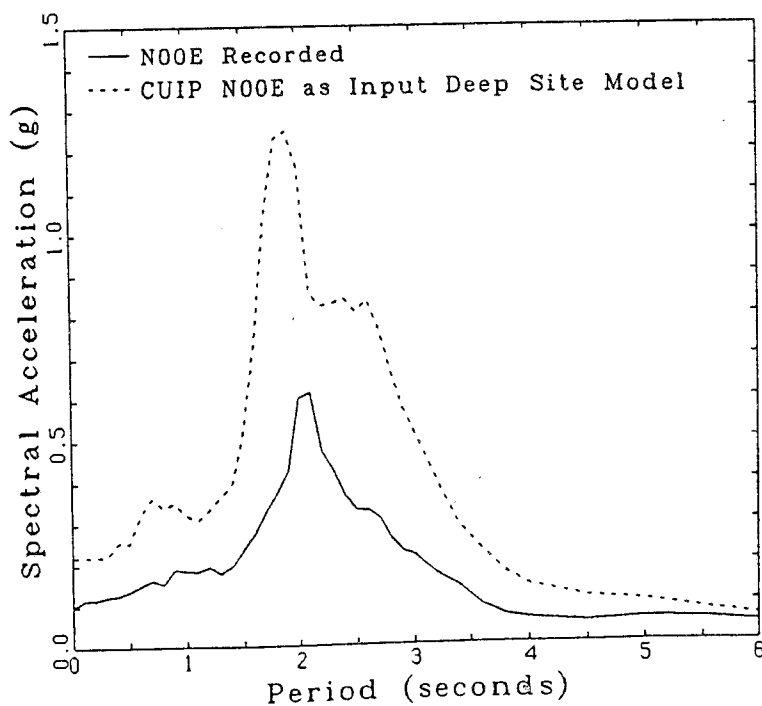


Figure 5.7: Response Spectra (5% Damping) of Recorded and Computed Motions in the N00E Direction at the SCT Site Using a Deep Site Model

propagating shear waves. The presence of surface wave motions in an earthquake record that cannot be reproduced using a recorded rock motion from the same earthquake as input has been reported before. Using data from an instrumented deep Japanese site, Ohta et al., (1977) have shown how a 1-D analysis underestimates the site response when significant surface waves are present. The case has been discussed in detail by Finn (1979).

5.2 Results of Analyses at the CAO Site

The response spectra of the motions computed for the CAO site, using the N90W and N00E components of the CUIP and CU01 records as input, are compared with the response spectra of the N90W and N00E motions recorded at the CAO site in Figures 5.8 and 5.9. Figure 5.8 shows that while the spectra of the computed motions compares well with that of the recorded motions for periods less than 2 seconds in the N90W direction, the match is not good for periods greater than 2 seconds. The spectra of the computed and recorded motions for the N00E component (Figure 5.9) do not match well at any period, since neither the amplitude nor the peak response periods match.

Scaling of the input motions will not cause a better match, as it did at the SCT site. If the input motions are scaled such that the spectra of the computed motions match the spectrum of the recorded motions around a period of 3.5 seconds the computed spectra are much greater than the spectrum of the recorded motions around a period of 1.5 seconds. In order for the

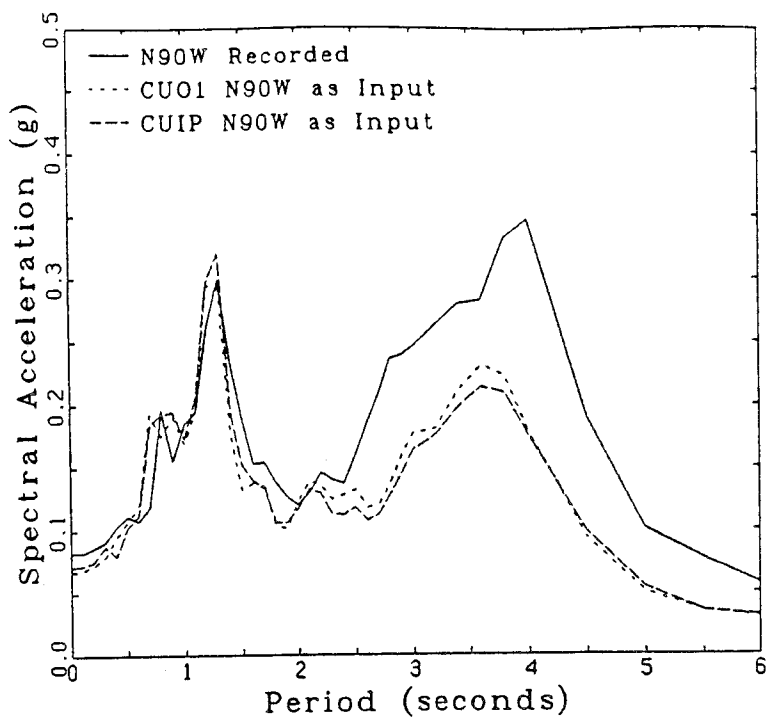


Figure 5.8: Response Spectra (5% Damping) of Recorded and Computed Motions in the N90W Direction at the CAO Site

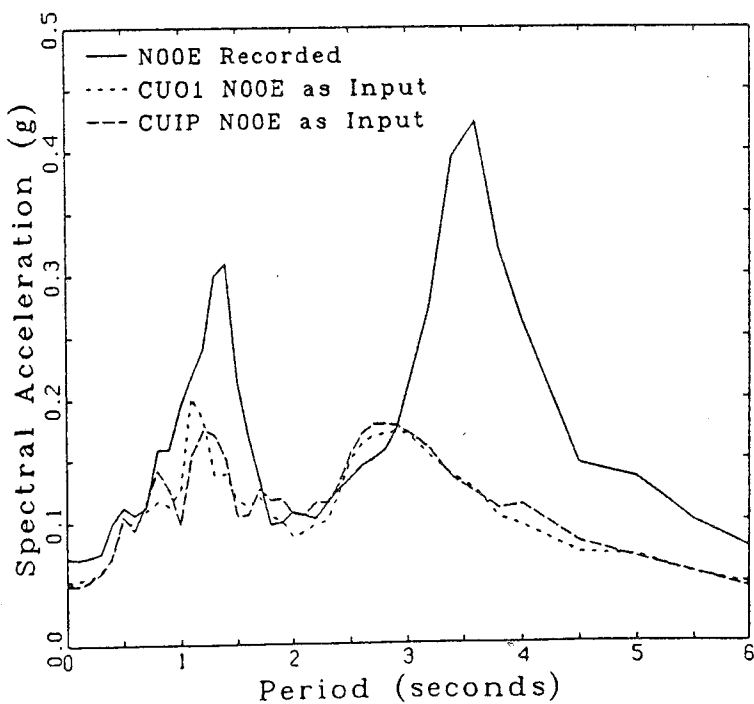


Figure 5.9: Response Spectra (5% Damping) of Recorded and Computed Motions in the N00E Direction at the CAO Site

computed spectra to match the peak of the spectrum of the recorded motions around a period of 3.5 seconds, the input motions had to be scaled as follows: the N90W component of the CUO1 motion, from .034g to .05g, the N90W component of the CUIP motion from .035g to .07g. The results of the analyses using scaled rock records as input is shown in Figure 5.10. For both the CUO1 and CUIP records the spectra of the computed motions are greater than the spectrum of the recorded motions over the period range from 0 to 2.5 seconds. Similar problems are encountered in the N00E direction.

5.3 Results of Analyses at the CAF Site

The spectra of the recorded motions and the spectra of the motions computed using the N90W and N00E components of the CUIP and CUO1 motions as input are shown in Figures 5.11 and 5.12. The match is not good for either component and, as at the CAO site, scaling does not allow a better match to be obtained. The difficulty in matching is caused by the fact that the spectra of the motions computed using the CUIP and CUO1 records have peaks at a period of 2.8 seconds while the spectra of the recorded motions have peaks at 2 seconds and at 3 seconds. Since a 1-D analysis of a site behaving in an approximately linear manner cannot have predominant periods not related by $1/2N-1$, one or both of the following may be responsible for the additional peak in the spectra of the recorded motions: the rock motions have been modified as they travel through the valley wall into the lakebed deposits, or surface waves in the lakebed deposits are

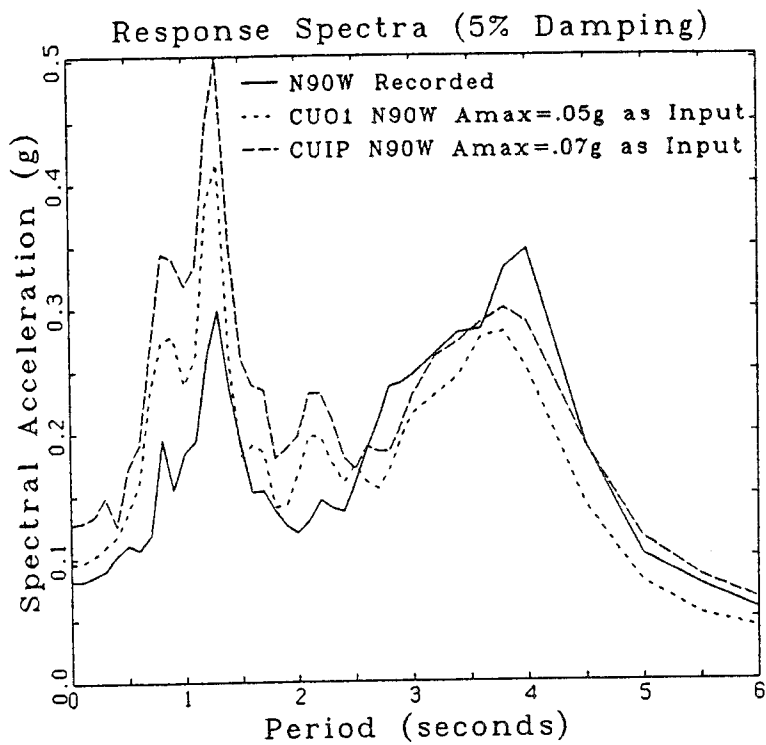


Figure 5.10: Response Spectra (5% Damping) of Recorded and Computed Motions in the N90W Direction at the CAO Site Using Scaled Input Motions

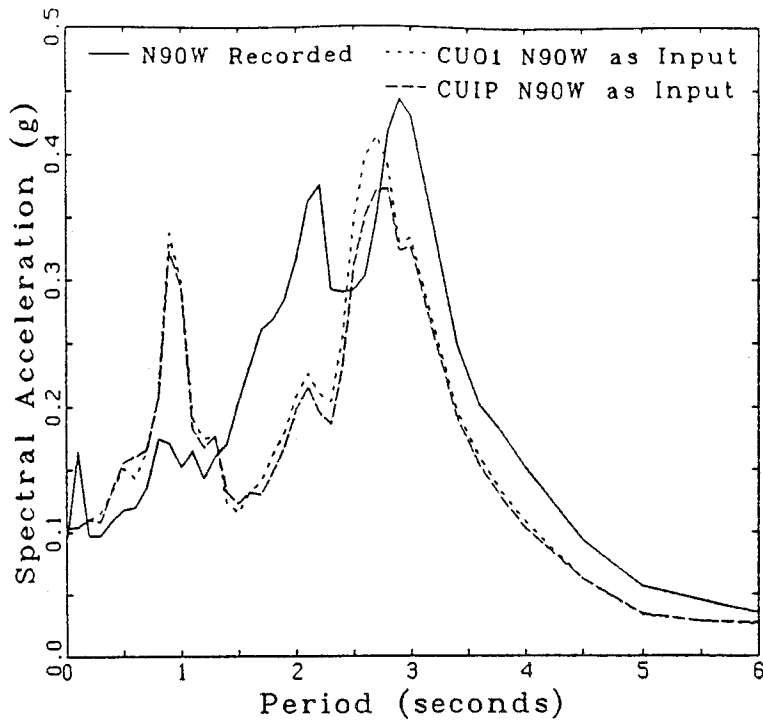


Figure 5.11: Response Spectra (5% Damping) of Recorded and Computed Motions in the N90W Direction at the CAF Site

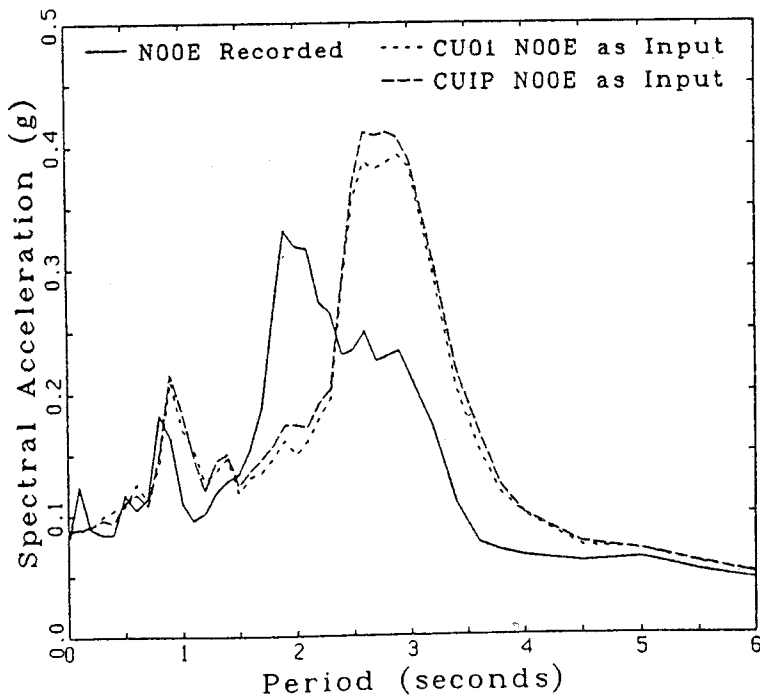


Figure 5.12: Response Spectra (5% Damping) of Recorded and Computed Motions in the N00E Direction at the CAF Site

adding to the motions at selected periods.

5.3 Summary of Analyses of Mexico City Sites Using Rock Outcrop Motions as Input

There are two factors that should be considered when performing dynamic analyses using recorded rock outcrop motions as input. The first is that rock motions may be altered as they enter the soil deposits due to refraction and reflection causing the motions in a hard layer taken as the base of a profile to be different from the recorded rock outcrop motions. Thus when the rock outcrop motions are used as input, the motions computed at the surface of the soil deposit may not be the same as the recorded motions.

Refraction and reflection may not be the only causes for the differences between the recorded and computed motions. Surface waves are often present in soft surficial layers and their passage adds to the response at a site at periods usually greater than one second. One dimensional analyses would not be able to reproduce these added motions since the surface waves would not be present in the rock outcrop motions. The effects of surface waves must be explored using two dimensional analyses.

In the analyses of Mexico City sites discussed in Chapter 4.0 and this chapter, the site models developed by Romo and Seed(1986) have been used as they are the most recent models available. If further site specific data becomes available these analyses could be repeated, but the overall conclusions of

these chapters would probably not change. While it is realized that there are problems with refraction and reflection and surface waves in a 1-D analysis, it is felt that the dominant characteristics of the response of some Mexico City sites have been reproduced and at sites where the motions were not reproduced possible causes have been discussed.

The procedures learned through the validation process of Mexico City site analyses will be applied to a deep site in Canada, namely the Fraser Delta in British Columbia. As with the Mexico City site analyses, the analysis of the Fraser Delta will begin by developing site models and the selection of representative input motions.

6.0 INPUT MOTIONS, SOIL PROFILES AND SOIL PROPERTIES FOR DYNAMIC ANALYSES OF FRASER DELTA SITES

The Fraser Delta is located in the southwest corner of British Columbia and forms the western edge of the Fraser Lowland. The Fraser Lowland has an area of 3000 km² and is bounded on the north by the Coast Mountains, on the south and southeast by the Cascade Mountains and in the west by the Strait of Georgia, as shown in Figure 6.1. The Fraser Lowland itself is part of a major structural depression extending from Alaska to California (Wallis, 1979).

The Fraser Delta consists of deep deposits of sand, silty clay and till. The geologic history and major deposits of the Fraser Delta are described in detail in Appendix I. Three sites, Annacis, Brighthouse and McDonald Farm, which are representative of the eastern, western, and northern portions of the delta, shown in Figure 6.2, will be analysed using selected representative input motions.

6.1 Selection of Representative Input Motions

The seismicity of the West Coast of British Columbia is reviewed to provide guidance in the selection of representative ground motions. The tectonics and seismicity of the West Coast of North America have been discussed by Milne et al.(1978), Hyndman and Weichert(1983), Heaton and Hartzell(1987) and Weichert and Rogers(1987). Figure 6.3 shows the plate boundaries responsible for the seismicity of the West Coast of

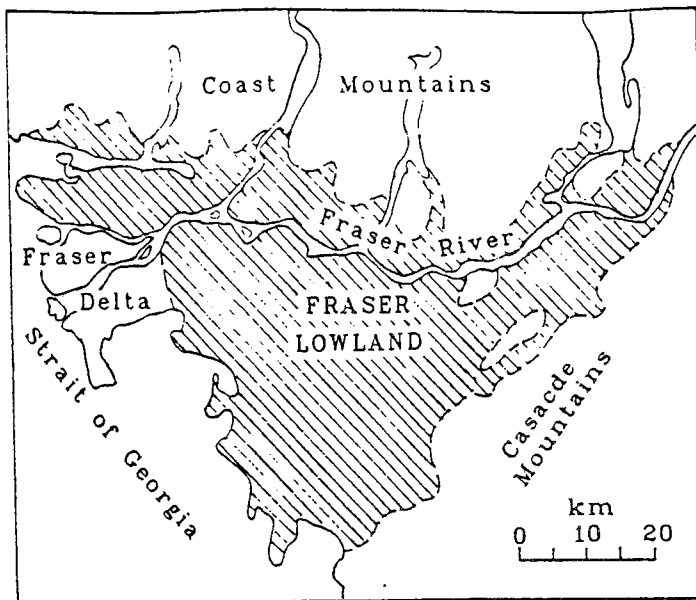


Figure 6.1: The Fraser Delta and Fraser Lowland
(Adapted from Armstrong, 1984)

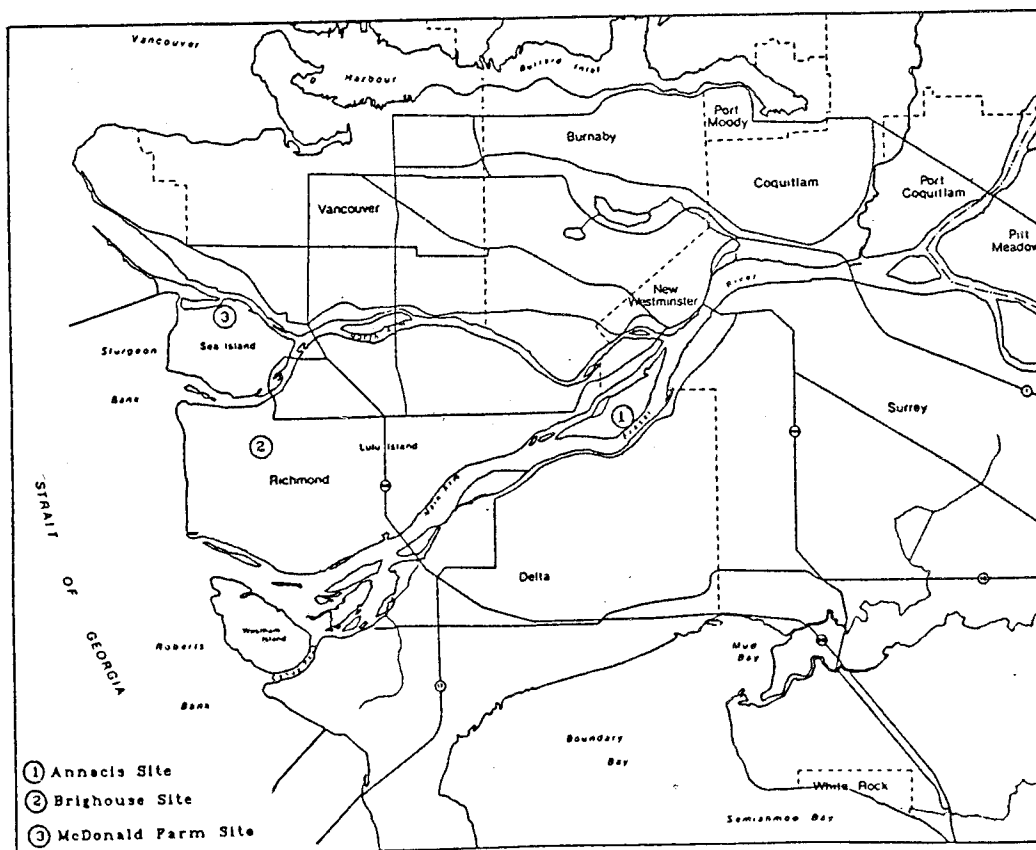


Figure 6.2: Location Map of the Delta Sites

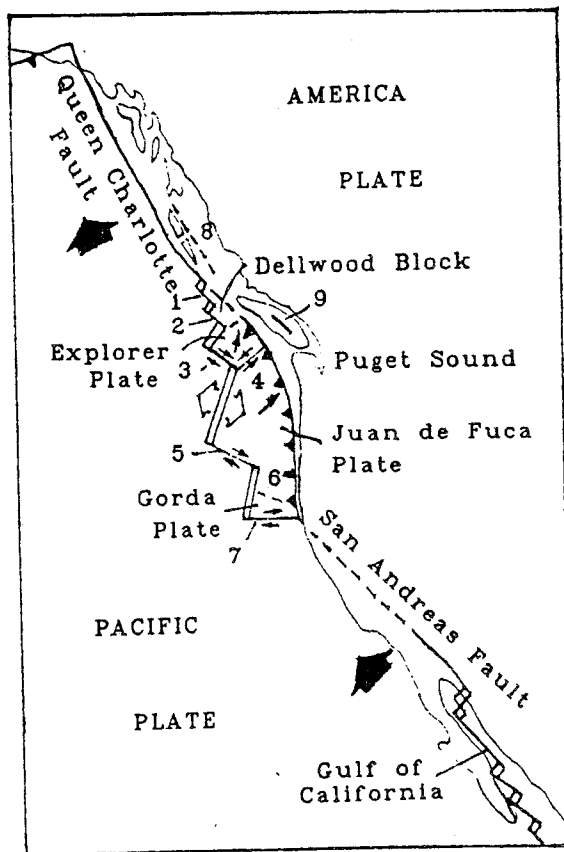


Figure 6.3: Plate Boundaries of the West Coast of North America: 1) Dellwood-Wilson, 2) Revere-Dellwood, 3) Sovanco, 4) Nootka, 5) Blanco, 6) Gorda, 7) Mendocino, 8) Sandspit, 9) Beaufort

(Adapted from Hyndman and Weichert, 1983)

North America. From the north end of Vancouver Island to Northern California a series of spreading ridges is driving the Juan de Fuca and Explorer Plates beneath the America Plate at rates of .5 to 1.5 cm/year and 3.5 to 4.6 cm/year respectively (Hyndman and Weichert, 1983). Outside of this area the Pacific and America Plates are in direct contact and are moving laterally to one another. In the area of direct contact along the Queen Charlotte fault the rate of relative movement is 5.5 cm/year (Hyndman and Weichert, 1983).

Slip along these boundaries causes earthquakes along the coast of British Columbia, Washington and Oregon. In addition to the earthquakes that occur on the plate boundaries, British Columbia and Washington are also affected by tension faulting earthquakes occurring beneath Puget Sound (Hyndman and Weichert, 1983). The combined effect of these sources produces a peak horizontal acceleration on firm ground in the Fraser Lowland of .2 g with a probability of exceedence of 10% in 50 years (NBCC, 1985).

Another possible source of earthquakes that would affect the Fraser Lowland has recently been suggested by Weichert and Rogers(1987) and Heaton and Hartzell(1987). These most recent studies were prompted by data from the 1985 Mexican earthquake. Based on comparisons of the plate configuration and seismic slip rates of the West Coast with other areas of the world with similar configurations, they propose that a large, subduction type earthquake, having a return period of 400-600 years and magnitude $M=8+$, could occur within 200 km of the Fraser Lowland.

The major seismic threat to the Fraser Delta in terms of maximum acceleration comes from the Puget Sound seismic zone and accordingly previous studies have used input motions that were representative of the motions expected from an earthquake in this zone as input. The N21E component of the 1952 record of the Kern County earthquake recorded at Taft, scaled to .2 and .25g, has been used as an input motion for Fraser Delta sites by Golder Associates(1983) and Wallis(1979). The response spectrum of the record scaled to .2 and .25 g is shown in Figure 6.4. The Taft record will be scaled to .2 and .25g and used as input motions in this study to verify the present analysis procedures by matching the responses computed by Golder Associates(1983) and Wallis(1979).

From the figure it can be seen that the Taft record contains little energy in the longer period range. The analyses of Mexico City lakebed sites have shown that the presence of long period energy can have a strong influence on long period sites. Significant long period energy could be contained in motions caused by the suggested subduction earthquake. To adequately represent the types of motion that could be caused in bedrock below the Fraser Delta by a large subduction earthquake several records will be selected. The recorded rock motions from the CU01 and CUIP sites will be used as input; being representative of the motions that could be caused by the subduction earthquake occurring at the outer limit of its 200 km range with a similar source mechanism. The Pasadena record used in the Mexico City analyses and scaled to .035g, with a range of

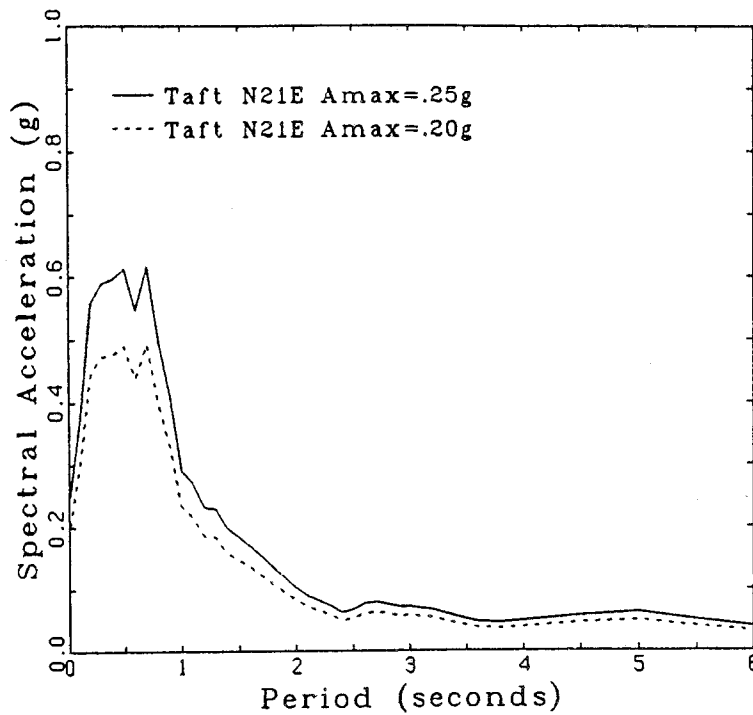


Figure 6.4: Response Spectra (5% Damping) of Motions Recorded at Taft During the 1952 Kern County Earthquake Scaled to .2 g and .25 g

predominant periods, will be used as input in order to bracket a range of motions that could be caused by the subduction earthquake occurring at the outer limit of its range.

The Pasadena record scaled to .07g with different predominant periods will be used as input in order to bracket the range of motions that could be caused by the subduction earthquake occurring within its 200 km radius. Finally, the epicentral motion recorded during the 1985 Mexican earthquake at the Caleto de Campos site will be used as input since it gives a possible upper range of acceleration for the subduction earthquake and has a similar source mechanism.

6.2 Soil Properties and Profile - Annacis Site

Soil profiles have been developed for the Annacis Site by both Golder Associates(1983) and Wallis(1979). The Golder Associates profile, shown in Figure 6.5, was chosen for use in this study because it is based on the most recent and extensive work at the site. The shear modulus profile shown in Figure 6.5 was determined from extensive crosshole seismic data and the maximum damping values were calculated using the equations of Hardin and Drnevich(1972). The dependence of shear modulus and damping on shear strain used by Golder Associates is shown in Figures 6.6 to 6.8. The curves were computed using the equations developed by Hardin and Drnevich(1972). In the silty clays the modulus-shear strain relationship was confirmed by laboratory testing to a shear strain of .01%.

For comparison, the range of modulus and damping dependence

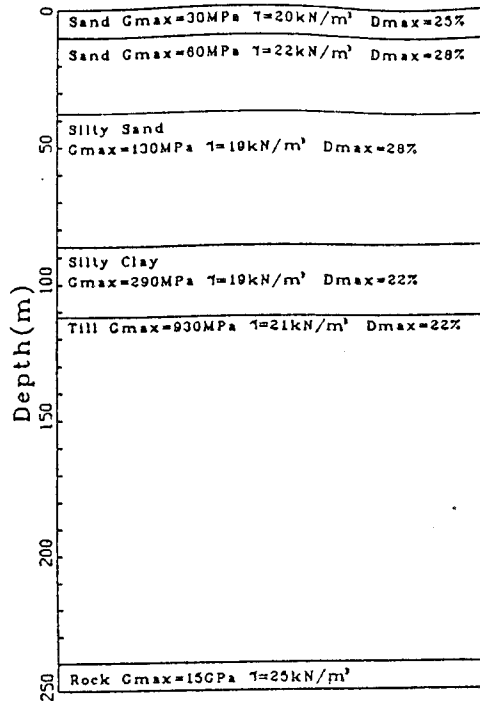


Figure 6.5: Soil Profile and Properties Developed by Golder Associates at the Annacis Site

(Adapted from Golder Associates, 1983)

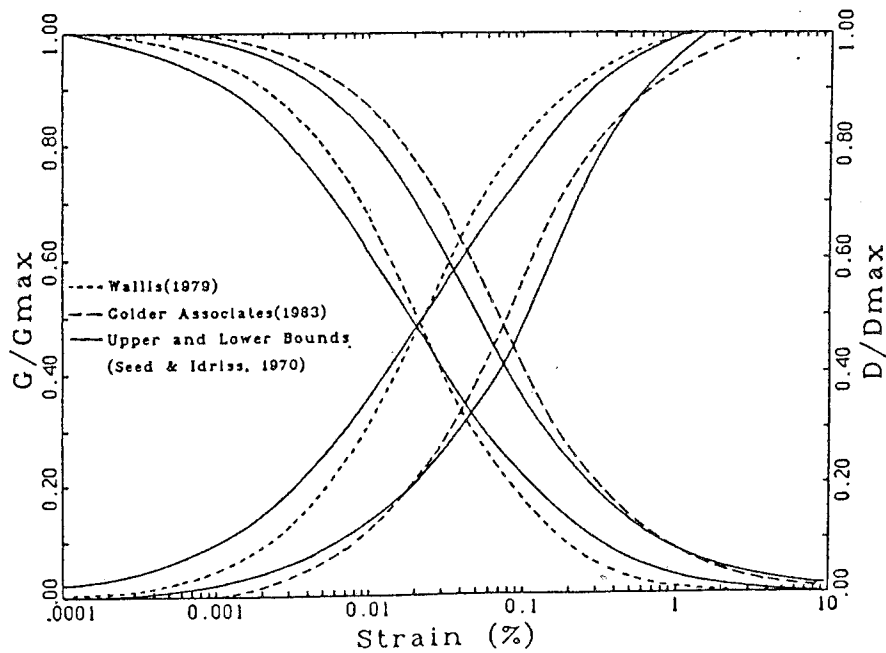


Figure 6.6: Shear Dependent Modulus and Damping for Sand

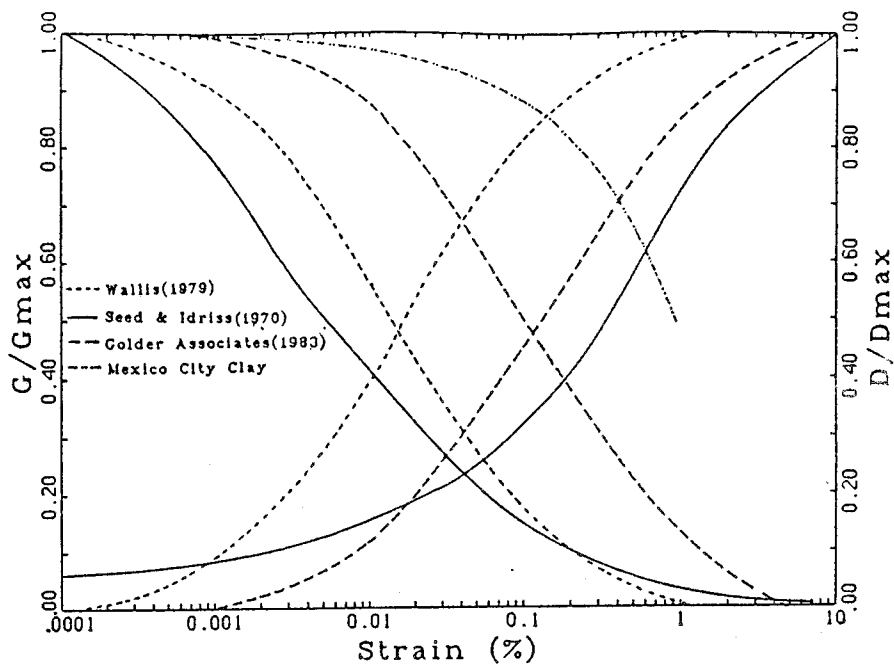


Figure 6.7: Shear Dependent Modulus and Damping for Silty Clay

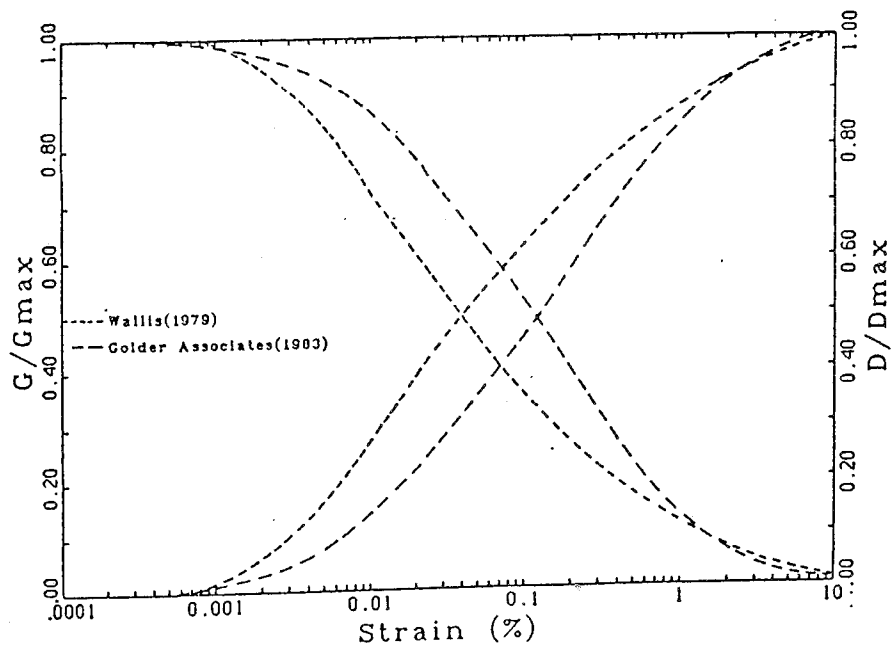


Figure 6.8: Shear Dependent Modulus and Damping for Till

suggested by Seed and Idriss(1970) for sands is also shown in Figure 6.6. From the figure it can be seen that the shear dependence of modulus and damping for Fraser Delta sands follows the suggested upper range.

The generalised curves of Seed and Idriss(1970) showing the dependence of shear modulus and damping ratio on shear strain are shown in Figure 6.7. Also shown are the curves for Mexico City clay, and for the Annacis silty clay determined by Golder Associates(1983) and Wallis(1979). It may be seen that the silty clays of the Fraser Delta exhibit less non-linear behaviour than typical clays but more than Mexico City clays. This will result in the silty clays of the Fraser Delta exhibiting more damping than Mexico City clays; thus their response will be lower and of shorter duration than that of Mexico City clays, but greater than typical clays.

6.3 Soil Properties and Profile - Brighthouse Site

The soil profile developed for the Brighthouse site by Wallis(1979) is shown in Figure 6.9. The values of shear moduli were calculated by Wallis using the equations given by Hardin and Black(1968) for sands and clays. The shear moduli values in the till were developed by Wallis from data collected by Murphy et al.(1978). The values for maximum damping were calculated by Wallis using the equations given by Hardin and Drnevich(1972).

The shear dependence of modulus and damping developed by Wallis using the equations given by Hardin and Drnevich(1972) for the sands, silty clays and till are shown in Figures 6.6 to

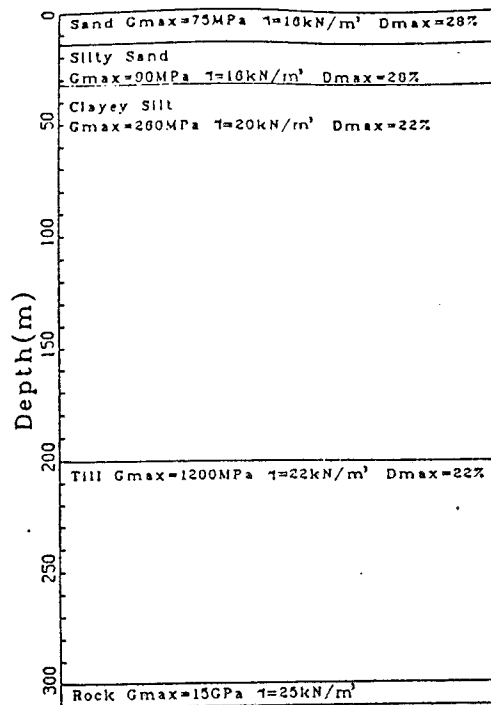


Figure 6.9: Soil Profile and Properties Developed by Wallis at the Brighthouse Site

(Adapted from Wallis, 1979)

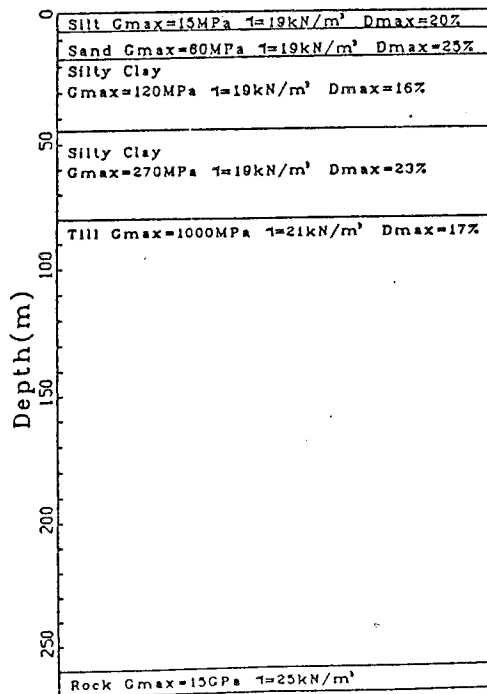


Figure 6.10: Soil Profile and Properties Developed at the McDonald Farm Site

6.8. Analyses were first done using the shear dependence relationships for moduli and damping developed by Wallis to allow comparison with his studies. Thereafter all analyses were conducted using the shear dependence relations developed by Golder Associates(1983) since they are based on the most recent and extensive work on the shear dependence of Fraser Delta soils.

6.4 Soil Properties and Profile - McDonald Farm Site

The soil profile developed at the McDonald Farm site (Figure 6.2) for this study is shown in Figure 6.10. The profile for the upper 30 m of the McDonald Farm site is based on data from Rice(1984); the depths to till and bedrock are based on cross sections from Armstrong and Hicock(1976). Maximum shear modulus values for the upper 45 m of soil at the site were based on downhole shear wave velocities measured by Rice(1984). Values of maximum damping in the soil above 45 m were calculated using data from Rice(1984) and the equations of Hardin and Drnevich(1972). Data for the shear modulus and damping values below 45 m were obtained from data developed for the Annacis Site by Golder Associates(1983). Although the two sites are 20 km apart the use of the same moduli may be justified because the same geological formations are present at both sites, namely deposits belonging to the Capilano, Vashon and Pre-Vashon stratigraphic units. The shear dependence of moduli and damping developed for Fraser Delta soils developed by Golder Associates(1983) was also used at the McDonald Farm site.

7.0 RESULTS OF DYNAMIC ANALYSES OF FRASER DELTA SITES

7.1 Results of Analyses at the Annacis Site

To confirm the profiles and properties used in the present study, the dynamic analysis of the Annacis site performed by Golder Associates(1983) was repeated. The results of this study compare very closely with the results of the previous study as shown in Figure 7.1.

Having confirmed the profile and properties used at the Annacis site, the effects of acceleration level and frequency content of the input motion on the response of the site will now be examined. Figure 7.2 shows the response spectrum of the motions computed using the Taft record scaled to .05g. This level of acceleration is representative of the maximum acceleration expected below the Delta from a large far field earthquake. For comparison Figure 7.2 also shows the response spectrum of the motions computed using the Taft record scaled to .2g. This level of acceleration is representative of the maximum acceleration expected below the Delta from a near field earthquake in the Puget Sound area and is typical of earthquakes used for design. It can be seen that scaling the maximum input acceleration by a factor of 4, from .05g to .2g, only results in an increase in the peak spectral acceleration of a factor of 2, from .37g to .74g. The non-linear relationship between the peak spectral acceleration and the input acceleration is due to the non-linear softening of soil stiffness with strain. As the

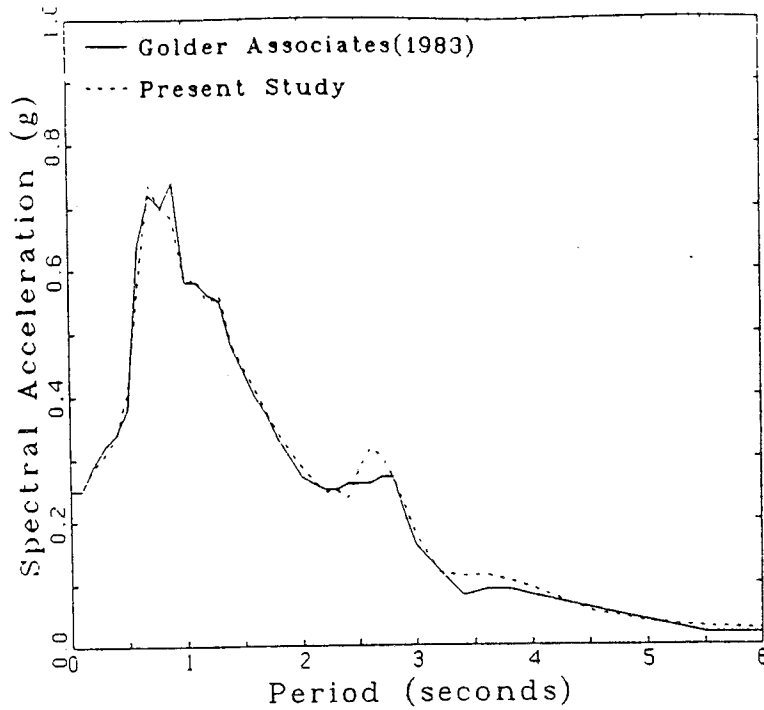


Figure 7.1: Response Spectra (5% Damping) of Computed Motions at the Annacis Site, Taft .25g as Input

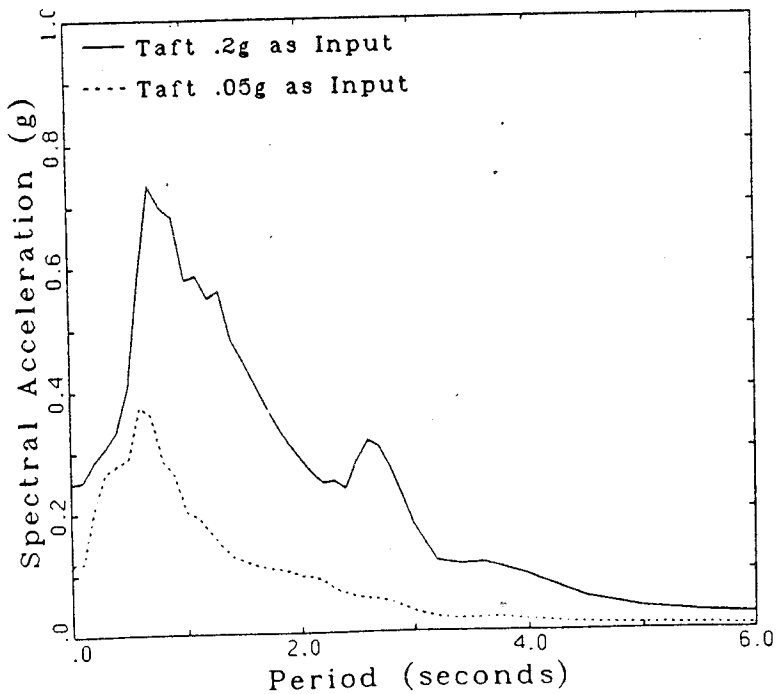


Figure 7.2: Response Spectra (5% Damping) of Computed Motions at the Annacis Site

input acceleration increases, the strains in the soil increase. The increased strains cause a non-linear reduction in soil stiffness governed by the curves shown in Figures 6.6 to 6.8.

The response of the Annacis site to the Pasadena motion scaled to .035 g with different predominant periods is shown in Figures 7.3 to 7.6. These figures show the response spectrum of the motions computed at the Annacis site along with the response spectrum of the input Pasadena motion. As the predominant period of the input motion (the peak of the response spectrum of the input motion) is increased towards the natural period of the site, the response of the site increases, as shown by the increasing peak spectral acceleration in Figures 7.3 to 7.6. Because strain softening occurs, the maximum response occurs not when the predominant period of the input motion and the initial natural period of 2 seconds coincide, but rather when the predominant period of the input motion and the first period of the site during shaking coincide. The first period of the site during shaking is computed from the eigen values of the site using the softened modulus values. The maximum response occurs when the input motion has a predominant period of 2.5 seconds (Figure 7.6). Figure 7.6 shows that resonance similar to that which occurred in Mexico City during the 1985 earthquake may occur in the Fraser Delta if the frequency of the majority of the energy in the input motions is similar to the natural frequency of sites in the Delta. Resonance is able to occur at Delta sites because of the limited strain softening that takes place during shaking.

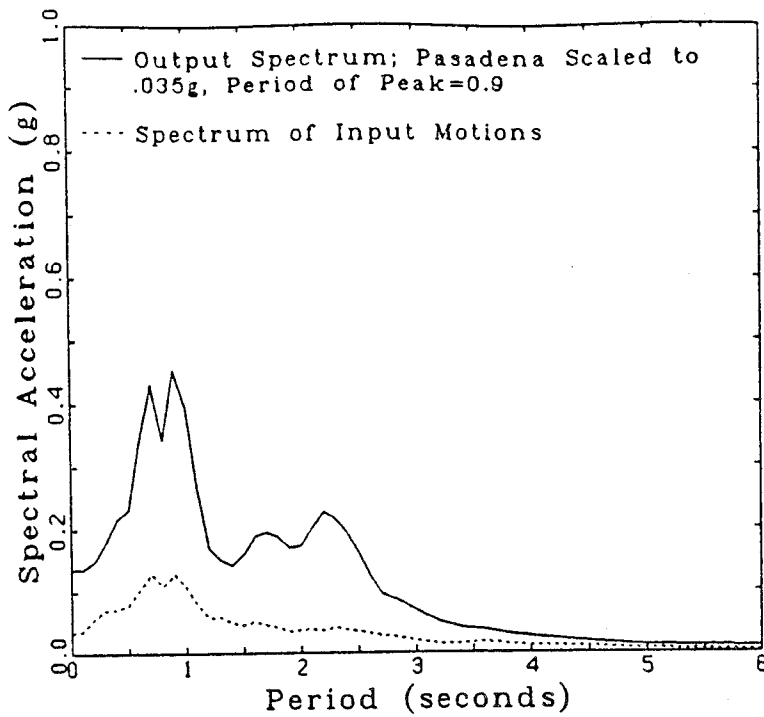


Figure 7.3: Response Spectra (5% Damping) of Input and Computed Motions at the Annacis Site

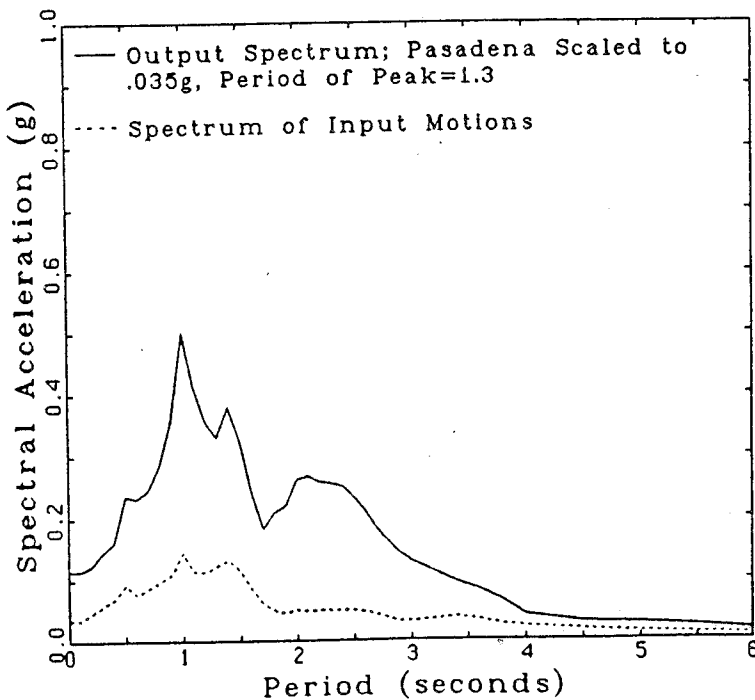


Figure 7.4: Response Spectra (5% Damping) of Input and Computed Motions at the Annacis Site

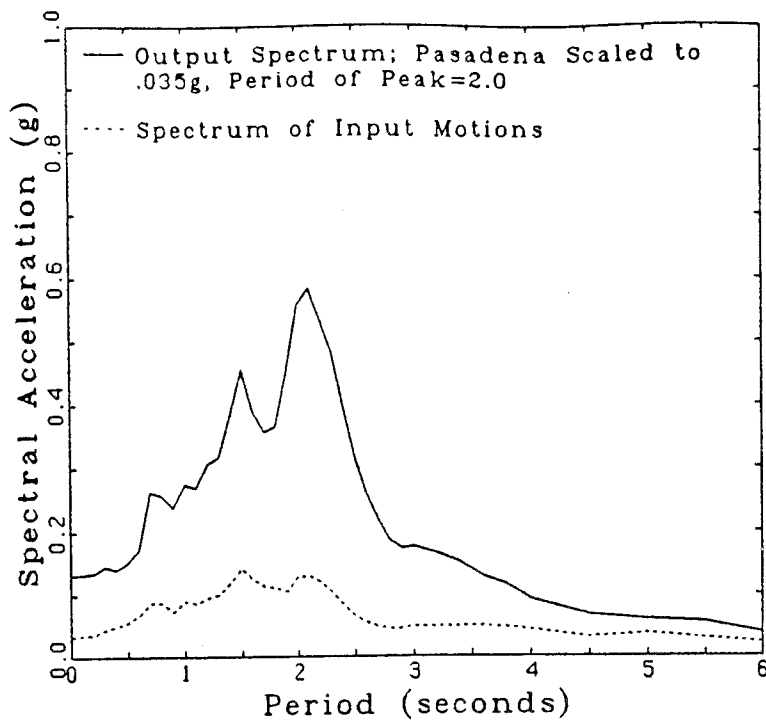


Figure 7.5: Response Spectra (5% Damping) of Input and Computed Motions at the Annacis Site

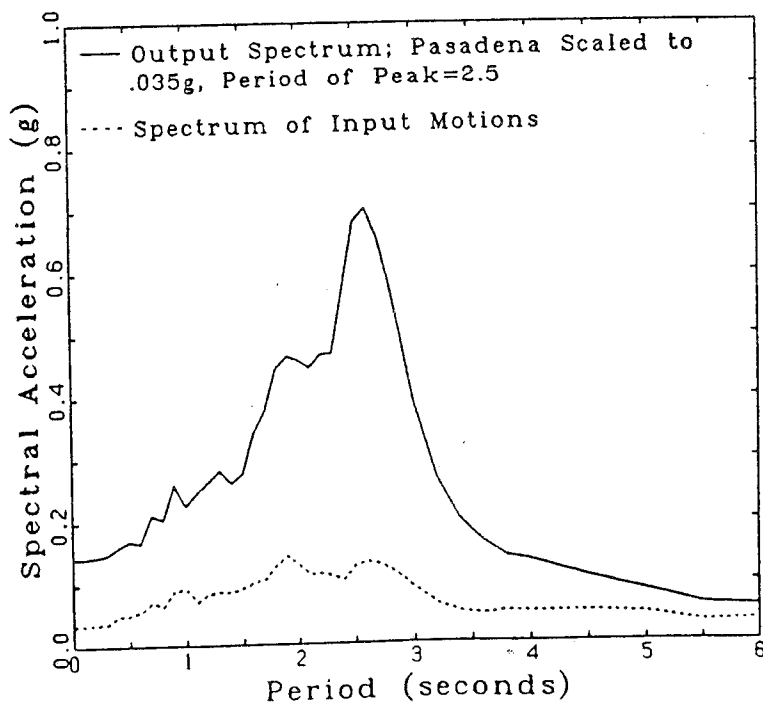


Figure 7.6: Response Spectra (5% Damping) of Input and Computed Motions at the Annacis Site

Figures 7.3 to 7.6 also show the importance of the predominant period of the input motion on site response apart from its relationship with site period. Examination of the figures shows that the period at which the maximum site response occurs is the predominant period of the input motion. In fact, the general shape of the response spectrum of the computed motions follows the general shape of the response spectrum of the input motion. This result indicates that a peak in the response spectra of the motions computed or recorded at a site may not always correspond to a natural period of a site. It may, instead, correspond to the predominant period of the input motion.

The results of Figures 7.3 to 7.6 are summarized in Figure 7.7. The response is given at the first three periods of the site in terms of the period of the input motion. The site period is the period during shaking and not the initial period which depends only on the initial, unsoftened, modulus values. Figure 7.7 shows that as the predominant period of the input motion increases, the response of the site shifts from the second mode of the site to the first, and that when the predominant period of the input motion coincides with the site's first period, the site response increases rapidly.

Similar results are obtained if the free field CUIP motions recorded during the 1985 Mexican Earthquake are used as input motions at the Annacis Site as shown in Figure 7.8. A spectral response of .5 g is obtained at a period of 2.5 seconds despite the low levels of input shaking of .035 g and .032 g for the

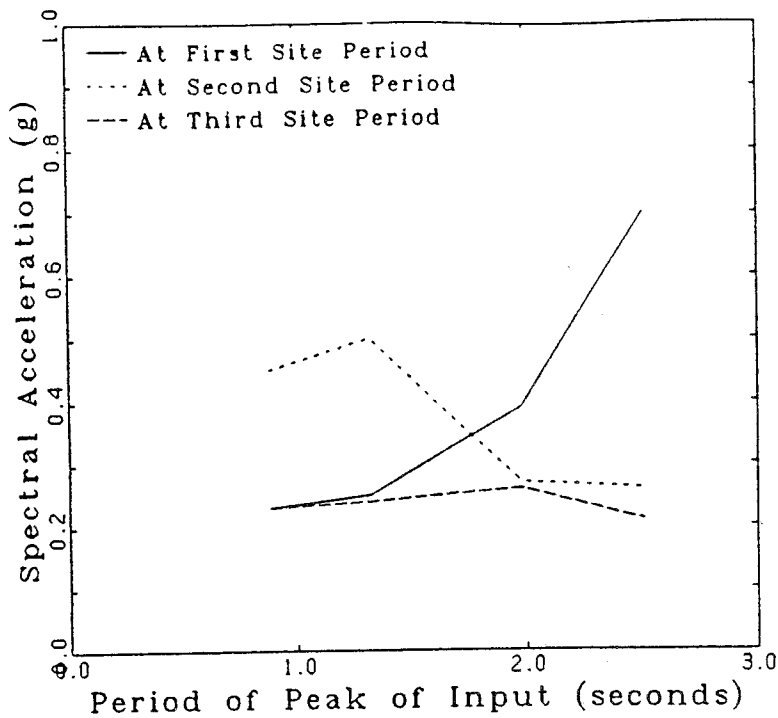


Figure 7.7: Spectral Acceleration (5% Damping) as a Function of the Predominant Period of the Input Motion

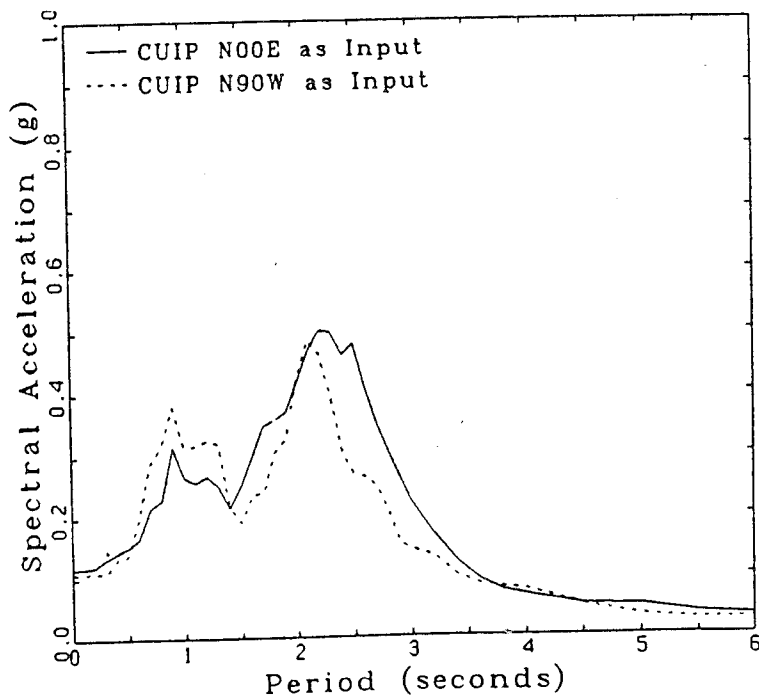


Figure 7.8: Response Spectra (5% Damping) of Computed Motions at the Annacis Site

N90W and N00E components.

The response of the Annacis site to the Pasadena record scaled to .07 g with a range of predominant periods is shown in Figure 7.9. The figure shows that the maximum site response is at a period of 1.3 seconds, which is shorter than the period of maximum response of 2.5 seconds computed using the Pasadena record scaled to .035g (Figure 7.7). The reason for this difference is apparent upon examination of Figure 7.10 which shows the dependence of spectral response on the predominant period of the input motion. Figure 7.10 shows that the maximum site response occurs when the predominant period of the input motion corresponds to the second natural period of the site during shaking. This is in contrast to the analyses performed using the Pasadena record scaled to .035g where the maximum site response occurred when the predominant period of the input motion matched the first period of the site.

The site response to the CALE motions is shown in Figure 7.11. The site exhibits a large response at 2.2 seconds corresponding to the predominant period of the input motion (Figure 2.19). The site has another large response at a period of 1 second corresponding to another peak in the response spectrum of the input motion.

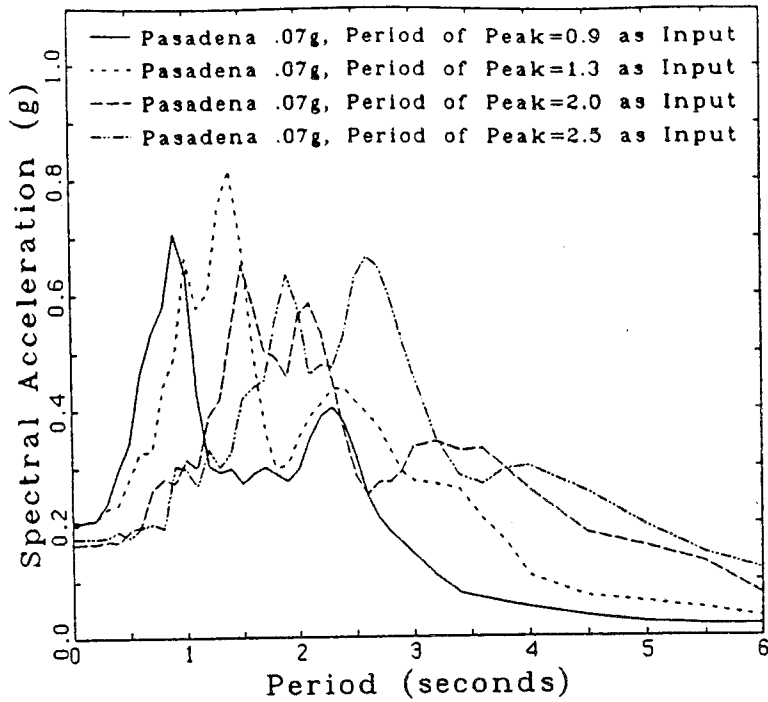


Figure 7.9: Response Spectra (5% Damping) of Computed Motions at the Annacis Site

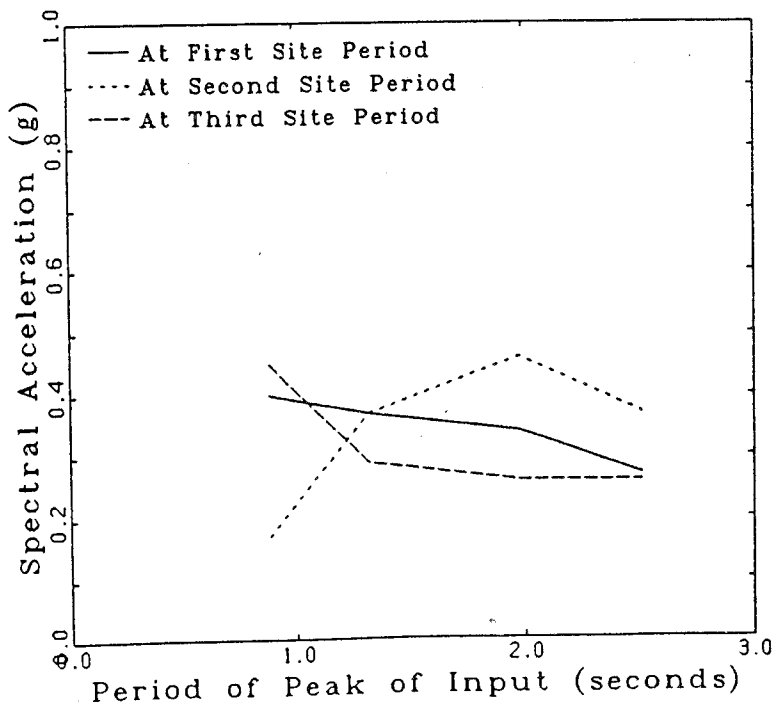


Figure 7.10: Spectral Acceleration (5% Damping) as a Function of the Predominant Period of the Input Motion

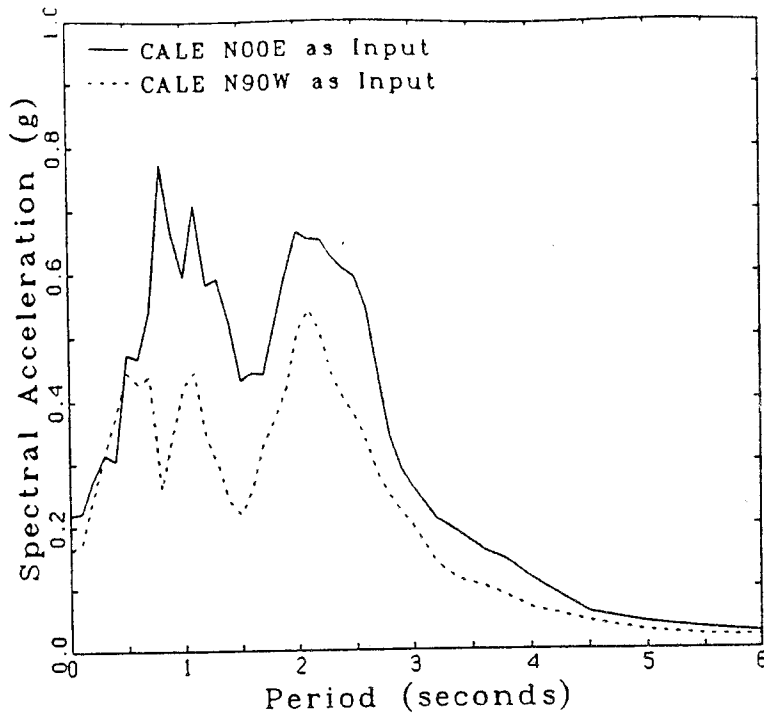


Figure 7.11: Response Spectra (5% Damping) of Computed Motions at the Annacis Site

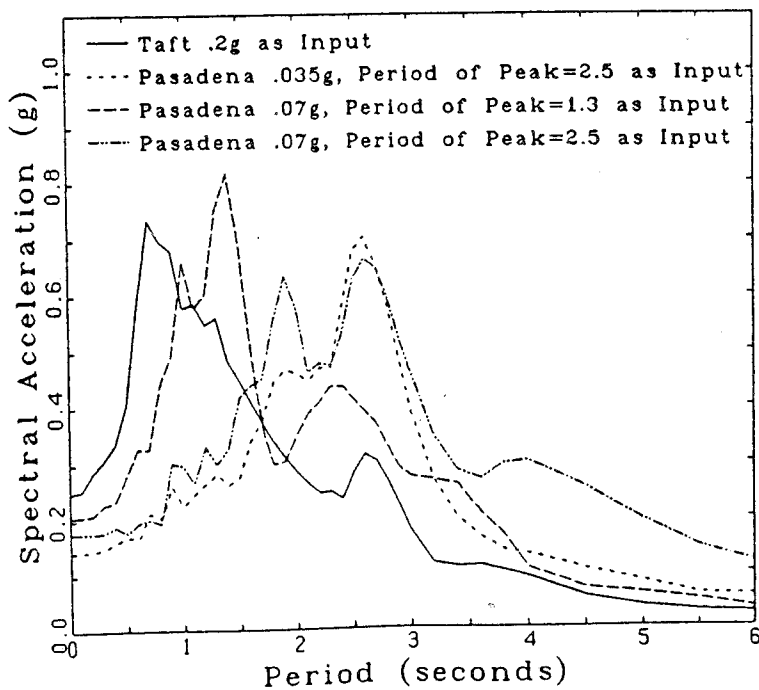


Figure 7.12: Response Spectra (5% Damping) of Computed Motions at the Annacis Site

7.2 Summary of Analyses at the Annacis Site

The response of the Annacis Site to low level, long period motions is significant with resonance occurring when the predominant period of the input motion and a period of the site coincide. The long period Pasadena motions with accelerations of .035 and .07g cause a larger response at periods greater than 1 second than the Taft record with a maximum acceleration of .2g as shown in Figure 7.12. The non linearity of site response is also shown in Figure 7.12 by the fact that the site response is as great under the influence of the Pasadena motion scaled to .035 g as it is to the Pasadena motion scaled to .07 g with the same predominant period of 2.5 seconds.

Since low level long period motions can cause large responses at the Annacis Site, the effects of a possible far field subduction earthquake should be considered in the determination of design spectra. This is achieved through the use of input motions covering a wide range of frequency contents and acceleration levels.

The response spectra in Figure 7.12 show that long period structures at the Annacis site will have very strong responses during a large far field earthquake. For a large, near field earthquake, which would cause baserock motions similar to the Taft record scaled to .2g, the response of long period structures at the Annacis site will not be as great. This is due to the fact that the increased strain softening caused by the increased input accelerations reduces site response through increased damping and reduced modulus. Also, the predominant

period of the baserock motions from a large, near field, earthquake would be shorter than the natural period of the Annacis site. Because of this, resonance would not occur, and surface motions with predominant periods in the range of long period structures would be less.

7.3 Results of Analyses at the Brighthouse Site

Following the same procedure used at the Annacis Site, the dynamic analysis by performed by Wallis(1979) was repeated as shown in Figure 7.13 as a check on procedures. The shear dependence of modulus and damping developed by Wallis (1979) (Figures 6.6 to 6.8) were used in the analysis. For all subsequent analyses, the shear dependence of modulus and damping developed by Golder Associates(1983) (Figures 6.6 to 6.8) was used since it is based on the most recent and extensive study on the shear dependence of Fraser Delta soils. The change in response from the use of the shear dependence relations developed by Wallis(1979) and Golder Associates(1983) is shown in Figure 7.14. The huge difference in response emphasizes that dynamic analyses should be conducted with site specific properties including site specific variations in modulus and damping with shear strain.

The results of the dynamic analyses of the Brighthouse Site using the Golder Associates shear dependence of modulus and damping are summarized in Figures 7.15 and 7.16. The results are similar to the results obtained at the Annacis Site because the initial elastic periods of the sites are similar. The

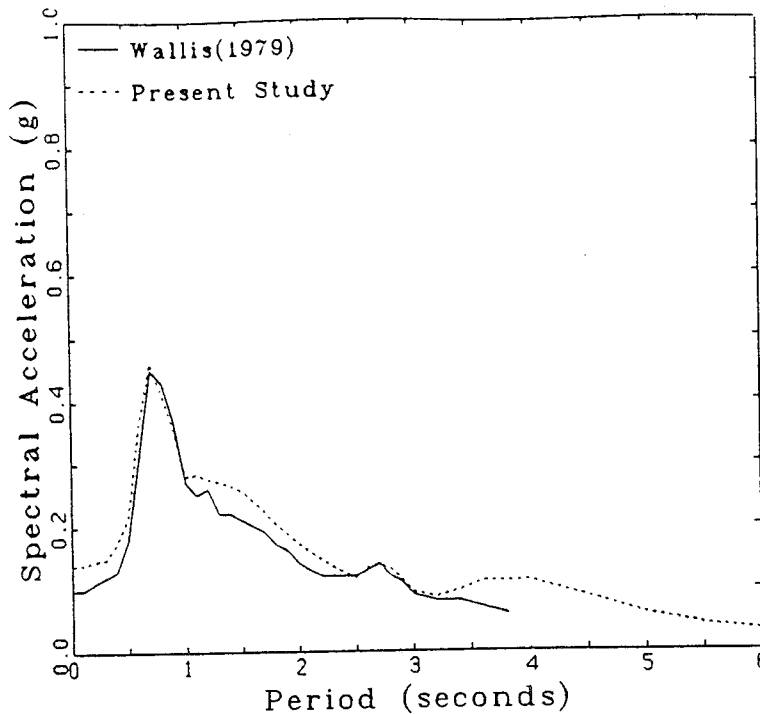


Figure 7.13: Response Spectra (5% Damping) of Computed Motions at the Brighthouse Site, Taft .25g as Input

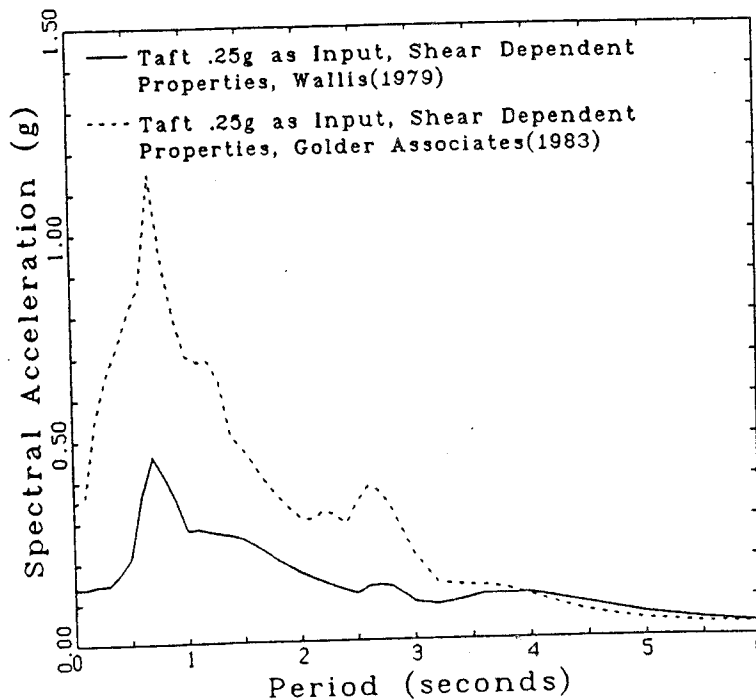


Figure 7.14: Response Spectra (5% Damping) of Computed Motions at the Brighthouse Site Showing Dependence of Site Response on Shear Dependence of Modulus and Damping

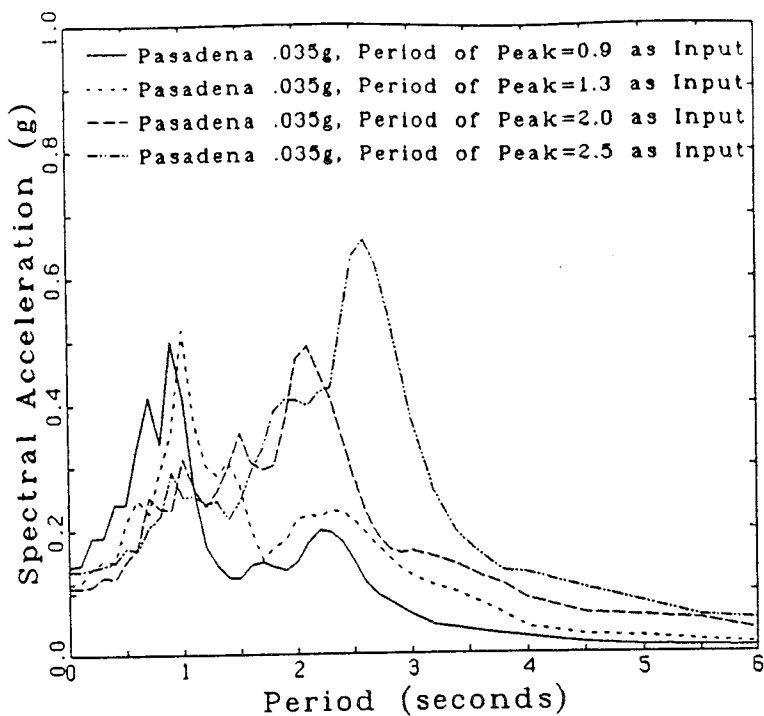


Figure 7.15: Response Spectra (5% Damping) of Computed Motions at the Brighthouse Site

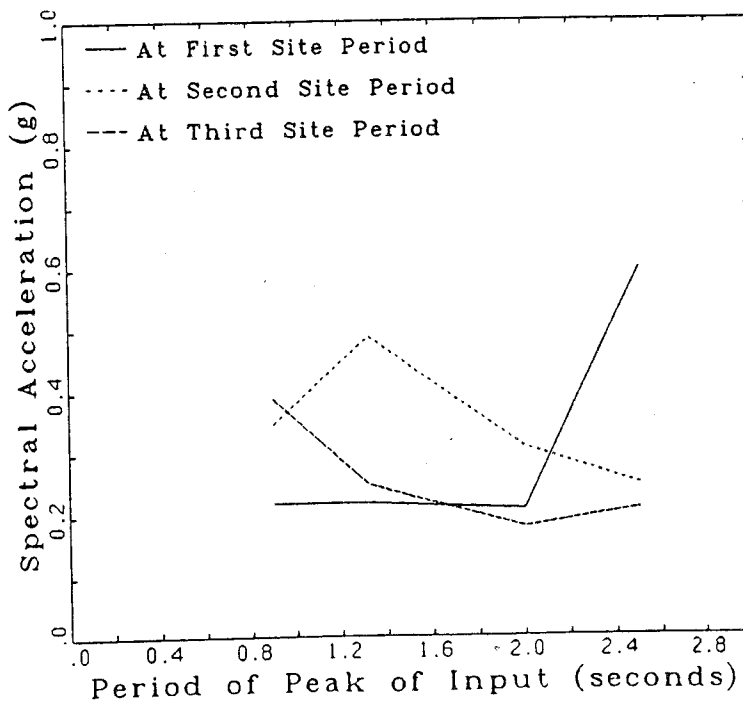


Figure 7.16: Spectral Acceleration (5% Damping) at the Brighthouse Site as a Function of the Predominant Period of the Input Motion

elastic periods of the first modes of vibration are 1.9 seconds at the Annacis Site and 2.3 seconds at the Brighthouse Site. The figures show that as the predominant period of the input motion increases towards the natural period of the site, the maximum response of the site shifts from the second and third modes of site response to the first (Figure 7.16). If the predominant period of the input motion matches a natural period of the site, resonance, with its accompanying large response, occurs (Figure 7.15).

As was noted at the Annacis Site, Figure 7.17 shows that low level input motions can cause a larger site response at certain periods than higher level input motions. In the figure, the computed site response for periods between 2 and 3 seconds is greater using the Pasadena motion scaled to .035 g and the epicentral record from the Mexican Earthquake ($A_{max}=.14g$) than it is using the Taft record scaled to .25 g. The large site response from .5 to 1 second to the Taft input motion is due to the coincidence of the predominant period of the Taft record with the second mode of vibration of the site.

7.4 Results of Analyses at the McDonald Farm Site

The results of the analyses using the Pasadena record scaled to .035 g with different predominant periods are shown in Figure 7.18. As at the Annacis and Brighthouse sites, maximum response is achieved by modifying the predominant period of the input motion until it matches the first natural period of the site during shaking. The McDonald Farm site is shallower than

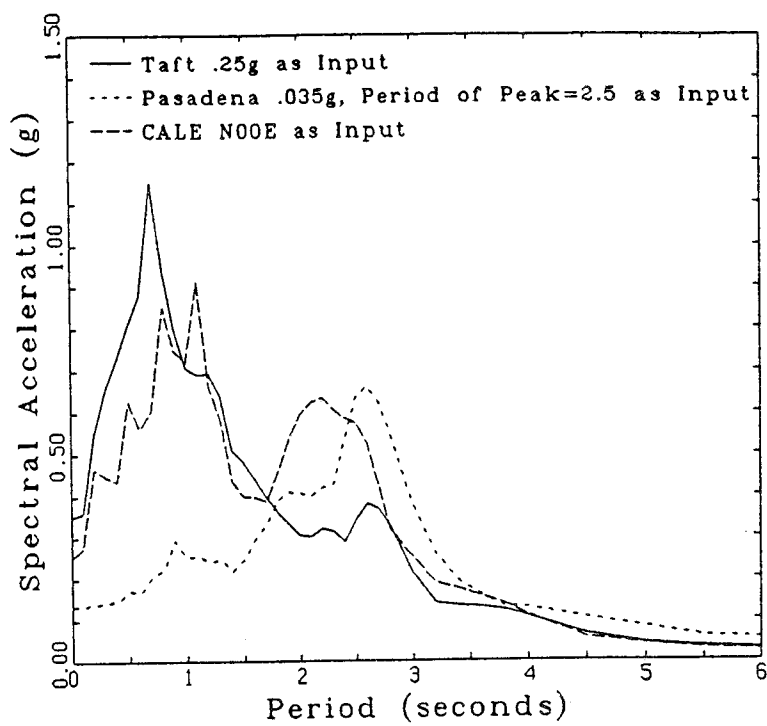


Figure 7.17: Response Spectra (5% Damping) of Computed Motions at the Brighthouse Site

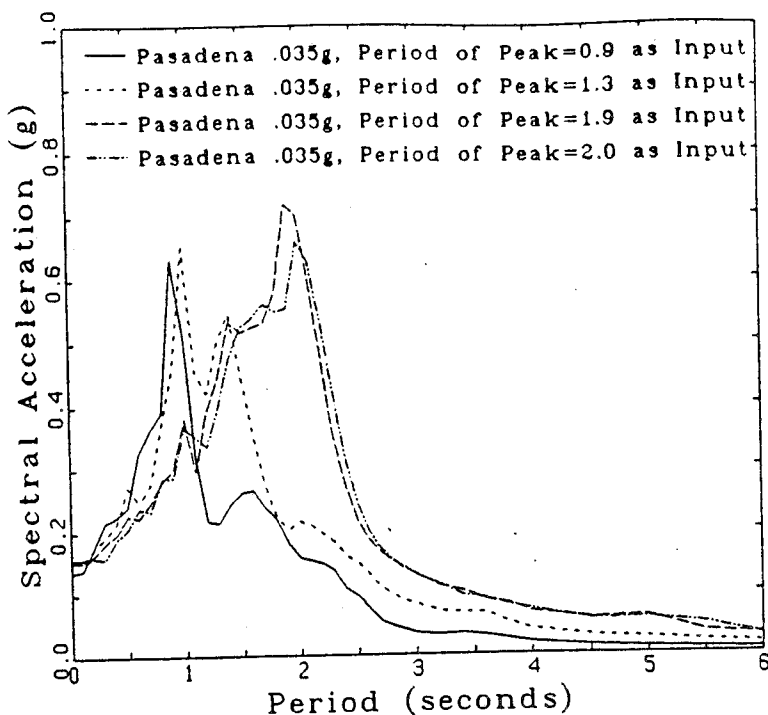


Figure 7.18: Response Spectra (5% Damping) of Computed Motions at the McDonald Site

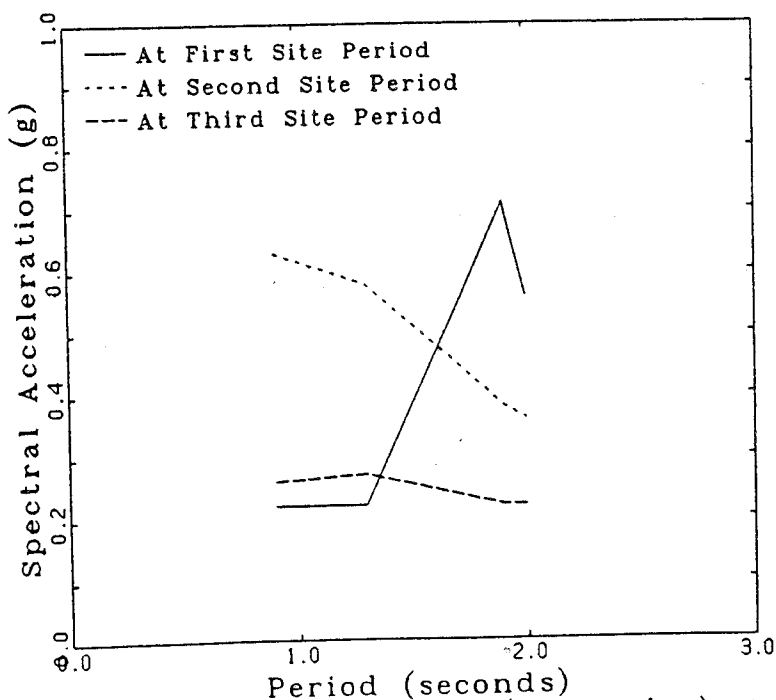


Figure 7.19: Spectral Acceleration (5% Damping) at the McDonald Farm Site as a Function of the Predominant Period of the Input Motion

the Annacis and Brighthouse sites, and thus has a shorter natural period. Therefore the maximum response occurs at a shorter period. The maximum response occurs when the predominant period of the input motion is 2.1 seconds rather than 2.5 and 2.6 seconds as at the Annacis and Brighthouse Sites. Figure 7.19 shows that as the predominant period of the input motion increases, the peak site response shifts from the second mode of the site to the first. Figures 7.18 and 7.19 also show that if the predominant period of the input motion exceeds the site period, the response decreases.

A plot of the response of the McDonald Farm site to several types of input motion is shown in Figure 7.20. The site has a large response to the Taft motion because the predominant period of the input motion corresponds to the second mode of vibration of the site. The large response to the CALE motion is caused by the coincidence of the spectral peaks in the record at 2 seconds and from .5 to 1 seconds (Figure 2.19) with the first, second and third modes of vibration of the site.

7.5 Summary of Analyses of Fraser Delta Sites

The primary observation that can be drawn from these analyses is the importance of the frequency content of the input motion on site response. The maximum spectral response of a site usually occurs close to the same period as the predominant period of the input motion (Figures 7.3 to 7.6). If the predominant period of the input motion coincides with a natural period of the site the response increases and the greatest

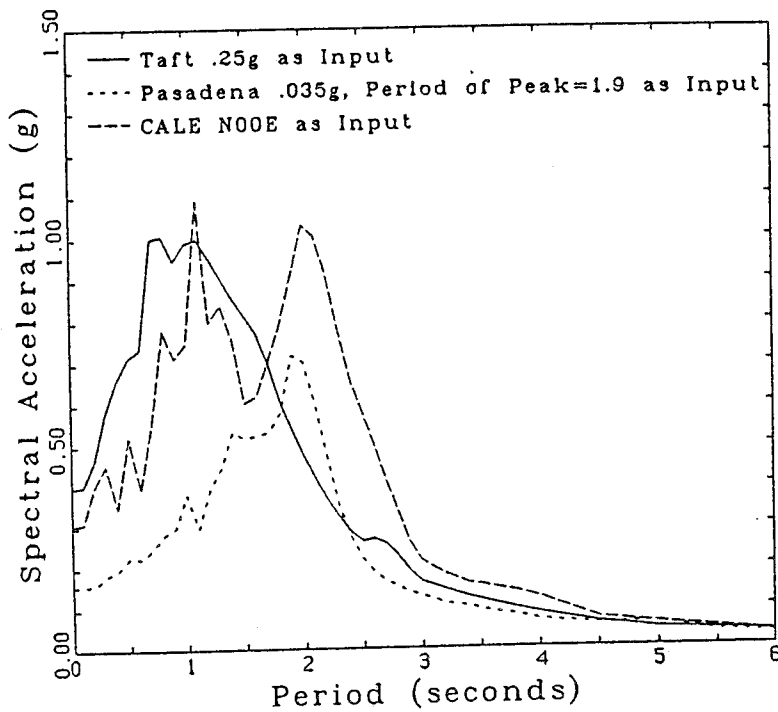


Figure 7.20: Response Spectra (5% Damping) of Computed Motions at the McDonald Site

response occurs when it coincides with the first natural period of the site (Figures 7.7, 7.10, 7.16, and 7.17).

These results show that structures with periods greater than one second can be affected by a large, far field, earthquake generating motions as low as .035g in the underlying bedrock. This is an important finding since prior to the Mexican earthquake of 1985 the effects of far field earthquakes had not been considered when developing design spectra for Fraser Delta sites. In future, when design spectra are being generated using dynamic analyses, input motions covering a broad range of frequency contents and acceleration levels should be used as input in order to properly define the response of the site.

The analyses also demonstrated the importance of using site specific properties when obtaining design spectra from dynamic analyses. Very large differences in spectral response can result from differences in the effects of shear strain on modulus and damping ratio. Indeed, the large amplifications in ground motion at Mexico City would not have occurred were it not for the limited strain softening that occurred over the strain range developed during the earthquake.

8.0 REVIEW OF RESULTS AND SUGGESTIONS FOR FURTHER STUDY

8.1 Review of Mexico City Analyses

The analyses of the three Mexico City sites showed that the heavy damage that occurred at lakebed sites during the 1985 Mexican earthquake was caused by the large amplification of bedrock motions and the long duration of the shaking. The large amplification was caused by the coincidence of the the predominant period of the input motions with the natural period of the lakebed sites. The predominant period of the input motion coincided with the long natural periods of the lakebed sites because of the large epicentral distance and the presence of strong, long period motion in the epicentral record due to the source mechanism. Resonance was able to develop and the shaking was of long duration because limited strain softening took place in the soils underlying the lakebed area of Mexico City. This prevented the modulus from decreasing and the damping from increasing both of which would reduce site response and the duration of shaking.

The analyses of the Mexico City lakebed sites emphasized the importance of three aspects of dynamic analysis. The first is that site specific soil properties as well site specific dependence of modulus and damping on shear strain must be used. The spectra of the recorded motions cannot be matched if site specific properties are not used.

The second area is the possibility of input motions having

predominant periods similar to the natural period of the site should be considered when developing design spectra for a site. To fully determine the response of a site to earthquake motions a number of input motions spanning a wide range of acceleration levels and predominant periods should be used.

Finally, the effects of focussing of earthquake motions and the presence of surface waves should be considered through the use of 2-D analyses since these effects can cause the response of a site to vary by 60% from one component to the other.

8.2 Review of Fraser Delta Analyses

The analysis of Fraser Delta sites reiterated the lessons from the Mexico City analyses as well as introducing a final point. The possibility of a subduction earthquake generating motions with predominant periods close to the natural periods of Delta sites must be considered when developing design spectra for Fraser Delta sites. Analyses of typical motion from such earthquakes leads to increased spectral acceleration response in the long period range above that derived from earthquake sources such as the Puget Sound area usually taken into account. These define the design spectrum primarily in the short period range with periods less than 1 to 1.5 seconds.

8.3 Suggestions for Further Research

Because 2-D effects affected the response at Mexico City sites, analyses using a 2-D program such as Tara-3 (Finn et al., 1980) would be helpful in determining if 2-D effects could be reproduced.

In the analyses of Fraser Delta sites the response was highly dependent on the soil properties chosen, especially the strain dependence of modulus and damping. Laboratory testing to determine the strain dependence of delta soils would aid in reducing the variability of future analyses. Additional deep drilling and geophysical work would also improve the results of dynamic analyses by refining the soil profiles and properties at depth. Work of this type is currently underway and, once completed, more refined analyses of the response of Fraser Delta sites may be made.

A more detailed study of the motions expected from the potential subduction earthquake would aid in defining the areas of the Delta that may undergo resonance and increased spectral response.

Finally, the Fraser Delta contains extensive deposits of saturated fine to medium sand. Pore pressure generation within these deposits would affect the site response by changing the resonant response of the site. If liquefaction occurred, the types of damage to be expected would change from those associated with strong shaking to those associated with settlement and ground instability. Laboratory work to determine the volume change characteristics and permeability of the sands

would allow effective stress dynamic analyses to be performed using programs such as Desra-2 (Lee and Finn, 1978). Analyses such as these would give a better indication of the types of motion that could be expected on the Fraser Delta during an earthquake.

REFERENCES

- Armstrong, J.E., (1955), "Surficial Geology of the Vancouver Area, British Columbia," G.S.C., Paper 55-40.
- Armstrong, J.E., (1981), "Post Vashon Glaciation, Fraser Lowland, British Columbia," G.S.C., Bulletin 322.
- Armstrong, J.E., (1984), "Environmental and Engineering Applications of the Surficial Geology of the Fraser Lowland, British Columbia," G.S.C., Paper 83-23.
- Armstrong, J.E. and Hicock, S.R., (1976), "Surficial Geology Map Vancouver," G.S.C., Map 1486A.
- Bard, P.Y. and Bouchon, M., (1980), "The Seismic Response of Sediment Filled Valleys, Part 1: The Case of Incident SH Waves," Bulletin of the Seismological Society of America, Vol. 70, pp 1263-1286.
- Blunden, R.H., (1973), "Urban Geology of Richmond British Columbia," University of British Columbia, Department of Geology, Report No. 15.
- Canadian National Committee on Earthquake Engineering, 1986. Committee discussions on seismic provisions of the National Building Code.
- Clague, J.J. and Luternauer, J.L., (1982), "Excursion 30A: Late Quaternary Sedimentary Environments, Southwestern British Columbia," Field Excursion Guidebook, Eleventh International Conference on Sedimentology, Hamilton.
- Duke, C.M., (1958), "Effects of Ground on Destructiveness of Large Earthquakes," Journal of Soil Mechanics and Foundation Division, A.S.C.E., Vol. 84, No. SM3, Proc. Paper

1730, pp 1-23.

Duke, C.M. and Leeds, D.J., (1959), "Soil Conditions and Damage in Mexico City Earthquake of July 28, 1957," Bulletin of the Seismological Association of America, Vol. 49, No. 2, pp 179-191.

Esteva, L. and Villaverde, R., (1973), "Seismic Risk, Design Spectra and Structural Reliability," Proceedings, 5th World Conference on Earthquake Engineering, Rome, 1973, Vol. 2.

Finn, W.D.L., (1979), "Role of Foundation Soils in Seismic Damage Potential," Proceedings, Third Canadian Conference on Earthquake Engineering, Montreal, Vol. 1, pp. 77-115.

Finn, W.D.L., Yogendrakumar, M., Yoshida, N. and Yoshida, H., (1986), "TARA-3: A Program for Non Linear and Dynamic Effective Stress Analysis," Soil Dynamics Group, University of British Columbia, Vancouver, B.C.

Golder Associates, (1983), "Report to the Province of British Columbia Ministry of Transportation and Highways on Foundation Soil Structure Interaction Analysis Annacis Island Bridge Main Span," Vol. I and II.

Gutenberg, B., (1957), "Effects of Ground on Earthquake Motion," Bulletin of Seismological Society of America, Vol. 47, No. 3, pp 221-251.

Hardin, B.O. and Black, W.L., (1968), "Vibration Modulus of Normally Consolidated Clay," Journal of Soil Mechanics and Foundation Division, A.S.C.E., Vol. 94, No. SM2, Proc. Paper 5833, pp 353-369.

- Hardin, B.O. and Drnevich, V.P., (1972), "Shear Modulus and Damping in Soils: Design Equations and Curves," Journal of Soil Mechanics and Foundation Division, A.S.C.E., Vol. 98, No. SM 7, Proc. Paper 9006, pp 667-691.
- Heaton, T.H. and Hartzell, S.H., (1987), "Earthquake Harzards in Cascadia Subduction Zone," Science, American Association for the Advancement of Science, Vol. 236, April 10, 1987, pp 162-168.
- Herrera, I., Rosenblueth, E. and Rascon, O.A., (1962), "Earthquake Spectrum Prediction for the Valley of Mexico," Proceedings, 3rd World Conference on Earthquake Engineering, New Zealand, 1965, Vol. 1, pp 61-73.
- Hyndman, R.D. and Weichert, D.H., (1983), "Seismicity and Rates of Relative Motion on the Plate Boundaries of Western North America," Geophysical Journal of the Royal Astronomical Society, Vol. 72, pp 59-82.
- Johnston, W.A., (1923), "Geology of the Fraser River Delta," G.S.C., Memoir 135.
- Lee, K.W. and Finn, W.D.L., (1978), "DESRA 2: Dynamic Effective Stress Analysis of Soil Deposits," University of British Columbia, Vancouver.
- Leon, J.L., Jaime, A., Tabago, A., (1974), "Dynamic properties of Soils Preliminary Study," Institute of Engineering, UNAM.
- Lo, K.Y., (1962), "Shear Strength Properties of a Sample of Volcanic Material of the Valley of Mexico," Geotechnique, Vol. 12, 1962, pp 303-316.

- Marsal, R.J., (1959), "Foundation Problems in Mexico City," Proceedings, 1st Pan American Conference on Soil Mechanics and Foundation Engineering, Mexico City, September, 1959, Vol. 3.
- Marsal, R.J., (1975), "The Lacustrine Clays of the Valley of Mexico," Contribution of the Institute of Engineering to the International Clay Conference, Mexico City, 1975.
- Marsal, R.J. and Mazari, M., (1959), "The Subsoil of Mexico City," Contribution of the Institute of Engineering to the First PanAmerican Conference on Soil Mechanics and Foundation Engineering, Mexico City, 1959.
- Marsal, R.J. and Rasines, H., (1960), "Pore Pressures and Volumetric Measurements in Shear Tests," Proceedings, 1st Pan American Conference on Soil Mechanics and Foundation Engineering, Mexico City, Preprint.
- Mathews, W.H. and Shepard, F.P., (1962), "Sedimentation of the Fraser River Delta, British Columbia," Bulletin of the American Association of Petroleum Geologists, Vol. 46, No. 8.
- Mesri, G., Rokhsar, A. and Bohor, B.F., (1975), "Composition and Compressibility of Typical Samples of Mexico City Clay," Geotechnique 25, No. 3, pp 527-554.
- Milne, W.G., Rogers, G.C., Riddihough, R.P. and Hyndman, R.D., (1978), "Seismicity of Western Canada," Canadian Journal Earth Science, Vol. 15, pp 1170-1193.
- Mitchell, D., Adams, J., DeVall, R.H., Lo, R.C. and Weichert, D., (1986), "Lessons from the 1985 Mexican Earthquake,"

Canadian Journal of Civil Engineering, Vol. 13, No. 5, pp 535-557.

Murphy, D.J., Koutsoftas, D., Covey, J.N. and Fischer, J.A., (1978), "Dynamic Properties of Hard Glacial Till," Earthquake Engineering and Soil Dynamics Specialty Conference, Pasadena.

National Building Code of Canada, (1975), Ottawa, Ontario.

Ohsaki, Y., (1969), "The Effects of Local Soil Conditions Upon Earthquake Damage," Proceeding, Specialty Session 2, Seventh International Conference on Soil Mechanics and Foundation Engineering, Mexico City.

Ohta, T., Niva, M. and Andoh, H., (1977), "Seismic Motions in the Deeper Portions of Bedrock and in the Surface and Response of Surface Layers," Proceedings, 4th Japan Earthquake Engineering Symposium, Tokyo, pp 129-136 (in Japanese).

Rice, A.H., (1984), "The Seismic Cone Penetrometer," M.A.Sc. Thesis, Dept. of Civil Engineering, U.B.C.

Romo, M.P. and Jaime, A., (1986), "Dynamic Characteristics of Some Clays of the Mexico Valley and Seismic Response of the Ground," Technical Report, DDF, (in Spanish).

Romo, M.P. and Seed, H.B., (1986), "Analytical Modelling of Dynamic Soil Response in the Mexico City Earthquake of September 19, 1985," in The Mexico Earthquakes-1985: Factors Involved and Lessons Learned, American Society of Civil Engineers, New York, N.Y., pp 148-167.

Rosenblueth, E., (1960), "Earthquake of 28 July 1957 in Mexico

City," Proceedings, 2nd World Conference on Earthquake Engineering, Tokyo and Kyoto Japan, July 1960, Vol. 1, pp 359-379.

Schnabel, P.B., Lysmer, J., and Seed, H.B., (1972), "SHAKE; A Computer Program for Earthquake Analysis of Horizontally Layered Sites," E.E.R.C. Report No. 72-12, University of California, Berkely, December, 1972.

Seed, H.B., (1986), Personal Communication.

Seed, H.B. and Idriss, I.M., (1969), "Influence of Soil Conditions on Ground Motions During Earthquakes," Journal of Soil Mechanics and Foundation Engineering, A.S.C.E., Vol. 95, No. SM1, Proc. Paper 6347, pp 99-137.

Seed, H.B. and Idriss, I.M., (1970), "Soil Moduli and Damping Factors for Dynamic Response Analyses," E.E.R.C. Report No. 70-10, University of California, Berkeley, December 1970.

Seed, H.B. and Idriss, I.M., (1969), "Characteristics of Rock Motions During Earthquakes," Journal of Soil Mechanics and Foundation Division, A.S.C.E., Vol. 95, No. 5, pp 1199-1218.

Seed, H.B., Ugas, C. and Lysmer, J., (1976), "Site-Dependent Spectra for Earthquake Resistant Design," Bulletin of Seismological Society of America, Vol. 66, No. 1, pp 221-243.

Singh, S.K., Astiz, L., and Hashov, J., (1981), "Seismic Gaps and Recurrence Periods of Large Earthquakes Along the Mexican Subduction Zone: A Re-examination," Bulletin of the Seismological Society of America, Vol. 47, No. 3, pp 221-

251.

Wallis, D.M., (1979), "Ground Surface Motions in the Fraser Delta Due to Earthquakes," M.A.Sc. Thesis, Department of Civil Engineering, University of British Columbia.

Weichert, D.H. and Rogers, G.C., (1987), "Seismic Risk in Western Canada," Proceedings, Earthquake Geotechnique, Vancouver, May 25, 1987, Vancouver Geotechnical Society.

Zeevaert, L., (1953), "Pore Pressure Measurements to Investigate the Main Source of Surface Subsidence in Mexico City," Proceedings, 3rd International Conference on Soil Mechanics and Foundation Engineering, Switzerland, 1953, Vol.3, pp 299-304.

APPENDIX--THE GEOLOGY OF THE FRASER LOWLAND

Geologic History of the Fraser Lowland

The history of the Fraser Lowland is extensively discussed by Clague and Lutenauer(1982) and Blunden(1973) and this summary is based primarily on information from these two works. The Fraser Lowland is underlain by deposits of Quaternary age. These deposits are up to 300 m thick and are underlain by freshwater sedimentary rocks of Tertiary age.

The Quaternary materials in the Fraser Lowland were laid down during alternating glacial and non-glacial periods. During these periods, there were also isostatic and eustatic fluctuations in sea level. Therefore, the Fraser Lowland deposits consist of a complex collection of glacial, glaciofluvial and ice contact materials alternating with marine, glaciomarine and deltaic sediments. The deposits that have been identified as to material type and age are listed in Table I. Although no one location will have a complete stratigraphic record due to the removal of stratigraphic units by later glacial and fluvial processes, a profile from bedrock to surface will contain some of the materials laid down in the following periods; Westlynn Glaciation, Highbury Non-glacial Interval, Semiahmoo Glaciation, Olympia Non-glacial Interval, Fraser Glaciation and the current non-glacial period.

Information on the materials laid down during the first three periods is poor since they have not been well studied and

Years B.P. (Thousands)	Time Stratigraphic Units	Geologic Climate Units	Lithostratigraphic Units
5	Holocene	Postglacial	Salish and Fraser River Sediments Fort Langley Formation Sumas Drift Capilano Sediments
--- 10 --- 18	Late Wisconsin	Fraser Glaciation	Vashon Drift
			Quadra Sand Coquitlam Drift
--- 26 ---	Middle Wisconsin	Olympia Nonglacial Interval	Cowichan Head Formation
--- >62 ---	Early Wisconsin and Pre-Wisconsin	Semiahmoo Glaciation Highbury Nonglacial Interval Westlynn Glaciation	Semiahmoo Drift Highbury Sediments Westlynn Drift

Table I: Stratigraphy of the Fraser Lowland

(Adapted from Armstrong, 1984)

they have been reworked by processes occurring in later periods. However, they have been grouped into the Westlynn Drift, Highbury Sediments and Semiahmoo Drift.

The age of Westlynn Drift materials has not been positively identified but they are the oldest sediments of Wisconsin age

found in the Fraser Lowland and are estimated to be at least 62,000 years old. Westlynn Drift materials consist of lodgement tills, glaciofluvial and glaciomarine deposits. These materials have been found during excavations for the Highbury Tunnel and in drillholes for the Annacis Bridge, Golder Associates (1983).

Highbury Non-glacial Interval materials have been dated at greater than 54,000 years of age and consist of marine sediments and fluvial deposits. These deposits are not exposed at ground surface but have been found in excavations for the Highbury Tunnel and in drillholes for the Port Mann and Annacis Bridges.

Semiahmoo Drift materials have been dated at greater than 31,000 to greater than 62,000 years old. Lodgement tills, glaciofluvial, glaciolacustrine, and marine sediments have been identified as Semiahmoo Drift. Semiahmoo Drift deposits are exposed at Mary Hill and have been found in the Highbury Tunnel excavations and in drillholes for the major bridges in the Fraser Lowland.

Following the Semiahmoo Glaciation came the Olympia Non-glacial interval and during this period from 62,000 years ago to 26,000 years ago the Cowichan Head formations were laid down. Cowichan Head deposits consist of marine, fluvial, slope and organic deposits. They are exposed at Mary Hill and have been identified in Highbury Tunnel excavations.

The Fraser Glacial period followed the Olympia Non-glacial interval and during this time Quadra Sand, Coquitlam Drift and Vashon Drift materials were laid down. This period lasted from 26,000 years ago to 11,000 years ago.

Quadra Sand was laid down during the growth of the ice sheet beginning 29,000 years ago and peaking 17,000 years ago. Quadra sand deposits consist of glaciofluvial and glaciomarine deposits of a well sorted fine to medium sand. Although Quadra Sand is only exposed along the Point Grey Cliffs, the south slope of Maillardville and the edge of the Surrey Upland, Clague and Lutenauer(1982) believe that Quadra Sand was laid down over most of the Fraser Lowland and Georgia Depression in deposits up to 500 m thick. This vast deposit was then removed by the advancing ice sheet. As well as the above exposures Quadra Sand has been identified at the Highbury Tunnel and in drillholes for the Knight St. Bridge.

The Coquitlam drift materials were laid down at the same time as Quadra Sand by glaciers advancing out of the Coast Mountains. Coquitlam Drift materials are exposed at Mary Hill and the north slope of Port Moody but have not been identified in drillholes for the major bridges indicating that it was a local advance preceding the main ice sheet.

The peak of the Fraser Glaciation occurred roughly 17,000 years ago at which time the ice sheet extended 300 km south of Vancouver. During the period from the peak until the time when the Fraser Lowland became ice free 11,000 years ago the Vashon Deposits were laid down. These deposits consist of lodgement tills up to 25 m thick and glaciomarine deposits up to 60 m thick. Vashon drift covers much of the western Fraser Lowland as shown in Figure 1. Figure 1 also shows the exposures of deposits laid down before the peak of the Fraser Glaciation.

The pre-peak deposits correspond to Middle Wisconsin and earlier in terms of time stratigraphic units and were discussed above. Vashon deposits have also been identified in excavations for the Highbury Tunnel and in drillholes for the Knight St. Bridge.

Once the Fraser Lowland became ice free post-glacial materials consisting of Sumas Drift, Fort Langley Formation, Capilano Sediments, Salish Sediments, and Fraser River Sediments were laid down. Sumas Drift materials consist of lodgement tills up to 6 m thick and glaciofluvial deposits up to 45 m thick. Although they are exposed in Abbotsford, Maple Ridge and Fort Langley (Figure 1) they do not appear in drillholes in the Fraser Delta.

The Fort Langley Formation was laid down by readvances of a valley glacier from the Coast Mountains and consists of lodgement tills up to 5 m thick, glaciofluvial deposits up to 50 m thick and glaciomarine deposits up to 6 m thick. The Fort Langley Formation is exposed over most of the Fraser Lowland east of Abbotsford as shown in Figure 1. Fort Langley materials do not appear below the Fraser Delta.

Capilano Sediments consist of glaciomarine deposits up to 15 m thick, marine deposits up to 15 m thick and fluvial deposits up to 20 m thick. Capilano Sediments outcrop in the Capilano and Seymour River valleys, Point Grey, and most of the Surrey Uplands (Figure 1). They have also been identified in drillholes for the major bridges on the Fraser Delta.

Salish Sediments consist of marine deposits up to 8 m thick in Boundary Bay, fluvial deposits up to 20 m thick in the Pitt,

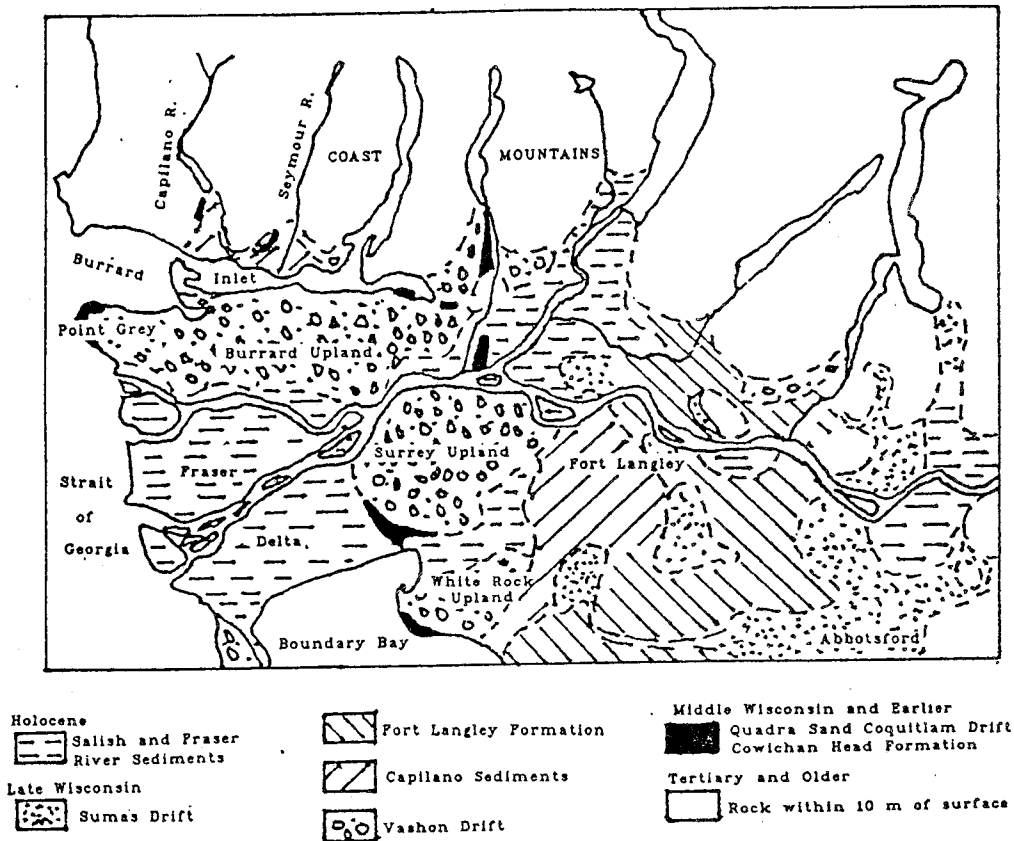


Figure 1: Quaternary Deposits of the Fraser Lowland

(Adapted from Armstrong, 1984)

Capilano, and Seymour River valleys, lacustrine deposits up to 20 m thick and organic deposits up to 20 m thick in the peat bogs of Lulu Island and Western Delta.

Although the Sumas, Fort Langley, Capilano and Salish sediments were laid down concurrently there are major differences between them in material type. Also much of the Sumas and Fort Langley formations have been overridden by ice whereas the Capilano and Salish Sediments have not been overridden by ice.

Fraser and Salish Sediments are the most recent sediments to be laid down and are still being deposited. Fraser sediments consist of marine sediments up to 185 m thick and fluvial deposits up to 215 m thick. The Fraser Sediments that form the Fraser Delta on which the Municipality of Richmond lies and the history of the Fraser Delta itself will now be discussed.

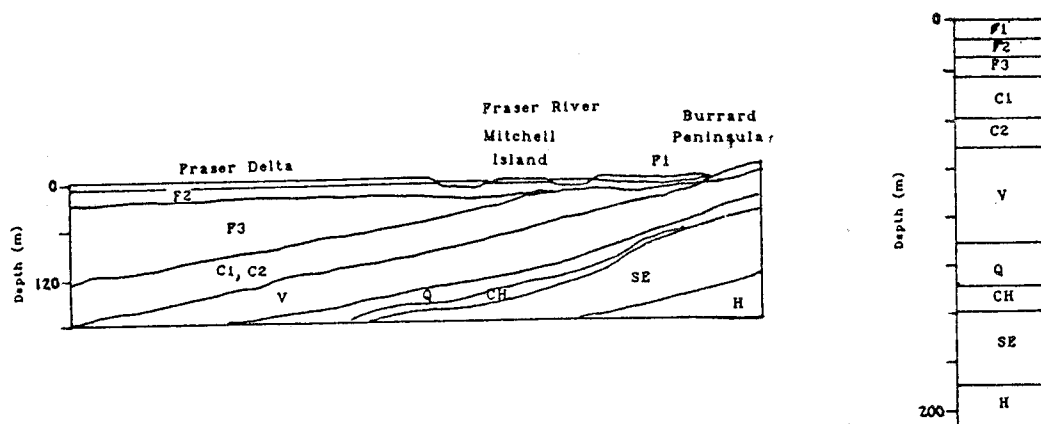
Geological History of the Fraser Delta

Once the ice had disappeared from the Fraser Lowland approximately 11,000 years ago the Fraser Delta began to develop. When the delta first began, the present location of Richmond was 40 km out to sea and thus only fine materials were carried as far as Richmond. Because the Fraser River was carrying large volumes of material from the retreating ice sheet the delta front moved 20 km from Haney to New Westminster in the period between 11,000 and 10,000 years ago. In the next 5,000 years, the delta grew to the present position of Ladner and would have grown further had the sea level not risen from its

position of 12 m below today's level to within 1 m of today's level, Clague and Luternauer(1982). At this time sediments reaching the location of Richmond still consisted of fine materials being deposited in a marine environment but volumes would be increasing since the Richmond location would now be 10 km out to sea rather than 40 km. During the time between 5,000 years ago and the present the delta grew from Ladner to its present position and the sea rose the remaining 1 m to its present level. As the delta front approached Richmond, sands rather than silts and clays would be laid down and once the delta front passed a given location finer overbank deposits would be laid down.

Current growth of the delta is still high; averaging 2.3 m/year at 6 m depth and 8.5 m/year at 90 m depth, Mathews and Shepard (1962). However, growth is uneven across the delta front especially since the addition of jetties on the north and south arms of the river.

From the history of the delta, a typical profile in Richmond can be developed. At the base would be sedimentary bedrock overlain by ice loaded Early Wisconsin tills, Middle Wisconsin glaciomarine and glaciofluvial deposits, Late Wisconsin tills and finally non ice loaded Holocene deposits. The Holocene deposits would consist of fine grained marine sediments overlain by sand sized marine and tidal flat deposits which in turn would be overlain by fine overbank deposits. This stratigraphic profile is confirmed by exploration in the delta the results of which are shown as a cross section in Figure 11.



Fraser River Sediments (F)

- F1 Channel and floodplain silty sand
- F2 Deltaic and channel fine to coarse sand
- F3 Deltaic fine sand to clayey silt, includes estuarine deposits

Capilano Sediments (C)

- C1 Glaciomarine stony silt to clay loam
- C2 Marine silt loam to clay loam

Vashon Drift (V)

Quadra Sand (Q)

Cowichan Head Formation (CH)

Semiahmoo Drift (SE)

Highbury Sediments (H)

Figure II: Cross Section and Borehole at Mitchell Island

(After Armstrong, 1984)

The ages of the stratigraphic groups shown in Figure II are given in Table I.

Geology of the Fraser River Delta

The Fraser Delta extends 15 to 23 km west and south of New Westminster and the tidal flats extend another 4 to 5 km seaward. The delta then dips at an average angle of 1.5° downward into the Strait of Georgia terminating in about 300 m of water 5 to 10 km seaward of the tidal flats, Clague and Luternauer (1982).

The geology of the delta was first discussed by Johnston(1923). Since then it has been covered in some detail by Armstrong(1955,1981,1984) and Armstrong and Hicock(1976). The history, geology and engineering properties have been collected and summarized by Wallis(1979).

The surficial deposits shown in Figure II have been further categorized by their depth and the thickness of the underlying sand deposits as shown in Figure III. From the figure it can be seen that Sea Island and Western Lulu Island have 2 m of surficial overbank deposits underlain by up to 25 m of sand. The eastern portion of Lulu Island, except for an abandoned channel running from the southeast to the northwest, has up to 8 m of peat overlying 2 m of silt and up to 25 m of sand. The sand beneath the surficial deposits varies from loose to dense and fine to coarse and often contain silt lenses. Below the sands are more than 40 m of soft to firm clayey silt. Beneath the soft to firm clayey silts are stiff, post glacial, marine,

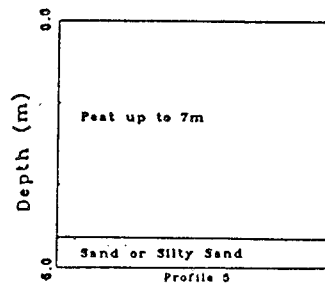
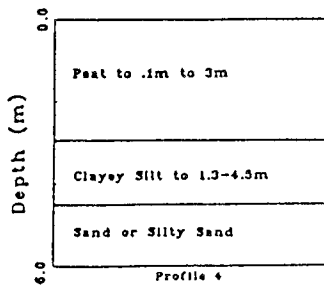
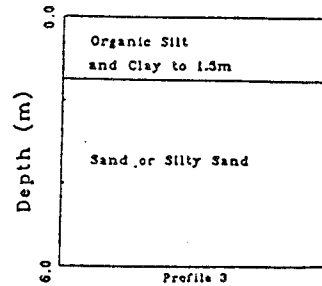
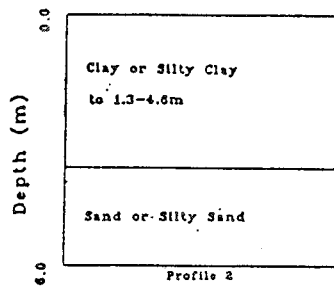
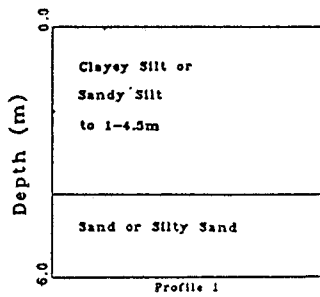
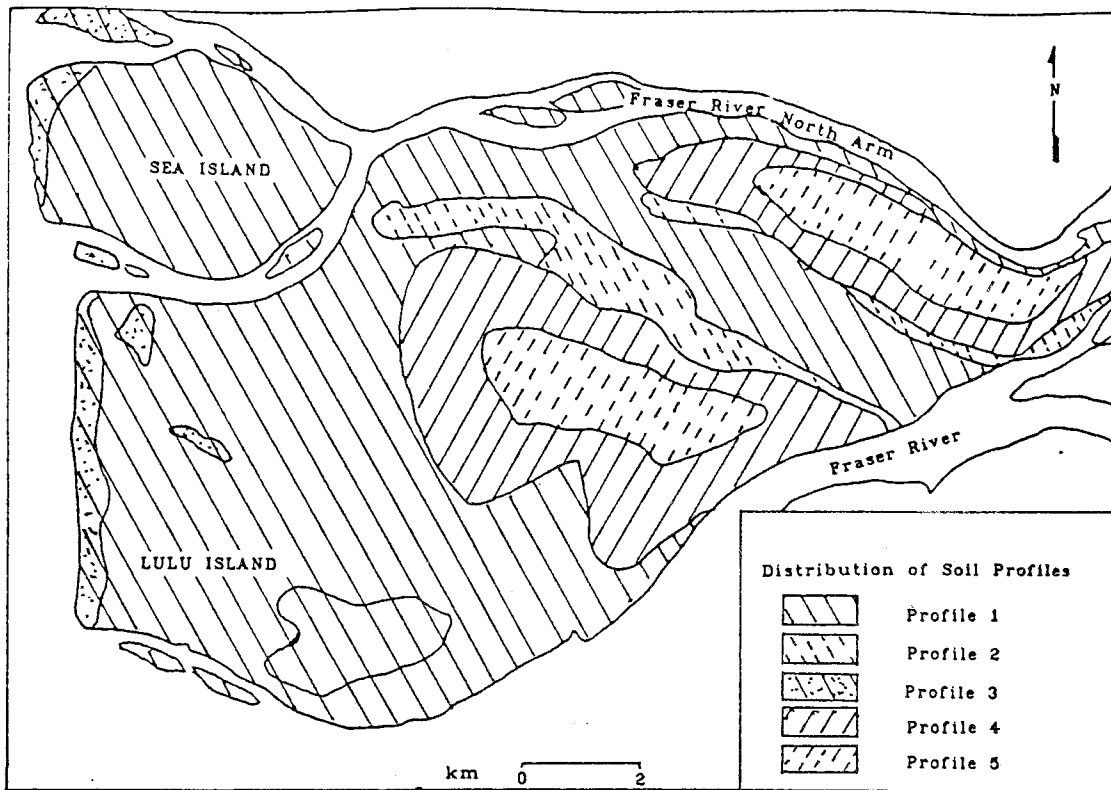


Figure III: Soil Type and Depth of Surficial Deltaic Deposits in Richmond

(Adapted from Wallis, 1979)

clayey silts and silty clays. Finally the ice loaded lodgement tills, glaciomarine and glaciofluvial deposits are encountered.

Estimates of the thickness of the post glacial sediments vary greatly. Mathews and Shepard(1962) estimate the average thickness of post glacial sediments to be 120 m. This figure was arrived at by dividing the present area of the delta into the annual volume of sediments multiplied by the age of the delta. Thus the sediments will be greater than 120 m thick in the center of the delta and shallower on the north edge and around Point Roberts.

The thickness of the ice loaded materials below the post glacial deposits is not well known. Blunden(1973) estimates depth to bedrock from ground surface to be 200 to 300 m.